GEOLOGICA ULTRAIECTINA

Mededelingen van de
Faculteit Aardwetenschappen
Universiteit Utrecht

No. 214

Biogenic silica cycling in the upwelling area on the Somalian Margin

Erica Koning

GEOLOGICA ULTRAIECTINA

Mededelingen van de
Faculteit Aardwetenschappen
Universiteit Utrecht

No. 214

Biogenic silica cycling in the upwelling area on the Somalian Margin

Erica Koning

ISBN 90-5744-072-5

Biogenic silica cycling in the upwelling area on the Somalian Margin

De kringloop van biogeen silica in het opwellingsgebied van de Somalische continentale helling

(met een samenvatting in het Nederlands)

Proefschrift

ter verkrijging van de graad van doctor
aan de Universiteit Utrecht
op gezag van de Rector Magnificus Prof. Dr. W.H. Gispen
ingevolge het besluit van het College voor Promoties
in het openbaar te verdedigen
op vrijdag 22 februari 2002 des middags te 4.00 uur

door

Frederica Angenita Koning

geboren op 23 september 1957 te Utrecht

Promotor: Prof. Dr. P. Van Cappellen
Department of Geochemistry
Utrecht University
Utrecht, The Netherlands

Co-promotor: Dr. Ir. W. van Raaphorst
Department of Marine Chemistry and Geology
Royal Netherlands Institute for Sea Research
Den Burg, The Netherlands

The research described in this thesis was carried out at the Department of Marine Chemistry and Geology of the Royal Netherlands Institute for Sea Research, P.O. Box 59, 1780 AB Den Burg, The Netherlands. This study was supported by NIOZ and by the Ministry of Education, Culture and Science (Ministerie van Onderwijs, Cultuur en Wetenschappen), within the framework of NEBROC, the NEtherlands- BRemen OCeanography co-operation.

All in a hot and copper sky,
The bloody sun at noon,
Right up above the mast did stand,
No bigger than the moon.

S.T. Coleridge,
The Rime of the Ancient Mariner

CONTENTS

CHAPTER 1

Introduction and summary

THE OCEANIC SILICA CYCLE

Silicon is one of the most abundant elements on earth. It occurs most often combined with oxygen as silica (SiO_2) in rocks and minerals (Iler, 1979), and weathering and erosion of these materials supplies silica to rivers, estuaries and to the surface waters of the oceans.

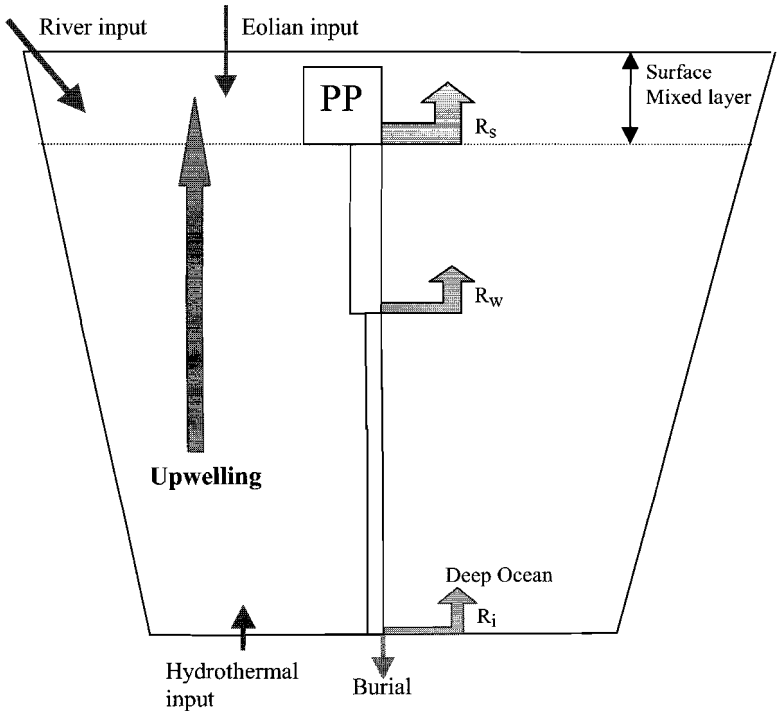

Fig. 1: The silica cycle in the oceans. PP represents primary production of biogenic silica in the surface waters. Gray arrows indicate dissolution of biogenic silica in the surface mixed layer (R_s), in the water column below the mixed layer (R_w) and at the sediment-water interface (R_i). The striped arrow indicates upwelling of silicic acid-rich deep water to the surface layer.

As a whole, the oceanic silica cycle is in steady state, indicating that input of silica to the oceans, through rivers, eolian transport and hydrothermal sources balances output through burial (Calvert, 1968; Broecker and Peng, 1982; Nelson et al., 1995; Tréguer et al., 1995). A schematic view of the ocean silica cycle is given in Fig. 1.

At the pH and ionic strength of seawater, dissolved silica occurs mostly as the monomeric silicic acid, H_4SiO_4 (Libes, 1992). Silicic acid is one of the major nutrients in the marine environment as it is utilized by diatoms, radiolarians, silicoflagellates and siliceous sponges to produce skeletal material composed of opal or biogenic silica. Upon their death, the skeletal remains may remain in the surface layer for a limited period of time due to mixing, but will eventually sink to the sea floor, often as constituent of fecal pellets (Bathman et al., 1990; Nelson et al., 1996). Because the water column is undersaturated with respect to silicic acid (Hurd, 1973), siliceous particles dissolve during settling, both in the surface layer and in the upper water column (R_s and R_u, Fig. 1). Direct measurement of production and dissolution rates indicate that 10-100% of the silica produced in the euphotic zone dissolves in the upper 50-100 m (Ragueneau et al, 2000). An overall mean of about 60% of the biogenic silica production is believed to dissolve in the upper water column above 1000m (Nelson and Goering, 1977; Nelson and Gordon, 1982; Nelson et al., 1995; Brzezinski and Nelson, 1995; Tréguer et al., 1995; Gersonde and Wefer, 1987). Silicic acid concentrations will therefore be low in the surface layer, where silicic acid is utilized, and increase with depth where dissolution dominates (Fig. 2a).

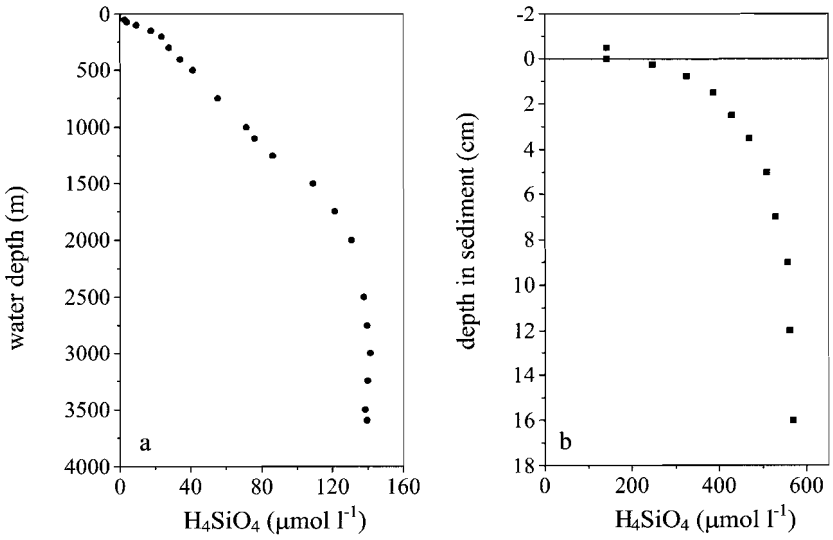

Fig. 2: Typical examples of silicic acid profiles from the water column (2a) and from interstitial waters from the sediment (2b). Both profiles are from the Somali Basin, Indian Ocean.

The age of the bottom water is reflected in the silicic acid concentrations. Young bottom waters, in the North Atlantic Ocean, have lowest silicic acid concentrations (20 μmol l^{-1}), while the oldest bottom waters, in the northeast Pacific Ocean, have highest silicic acid concentrations (160 μmol l^{-1}). Intermediate bottom water concentrations, ~120 μmol l^{-1}, are found in the Southern and Indian Oceans (Broecker and Peng, 1982). From the biogenic silica particles that escape dissolution in the water column during settling and reach the sea floor, an additional fraction dissolves at the sediment-water interface and in surficial sediments, leaving only ~2.5% of the original BSi production to be buried deeper in the sediment (Sayles et al., 1994; Koning et al., 1997).

Upon burial, dissolution continues, giving rise to pore water silicic acid concentrations well above those in the overlying water (Fig. 2b). The concentration gradient results in an efflux of silicic acid across the sediment-water interface, thereby returning dissolved silica to the water column. Through upwelling, deep water enriched in dissolved silica can be transported to the surface layer, where the silica can be utilized again by diatoms and other organisms. The buried biogenic silica will ultimately return to the oceanic silica cycle through sea-floor spreading, mountain uplift, weathering and erosion (Chester, 2000).

THE IMPORTANCE OF BIOGENIC SILICA IN UPWELLING AREAS

Diatoms are the major primary producers in the oceans and can often dominate the phytoplankton community, particularly in the early stage of blooms (Officer and Ryther, 1980; Cadee, 1986; Conley and Malone, 1992). The general competitive advantage of diatoms over flagellates lies both in a better photosynthetic capacity and in lower maintenance energy requirements (Billen et al., 1991). In spring, this may result in extensive diatom blooms in large areas of the oceans and in coastal seas. The diatoms in turn are grazed upon by foraminifera and copepods. Besides the major nutrients nitrogen and phosphorous and the micronutrients and trace elements required by all autotrophs, diatoms have an absolute requirement for silicon (Darley and Volcani, 1969; Brzezinski et al., 1990). Thus, growth will be inhibited when surface waters become depleted in silicic acid after which the phytoplankton assemblage shifts from diatoms to flagellates, species that require only nitrogen and phosphorous (Officer and Ryther, 1980).

In upwelling areas, however, constant replenishing of nutrients takes place, thus maintaining silicic acid concentrations favorable for diatom productivity for an extended period of time. As a consequence, biogenic silica production is relatively large in upwelling areas. Depending on the nutrient level and the actual hydrographic conditions, a succession of diatom species will subsequently dominate the upwelling-associated phytoplankton bloom. Between the different diatom species, cell size, thickness of skeleton walls and the presence of microscopic pores and spines vary considerably and such variations in surface/volume ratio (i.e. the amount of reactive surface exposed) and cell size will obviously influence their susceptibility to dissolution. While the living diatoms are protected against dissolution by the presence

of organic coatings surrounding the cell, upon death of the organisms the rate of dissolution of the silica walls increases (Lewin, 1961; Kamatani, 1982).

For all diatom species, the extent of recycling will depend on the residence time of the particles in the water column, especially in the warm surface waters (Ragueneau et al., 2000). Processes that increase sinking speed, such as a high Si:cell ratio, aggregation and grazing, will therefore promote export of biogenic silica from the surface layer to the sea floor. Summarizing, the high rates of diatom productivity that are maintained over prolonged periods of time in areas where upwelling of deep water occurs are expected to result in enhanced export fluxes of diatoms from the photic zone to the sediment surface.

PRESERVATION OF BIOGENIC SILICA IN THE SEDIMENTS

Although only a small portion of the siliceous organisms produced in the upper water column survives dissolution and is buried in the sediments, the abundance of diatoms in deep-sea sediments reflects the general pattern of productivity in the overlying waters (Lisitzin, 1972; Thunell et al., 1994; Broecker and Peng, 1982). Often however, the specific diatom species composition in the sediments fails to reflect that of the living phytoplankton, apparently because the more delicate species with a large surface area tend to dissolve and only the dissolution-resistant skeletons are preserved (Lewin, 1961; Dixit et al., 2001).

From silicic acid pore water profiles, dissolution is evident in the upper few centimeters of the sediment (Fig. 2b). Once the diatom frustules have been buried below the sediment mixing depth, however, dissolution appears to be of minor importance (Koning et al., 2001). Apparently, the transfer of biogenic silica from the water column to the sediment-water interface and subsequently into the sediment represents the crucial step in the preservation of biogenic silica. Elevated solute concentrations in the pore water, notably dissolved metals and specifically aluminium, promote the diagenetic alteration of biogenic silica, lower its solubility and dissolution rate, and may favor preservation over dissolution. Dissolution rates on the sea floor depend on ambient temperature, bottom water concentrations of silicic acid, sedimentation rate, reactive surface area of the diatoms and composition of the lithogenic fraction of the sediment (Van Cappellen, 1996; Kamatani and Riley, 1979; Dixit et al., 2001). Biogenic silica dissolution rates increase with increasing temperature and high degree of undersaturation, i.e. low silicic acid bottom water concentrations. High sedimentation rates reduce the exposure time to undersaturated bottom waters and thereby promote burial (Riedel, 1959; Pokras, 1986). The reactive surface area of biogenic silica particles is an important factor that controls dissolution. Dissolution is a surface process, initiated by the adsorption of an OH ion in the spaces between the oxygen ions on the particle surface (Iler, 1979). During dissolution, these reactive surface areas are progressively eliminated as silica dissolves from and reprecipitates on the particle surface (Van Cappellen, 1996; Van Cappellen and Qiu, 1997).

The incorporation of small amounts of aluminium in the matrix of biogenic silica has been shown to effectively lower the solubility (Lewin, 1961; van Bennekom, 1991). Aluminium can be incorporated into the diatom frustule during biosynthesis (van Beusekom, 1990; van Bennekom et al; 1991), but levels will not exceed 0.8%. Since up to 6% is found in diatoms in surface sediments from the Angola Basin, an additional post-mortem incorporation process must occur during early diagenesis (van Bennekom, 1996). Concentrations of dissolved aluminium are low in bottom waters, but in pore waters, dissolved aluminium originating from the lithogenic fraction of the sediment is present in concentrations that are sufficiently high to facilitate these diagenetic incorporation processes. In the Southern Ocean, negative correlations were observed between the concentration of aluminium and silicic acid in the pore water, on the one hand, and between the concentration of aluminium in the pore water and the solubility of biogenic silica, on the other hand (van Beusekom et al., 1997; Van Cappellen and Qiu, 1997). Recent studies showed both structural incorporation of aluminium in the diatom lattice and co-precipitation of silica and aluminium originating from the lithogenic fraction of the sediment (Dixit et al, 2001; Gehlen et al., 2001).

Summarizing, early diagenetic processes taking place at the sediment-water interface appear to be the major control on biogenic silica and diatom preservation. Once buried below the sediment-water interface, biogenic silica can be traced in sediments that are several 100,000 years old, where it provides information about productivity patterns of diatoms on geological time scales. Consequently, the alternating presence and absence of upwelling indicating diatom species in the sediment record may reflect the changes in upwelling intensity in the geological past (e.g. Sirocko et al.,, 1993; Sirocko, 1996). Biogenic silica and diatoms therefore have potential as a proxy for paleoproductivity (Lyle et al., 1988; Mortlock et al., 1991), provided that the mechanisms controlling the cycle of production, dissolution and burial of silica in the modern ocean are understood. A prerequisite for such studies is a reliable method to quantify biogenic silica in the water column, in sediment traps and in the sediment.

UPWELLING AREAS

Upwelling is the major transport mechanism for silicic acid-rich deep waters to the photic zone, where it can be utilized by phytoplankton. Upwelling of deep water takes place in open ocean areas in the Equatorial Atlantic and Pacific Oceans and in the Southern Ocean. In the Equatorial region, the most extensive areas of upwelling are found just south of the Equator, in association with the Equatorial Counter Current. Associated with the Circumpolar Current in the Southern Ocean are both areas where surface waters converge and downwelling occurs, and areas where when surface currents diverge and where upwelling takes place.

Besides open-ocean upwelling areas, high diatom productivity related to coastal upwelling is found along the continental margins of the continents. In these areas, surface waters are driven away from the coastal boundary in response to wind stress

and replaced by nutrient-rich subsurface waters (Suess and Thiede, 1983). Almost all the important coastal upwelling regions are found along the eastern margins of the oceans e.g. Peru, the northeast Pacific, Namibia, the Angola Basin, Cape Blanc and the Iberian Margin. The only major upwelling area on a western ocean margin is that along the Somali coast, associated with the seasonal Indian Ocean Monsoon. In this thesis, we will focus on the upwelling area on the Somali Margin in the Indian Ocean.

THE INDIAN OCEAN

In the NW Indian Ocean, intense coastal upwelling is present during boreal summer (Clemens et al., 1991; Brock et al., 1992), related to the SW Indian Monsoon. The SW Indian Monsoon is one of the major climate systems of the world, impacting large portions of both Africa and Asia (Overpeck et al., 1996). The seasonal occurrence of SW and NE monsoonal winds and associated surface currents is closely linked to the greater heat capacity of the ocean relative to the surrounding landmasses (Fein and Stephens, 1987). In winter, the continent cools relative to the Southern Indian Ocean, resulting in NE monsoonal winds forcing a Somali Current that flows from north to south (Fig. 3a).

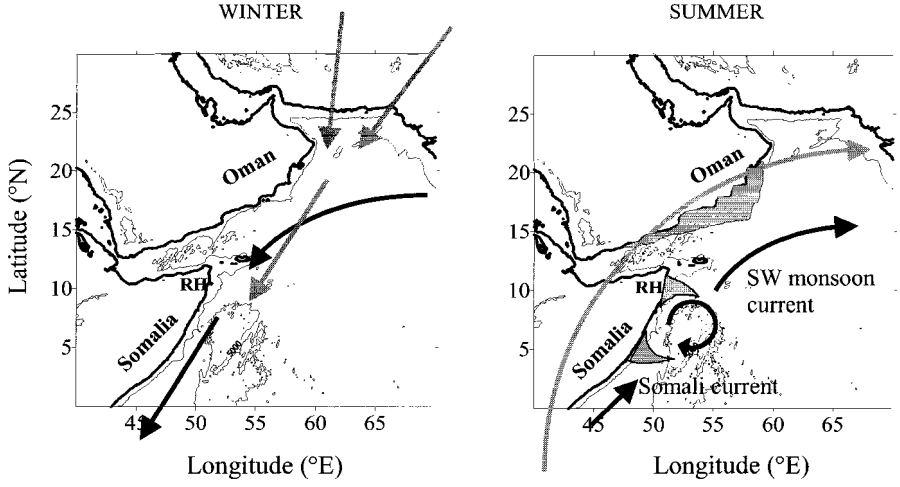

Fig. 3: Wind and current patterns in the northwestern Indian Ocean during summer (left panel) and winter (right panel). Grey arrows indicate major wind trajectories. Black arrows indicate the direction of the surface currents. Grey areas indicate upwelling. RH indicates Cape Ras Hafun.

In early spring, the Tibetan Plateau warms rapidly relative to the Southern Indian Ocean, resulting in the formation of an area of low atmospheric pressure above the Himalayas, while pressure above the relatively cold Southern Indian Ocean is high. Due to this pressure gradient, southwesterly winds rapidly gain strength along the coast of Somalia and persist at high velocities during the entire SW monsoon until late September (Prell, 1984; Webster, 1987). In response, coastal upwelling is generated and a succession of large, anti-cyclonic eddies develops, bound by wedges of cold, upwelled water off the coast at about 5 and 10°N (Fig. 3b). The eddies migrate northward, along with the Somali current (Brock et al., 1992; Fischer et al., 1996; Schott, 1983; Schott et al., 1990; Rixen et al., 1996). Off Ras Hafun (RH, Fig. 3), the wedge of cold upwelled water remains almost continuously present during the SW monsoon. Further offshore, the wedges merge into filaments or jets curving along the eddy margin, advecting high concentrations of upwelled nutrients into the interior of the Somali Basin. The seasonal reversal in the surface circulation of the Indian Ocean (Nair et al., 1989) results in strong differences between the oligotrophic period during the NE monsoon, when productivity is almost as low as that of the Sargasso Sea (Smith and Codispoti, 1980), and the SW monsoon, when primary production is as high as 1-2.5 gC m^{-2} d^{-1} (Veldhuis et al, 1997).

Productivity however may vary widely on an annual basis. In years of low snowfall, the Tibetan Plateau is able to warm early and generate a stronger monsoonal circulation (Barnett, 1988; Prell and Kutzbach, 1992; Clemens et al., 1996). In contrast, a cold winter over the Northern Hemisphere and over the Tibetan Plateau results in a weakened pressure low and a weakened SW monsoon the following summer (Raman and Maliekal, 1985; Meehl, 1994). Consequently, a prolonged period of intensive snow and ice cover on the Tibetan Plateau as could have occurred in glacial times (Kuhle, 1998) would have reduced monsoonal upwelling for an extended period of time.

EARLY OBSERVATIONS ON THE SOUTHWEST MONSOON

The word monsoon originates from the Arabic word *mausim* that means a fixed time, a season. The notion of periodic changes in the direction of the winds, however, is a notion taught by navigators from the west. In indigenous thought, the monsoon is indeed the result of periodic reversal, but the realization of this reversal is with sun and rain, not winds (Zimmerman, 1987).

Merchant seamen have been sailing the Indian Ocean for 5000 years. Man's oldest shipping records for the Indian Ocean date from about 2300 B.C., from the ancient city-states of lower Mesopotamia. Early sailors engaged in the longstanding trade across the Persian Gulf and Northern Arabian Sea must surely have observed the seasonal change in winds there, and perhaps they scheduled their voyages according to the monsoon as well. No mention of those winds seems to have survived from that period, but a few merchant records hint of seasonality in this maritime traffic that may have been based on the monsoons. None of these early writers, however, spoke of ocean currents, let alone the semiannual reversal in surface currents of the Arabian

Sea, suggesting that little was known of the Indian Ocean circulation at that time (Warren, 1987).

With the decline of the Roman Empire in the third century, Mediterranean traders disappeared almost entirely from the Indian Ocean and reports of winds and currents are very meager in the next centuries. From the 7th century onwards, however, the Arabs made their prodigious conquests and a great development of maritime commerce started. From this period dates this early observation on the reversal of the surface current:

> *The sea flows during the summer month to the north-east, and during the winter month to the south-west - Ibn Khordazbeh, 9th century.*

The medieval geographers did not have any concept of horizontal circulatory gyres in the ocean, and they always spoke as currents as water periodically emptying out of one place and piling up in another. Hence the monsoon currents are conceived here essentially as an annual tide. Nevertheless, the description is roughly accurate for the North Indian Ocean with respect to both direction of flow and season. Apparently, the Arabic geographers were aware of the seasonal current reversal, but their knowledge of it was meager and none of them for example mentioned the powerful Somali current, even though Arabs had been on the East coast of Africa since the eighth century (Warren, 1987).

In the seventeenth century, a new perspective of the monsoons emerged with the development of modern science in Western Europe (Kutzbach, 1987). The new approach to science proclaimed that the first step toward understanding natural phenomena was experimental study, especially by accurate description, observation, survey and classification, followed by the theoretical interpretation of these phenomena, applying mathematics and physical laws. Atmospheric phenomena lent themselves particularly to this new approach, and because of its striking characteristics and its importance to life and commerce, the monsoon was among the first large-scale atmospheric circulation systems that was investigated. Most of the early observations were by passing merchant ships to the East Indies, many belonging to the East India Company, which held a monopoly over Indian trade for more than two centuries. Their observations were compiled in navigational atlases, e.g. by Findlay (1866), who described the Somali current and the Great Whirl, and the KNMI atlas (1889), showing wind speed and direction for the Indian Ocean and the Gulf of Aden. From the 1890's onward, specialized research vessels have visited the Indian Ocean with a purely scientific objective (e.g. Challenger, Snellius I Expedition, 1929-1930; John Murray Expedition, 1933-1934; International Indian Ocean Expedition, 1959-1960). During these early expeditions, the main focus was on observations of currents and measurements of physical and biological parameters. In 1992-1993, the Netherlands Indian Ocean Programme (NIOP) was carried out in the NW Indian Ocean, the Arabian Sea and off Kenya and the Seychelles, with the objective 'to study the effect, on both spatial and temporal scales, of the monsoon on the climate system in the northern Indian Ocean' (van Weering et al., 1997). The samples discussed in this thesis were recovered during legs C0, C1 and C2 of the sub-program 'Tracing a Seasonal Upwelling'.

In recent years, deep-sea sediment cores, ice cores, loess and lake records and tree rings have been studied to explain the forces driving the SW monsoon and its variability in the geological past (e.g. Shimmield and Mowbray, 1991; Xiao et al, 1999; Altabet et al, 1995; Gasse and van Campo, 1994; Thompson et al, 1997; Feng et al, 1999). Their results have shown that the intensity of the Indian Ocean monsoon and the associated upwelling has varied over glacial-interglacial time scales and that the processes that force the Indian Ocean climate are related to global climate variability. The glacial-interglacial variability in upwelling intensity would be reflected in a direct response of the diatoms that, in turn, are preserved in the biogenic silica record in the sediment (Sirocko, 1992; Sirocko et al., 1993; Sirocko, 1996). The biogenic silica content of the sediments could thus be used for paleo-productivity studies, provided a reliable method to detect even the minor amounts of biogenic silica found during glacial intervals, is available.

DEVELOPMENTS IN BIOGENIC SILICA ANALYSIS

The biogenic silica, or BSi, contents of the sediment can vary widely, depending on dilution with other biogenic and lithogenic components. Siliceous oozes, with BSi >80%, cover the sea floor in areas of the Southern Ocean and in the equatorial Pacific, while biogenic silica is <5% in most of the Atlantic and Indian Oceans, due to the dilution with $CaCO_3$ and land-derived material (Broecker and Peng, 1982). In coastal areas, minor amounts of biogenic material are deposited within a large lithogenic matrix. During early diagenesis, this lithogenic phase may interact with the biogenic silica in the sediment, thereby obscuring the distinction between biogenic and non-biogenic fractions. Most marine samples therefore consist of a number of silica containing fractions, a reactive silica phase of biogenic origin, which is therefore called biogenic silica or biogenic opal, clay minerals, alumino silicates, quartz, all more or less susceptible to dissolution in alkaline solutions. Under optimized analytical conditions, the reactive biogenic silica fraction should dissolve completely, while the contribution of non-biogenic siliceous components should be minor. For several decades, a succession of analytical techniques were developed and tested, many with a specific type of sample in mind.

In the last decades, several techniques have been employed to analyze biogenic silica in samples from the water column and in the sediments, e.g. spectroscopy, X-ray diffraction after transformation to cristobalite (Goldberg, 1958; Calvert, 1966), direct X-ray diffraction (Eisma and Van der Gaast, 1971), normative calculation (Leinen, 1977). Besides the techniques mentioned above, a number of wet-chemical leaching techniques have been developed that are considered to be the most sensitive technique for determining biogenic silica in marine sediments of various composition (DeMaster, 1981; Conley, 1998). Although all leaching techniques are based on the dissolution of reactive silica in an alkaline solution, experimental conditions vary widely. Most of the early wet-chemical leaching techniques (Hurd, 1973; Eggiman et al, 1980; DeMaster et al, 1981; Mortlock and Froelich, 1989) use Na_2CO_3 as a leaching agent because it was considered to preferentially attack opaline silica, while

sodium hydroxide was believed to attack alluminosilicates, cristobalite and fine-grained quartz as well. However, Krausse et al (1983) compared alkaline leachings with either sodium carbonate or sodium hydroxide and showed that, in contrast to earlier studies, a 0.2M NaOH extraction appeared to leach less silica from the mineral phase than 0.05 or 0.5M Na_2CO_3.

Furthermore, most of the early leaching techniques did not correct for dissolved silica leached from the lithogenic phase of the sediment. In 1981, DeMaster proposed a sequential leaching in 0.1M Na_2CO_3 with a sample taken after 1, 2, 3 and 5 hrs. His results showed that the diatoms are quantitatively dissolved in such a leaching solution in 2 hr or less and that dissolution of clay minerals contributed substantially to the concentration of silicic acid in the leaching solution. DeMaster proposed that the dissolution of clay minerals occurred independently from the dissolution of the reactive silica fraction and that extrapolation of this 'clay' dissolution line to time zero corrects for the contribution of non-biogenic silica and thus gives the biogenic silica content of the sample. In these experiments, the correction for the contribution of silica from the mineral phase was made on the basis of a small number of samples, commonly 5 or 6, introducing considerable errors in the intercept determined from extrapolation of this line (Conley, 1998). More importantly, this error is solely determined by the clay fraction of the sample and can thus cause considerably large relative errors at low BSi and high clay contents. In 1993, Müller and Schneider modified the sequential leaching proposed by DeMaster (1981) by applying an auto-analyzer system that allowed for a continuous recording of the mineral dissolution line and thus ensures an accurate estimate of the extrapolated intercept at time zero.

Recently, Kamatani and Oku (2000) described a new approach to correct for the non-biogenic content of the sample. They estimated the biogenic silica content of the sediment through linear regression of the extracted SiO_2 plotted against the simultaneously extracted aluminium. Because of the low sampling resolution, 5 samples taken at 20-minute intervals, errors can be large, particularly because most clay minerals do not dissolve homogeneously. Despite the major developments in analyzing biogenic silica described above, none of the techniques appears to be suited for complex samples with very low biogenic silica and high clay content (Conley, 1998). For this type of sediment, a new alkaline leaching method was developed, that measures both silicic acid and aluminium at 1-second intervals.

THIS THESIS

This thesis presents a study on the cycling and preservation of biogenic silica and diatoms in the upwelling area on the Somali continental margin in the NW Indian Ocean.

Chapter 2 describes an alkaline leaching technique for the simultaneous analysis of biogenic silica and aluminium in sediments, suitable for complex samples with low biogenic silica and with a high clay mineral content. Measuring aluminium facilitates the discrimination between silica from the biogenic (BSi) and the non-

biogenic fraction, because it originates almost solely from the lithogenic phase of the sediment. The method was tested using fine-grained silicagel, standard clay minerals, artificial sediment mixtures, and natural samples ranging from fresh diatoms to aged sediment from different depositional settings. To determine the BSi content, 4 different models each describing the dissolution curves, but of increasing complexity, were applied and for each different type of sample the optimum model was selected on the basis of F-test statistics. For mixtures of silicagel and clay minerals, the contribution of Si from dissolution of the clay was negligible compared to Si from silicagel. For natural samples, however, the dissolution curves varied with the age and composition of the sample. For fresh diatoms and Pleistocene siliceous oozes, first order dissolution curves were observed, but for sediments with high clay content, complex dissolution curves were observed and single-phase first order dissolution was exceptional. For most of these samples, the distinction between biogenic silica and the silica originating from dissolution of clays could be made on the basis of the Si/Al ratios and reactivity constants of the dissolving phases calculated with the models.

Chapters 3, 4 and 5 describe the cycling of biogenic silica at two stations 80 and 270 kilometers offshore on a transect on the Somali Margin (NW Indian Ocean). During the Netherlands Indian Ocean Programme (NIOP), settling particles were collected at these two sampling sites for nine months, from June 1992 to February 1993. One sediment trap array was deployed on the Somali slope directly below one of the main upwelling gyres and a second array, meant as a reference site to reflect pelagic sedimentation, was moored in the Somali Basin away from direct coastal upwelling influence. At the sediment below the traps, benthic landers were deployed and box cores and piston cores were recovered. Based on particulate fluxes of biogenic silica through the water column, silica burial fluxes into the sediments and the flux of dissolved silica across the sediment-water interface estimated from pore water profiles and from in-situ benthic chamber incubations, a mass balance was calculated for biogenic silica (chapter 3). Particulate fluxes collected in the sediment trap on the Somali slope show a distinct pattern, with high fluxes intercepted during the SW monsoon and low fluxes during the winter months. Particulate fluxes are lower in the Somali Basin, but show a similar pattern. Our results show that less than 10% of the biogenic silica arriving on the Somali Margin is buried in the sediments, due to efficient recycling at the sediment-water interface.

In chapter 4, the diatom species composition of the settling biogenic silica particles collected in the sediment traps was studied in detail and compared with the underlying sediment to determine the preservation of the various diatom species and to investigate the potential of biogenic silica as an indicator for changes in paleo-upwelling intensity. At both sampling sites, fluxes of diatoms increased by one order of magnitude during the upwelling season. However, species fluxes were distinctly lower in the Somali Basin than on the Somali slope, due to the diminished influence of upwelling away from the coast. On the Somali slope, a distinct seasonal diatom species succession of 'pre-upwellers', 'upwellers' and 'oceanic species' was apparent. A similar species sequence was found in the Somali Basin, however, the massive flux of *Chaetoceros* resting spores that characterizes the end of the SW monsoon is absent at this site away from the coast. Major dissolution takes place at the sediment-water

interface and results in the disappearance of the small, weakly silicified diatoms from the species assemblage. Less than 10% of the diatom assemblage escapes dissolution at the sediment-water interface and is buried in the sediment. Below the sediment mixing depth, dissolution appears to be of minor importance and the two diatom species that characterize the upwelling season, *Thalassionema nitzschioides* and *Chaetoceros* resting spores, dominate the diatom assemblage in the sediments and thereby reflect the upwelling in the surface layer of the water column.

In chapter 5, the conclusions drawn from the previous chapter are applied on a piston core recovered below the sediment trap on the Somali slope. In this piston core, the high-resolution biogenic silica accumulation record strongly reflects changes in upwelling intensity during the past 115 ky. In the Holocene, sampling at 50-year resolution provides a biogenic silica record that reflects variability on millennial and centennial time scales. Two long intervals of continuously increasing upwelling intensity occurred, suggesting a gradual deglaciation of the Tibetan Plateau with abrupt returns to colder conditions at the Holocene cold event (8.2 ky BP) and at the late Holocene aridification (5.9 ky BP). The diatom species assemblage of selected samples was studied in detail to determine the preservation of the upwelling-indicating diatoms. During intervals with elevated biogenic silica accumulation, 'upwelling' diatoms dominated, except for two samples in early isotope stage 3, when oceanic species dominated the assemblage. In glacial periods and cold stadials, biogenic silica accumulation rates were very low and diatoms were almost absent from the sediments. In the early Holocene and in isotope stage 5c, the upwelling indicating diatom species *Thalassionema nitzschioides* and *Chaetoceros* resting spores accumulated at up to 8 times the present day accumulation rates, indicating that upwelling induced diatom productivity was enhanced during these periods. Apparently, upwelling was more intense in the early Holocene and in the last interglacial than it is at present, but was of minor importance during glacial periods.

Summarizing, the study presented in this thesis shows that on the Somali Margin of the Indian Ocean, the biogenic silica record preserved in the sediments reflects the upwelling-induced primary productivity of diatoms in the surface waters. Although a major fraction of the biogenic silica dissolves in the water column and at the sediment- water interface and the small, weakly silicified diatoms disappear from the species assemblage, two important upwelling diagnostic diatom species survive dissolution and are preserved in the sediment. In the sediment record, the upwelling history of the NW Indian Ocean was successfully inferred from the fluctuations in biogenic silica accumulation and from the presence and absence of these upwelling indicating diatom species.

REFERENCES

Altabet, M.A., Francois, R., Murray, D.W., Prell, W.L. (1995). Climate-related variations in denitrification in the Arabian Sea from sediment $^{15}N/^{14}N$ ratios. Nature, 373, 506-509, 1995.

Barnett, T.P., Domenil, L., Schlese, U., Roeckner, E. (1988). The effect of Eurasian snow cover on global climate. Science, 239, 504-507.

Bathman, U.V., Noji, T.T., von Bodungen, B. (1990). Copepod grazing potential in late winter in the Norwegian Sea- a factor in the control of spring bloom development? Marine Ecology Progress Series, 60, 225-233.

Billen, G., Lancelot, C., Meybeck, M. (1991). N, P, and Si retention along the aquatic continuum from land to ocean. In: Mantoura, R.F.C., Martin, J.-M., Wollast, R. (Eds.) Ocean margin processes in global change. Wiley-Interscience, Chichester, New York, Brisbane, Toronto, Singapore, 19-44.

Brock J.C., McClain, C.R., Hay, W.W. (1992). A southwest monsoon hydrographic climatology for the northwestern Arabian Sea. Journal of Geophysical Research, 97, 9455-9465.

Broecker, W.S., Peng, T.-H. (1982). Tracers in the sea, Eldigio Palisades, New York. 690pp.

Brzezinski, M.A., Nelson, D.M. (1995). The annual silica cycle in the Sargasso Sea near Bermuda. Deep-Sea Research I, 42, 1215-1237.

Brzezinski, M.A., Olson, R.J., Chisholm, S.W. (1990). Silicon availability and cell-cycle progression in marine diatoms. Marine Ecology Progress Series, 67, 83-96.

Cadee, G.C. (1986). Recurrent and changing seasonal patterns in phytoplankton of the westernmost inlet of the Dutch Wadden Sea from 1969 to 1985. Marine Biology, 93, 281-289.

Calvert, S.E. (1966). Accumulation of diatomaceous silica in the sediments of the Gulf of California. Geological Society of America Bulletin, 77, 569-596.

Calvert, S.E. (1968). Silica balance in the ocean and diagenesis. Nature, 219: 919-920.

Chester, R. (2000). Marine Geochemistry. Blackwell Science, Oxford. 506pp.

Clemens, S., Prell, W., Murray, D., Shimmield, G., Weedon, G. (1991). Forcing mechanisms of the Indian Ocean monsoon. Nature, 353, 720-725.

Clemens, S.C., Murray, D.W., Prell, W.L. (1996). Nonstationary phase of the Plio-Pleistocene Asian monsoon. Science, 274, 943-948.

Conley, D.J., Malone, T.C. (1992). Annual cycle of dissolved silicate in Chesapeake Bay: implications for the production and fate of phytoplankton biomass. Marine Ecology Progress Series, 81, 121-128.

Conley, D.J. (1998). An interlaboratory comparison for the measurement of biogenic silica in sediments. Marine Chemistry, 63: 39-48.

Darley, W.M., Volcani, B.E. (1969). Role of silicon in diatom metabolism. Experimental Cell Research, 58, 334-342.

DeMaster, D.J. (1981). The supply and accumulation of silica in the marine environment. Geochimica et Cosmochimica Acta, 45, 1715-1732.

Dixit, S., Van Cappellen, P., van Bennekom, A.J. (2001). Processes controlling the solubility of biogenic silica and pore water build-up of silicic acid in marine sediments. Marine Chemistry, 73, 333-352.

Eggimann, D.W., Manheim, F.T., Betzer, P.R. (1980). Dissolution and analysis of amorphous silica in marine sediments. Journal of Sedimentary Petrologists, 51, 215-225.

Eisma D., van der Gaast, S.J. (1971). Determination of opal on marine sediments by X-ray diffraction. Netherlands Journal of Sea Research, 5, 382—389.

Fein, J.S., Stephens, P.W. (1987). Monsoons. Wiley, New York, 632 pp.

Feng, X., Cui, H., Tang, K. Conkey, L.E. (1999). Tree-ring δD as an indicator of Asian monsoon intensity. Quaternary Research, 51, 262-266, 1999.

Findlay, A.G. (1866). A directory for the navigation of the Indian Ocean. Richard Holmes Laurie, London, 1062pp.

Fischer, J., Schott, F., Stramma, L. (1996). Current and transports of the Great Whirl-Socotra Gyre system during the summer monsoon, August 1993. Journal of Geophysical Research, 101, 3573-3587.

Gasse, F., van Campo, E. (1994). Abrupt post-glacial climate events in West Asia and North Africa monsoon domains. Earth and Planetary Science Letters, 126, 435-456.

Gehlen, M., Beck, L., Calas, G., Frank, A.-M., van Bennekom, A.J., Beusekom, J.E.E. (2001). Unraveling the atomic structure of biogenic silica: Evidence of the structural association of Al and Si in diatom frustules. Geochimica et Cosmochimica Acta (in press)

Gersonde, R., Wefer, G. (1987). Sedimentation of biogenic siliceous particles in Antarctic waters from the Atlantic sector. Marine Micropaleontology, 11, 311-332.

Goldberg, E.D. (1958). Determination of opal in marine sediments. Journal of Marine Research, 17, 178-182.

Hurd, D.C. (1973). Interactions of Biogenic opal sediment and sea water in the central equatorial Pacific. Geochimica et Cosmochimica Acta, 37, 2257-2282.

Iler, R.K. (1979). The chemistry of silica. Wiley-Interscience, New York. 866 pp.

Kamatani, A. (1982). Dissolution rates of silica from diatoms decomposing at various temperatures. Marine Biology, 68, 91-98.

Kamatani, A., Riley, J. P. (1979). Rate of dissolution of diatom silica walls in seawater. Marine Biology, 55, 29-35.

Kamatani, A., Oku, O. (2000). Measuring biogenic silica in marine sediments. Marine Chemistry, 68, 183-264.

Koning, E., Brummer, G.J.A., van Raaphorst, W., van Bennekom, A.J., Helder, W. van Iperen, J.M. (1997). Settling, dissolution and burial of biogenic silica in the sediments off Somalia (northwestern Indian Ocean). Deep-Sea Research II, 44, 1341-1360.

Koning, E., van Iperen, J.M., van Raaphorst, W., Helder, W., Brummer, G.-J.A., van Weering, T.C.E. (2001). Selective preservation of upwelling-indicating diatoms in sediments off Somalia, NW Indian Ocean. Deep-Sea Research I, 48, 2473-2495.

Koninklijk Nederlands Meteorologisch Instituut (1889). Barometerstanden en winden in de Golf van Aden en den Indischen Oceaan bij Kaap Guardafui. KNMI, Utrecht, 21pp.

Krausse, G.L., Schelske, C.L. Davis, C.O. (1983). Comparison of three wet-alkaline methods of digestion of biogenic silica in water. Freshwater Biology, 13, 73-81.

Kuhle M. (1998). Reconstruction of the 2.4 million km^2 late Pleistocene ice sheet on the Tibetan Plateau and its impact on the global climate. Quaternary International, 45/46, 71-108.

Leinen, M. (1977). A normative calculation technique for determining opal in deep-sea sediments. Geochimica et Cosmochimica Acta, 41, 671-676.

Lewin, J.C. (1961). The dissolution of silica from diatom walls. Geochimica et Cosmochimica Acta, 21, 182-198.

Libes, S.M. (1993). An introduction to Marine Biogeochemistry. J. Wiley & Sons, Inc. New York, Chichester, Brisbane, Toronto, Singapore. 734pp.

Lisitzin, A.P. (1972). Sedimentation in the world ocean. Society of Economic Paleontologists and Mineralogists Special Publication, 17, 218p.

Lyle, M., Murray, D.W., Finney, B.P., Dymond, J., Robbins, J.M., Brooksforce, K. (1998). The record of late Pleistocene biogenic sedimentation in the eastern tropical Pacific Ocean. Paleoceanography, 3, 39-59.

Meehl, G.A. (1994). Coupled land-ocean-atmosphere processes and South Asian monsoon variability. Science, 266, 263-267.

Mortlock, R A, Froelich, P.N. (1989). A simple method for the rapid determination of Biogenic opal in marine sediments. Deep-Sea Research I, 36, 1415-1426.

Mortlock, R.A., Charles, C.D., Froelich, P.N., Zibello, M.A., Saltzman, J., Hays, J.D., Burckle, L.H. (1991). Evidence for lower productivity in the Antarctic Ocean during the last glaciation. Nature, 351, 220-223.

Müller, P.J., Schneider, R. (1993). An automated method for the determination of opal in sediments and particulate matter. Deep Sea Research I, 40, 425-444.

Nelson, D.M., Goering, J.J. (1977). Near-surface silica dissolution in the upwelling region off northwest Africa. Deep-Sea Research I, 24, 65-73.

Nelson, D.M., Gordon, L.I. (1982). Production and pelagic dissolution of biogenic silica in the Southern Ocean. Geochimica et Cosmochimica Acta, 46, 491-501.

Nelson, D.M., Tréguer, P., Brzezinski, M.A., Leynaert A., Quéguiner, B. (1995). Production and dissolution of biogenic silica in the ocean: Revised global estimates, comparison with regional data and relationship to biogenic silica sedimentation. Global Biogeochemical Cycles, 9, 359-372.

Officer, C.B., Ryther, J.H. (1980). The possible importance of silicon in marine eutrification. Marine Ecology Progress Series, 3, 83-91.

Overpeck, J., Anderson, D., Trumbore, S., Prell, W. (1996). The southwest Indian Monsoon over the last 18000 years. Climate dynamics, 12, 213-225.

Pokras, E.M. (1983). Preservation of fossil diatoms in Atlantic sediment cores: control by supply rate. Deep-Sea Research I, 33, 893-902.

Prell, W.L. (1984). Variation of monsoonal upwelling: a response to changing solar radiation, In: J. Hasen and T. Takahashi (Eds.) Climate processes and climate sensitivity. 29. AGU, Washington DC, 48-57.

Prell, W.L., Kutzbach, J.E. (1987). Sensitivity of the Indian monsoon to forcing parameters and implications for its evolution. Nature, 360, 647-652.

Ragueneau, O., Tréguer, P., Leynaert, A., Anderson, R.F., Brzezinski, M.A., DeMaster, D.J., Dugdale, R.C., Dymond, J., Fischer, G., François, R., Heinze, C., Maier-Reimer, E., Martin-Jézéquel, Nelson, D.M., Quéguiner, B.(2000). A review of the Si cycle in the modern ocean: recent progress and missing gaps in the application of biogenic opal as a paleoproductivity proxy. Global and Planetary Change, 26, 317-365.

Raman, C.R.V., Maliekal, J.A. (1985). A 'northern oscillation' relating northern hemisphere pressure anomalies and the Indian summer monsoon, Nature, 314, 430-432.

Riedel, W.R. (1959). Siliceous organic remains in pelagic sediments. Special publication nr. 7, Society of Economic Paleontologists and Mineralogists, 80-91.

Rixen, T., Haake, B., Ittekkot, V., Guptha, M.V.S., Nair, R.R. and Schluessel, P.(1996). Coupling between SW monsoon related surface and deep ocean processes as discerned from continuous particle flux measurements and correlated satellite data.
Journal of Geophysical Research, 101, (12), 28569-28582.

Sayles, F.L., Deuser, W.G., Goudreau, J.E., Dickinson, W.H., Jickells, T.D., King, P. (1996) The benthic cycle of biogenic opal at the Bermuda Atlantic Time Series site. Deep Sea Research I, 43, 383-409.

Schott, F. (1983). Monsoon response of the Somali Current and associated upwelling. Progress in Oceanography 12, 357-381.

Schott, F., Swallow, J.C., Fieux, M. (1990). The Somali Current at the equator: annual cycle of currents and transports in the upper 1000m and connection to neighboring latitudes. Deep-Sea Research I, 37, 1825-1848.

Shimmield, G.B., Mowbray, S.R. (1991). The inorganic geochemical record of the northwest Arabian Sea: a history of productivity variation over the last 400 K.Y. from sites 722 and 724, In: Prell, W.L., Niitsuma, N., et al., (Eds.) Proceedings of the Ocean Drilling Program, Scientific Results, Vol. 117, 409-429.

Sirocko, F., Sarnthein, M., Erlenkeuser, H., Lange, H., Arnold, M., Duplessy, J.C. (1993). Century-scale events in monsoonal climate over the past 24,000 years, Nature, 364, 322-324.

Sirocko, F. (1996). Past and present subtropical summer monsoons, Science, 274, 937-938.

Smith, S.L., Codispoti, L.A. (1980). Southwest monsoon of 1979: chemical and biological response of Somali coastal waters. Science, 209, 597-600.

Suess, E., Thiede, J. (1983). Introduction. In: Suess, E. and Thiede, J. (Eds), Coastal upwelling, its sediment record. Part A: responses of the sedimentary regime to present coastal upwelling. Plenum Press, New York and London, 1-10.

Thompson, L.G., Yao, T., Davis, M.E., Henderson, K.A., Thompson-Mosley, E., Lin, P.-N., Beer, J., Synal, H.-A., Cole-Dai, J., Bolzan, J.F. (1997). Tropical climate instability: the last glacial cycle from a Qinghai-Tibetan ice core, Science, 276, 1821-1825.

Thunell, R.C., Pride, C.J., Tappa, E., Muller-Karger, F.E. 1994. Biogenic Silica fluxes and accumulation rates in the Gulf of California. Geology, 22, 303-306.

Tréguer, P., Nelson, D.M., van Bennekom, A.J., DeMaster, D.J., Leynaert, A., Quéguiner, B. (1995). The silica cycle in the world ocean: A reestimate. Science, 268, 375-379.

Van Bennekom, A.J. (1996). Silica signals in the Southern Ocean. Wefer, G., Berger, W.H., Siedler, G., Webb, D.J. (Eds.) The South Atlantic. Springer-Verlag, Berlin, Heidelberg, New York, 345-354.

Van Bennekom, A.J., Jansen, J.H.F., van der Gaast, S.J., van Iperen, J.M., Pieters, J. (1989). Aluminium-rich opal: an intermediate in the preservation of biogenic silica in the Zaire (Congo) deep-sea fan. Deep-Sea Research I, 36, 173-190.

Van Bennekom, A.J., Buma, A.G.J., Nolting, R.F. (1991). Dissolved aluminium in the Weddell-Scotia Confluence and effect of Al on the dissolution kinetics of biogenic silica. Marine chemistry, 35, 423-434.

Van Beusekom, J.E.E. (1989). Wechselwirkungen zwischen gelöstem Aluminium und Phytoplankton in marinen Gewässern. PhD Thesis, University of Hamburg, Germany. 164p.

Van Beusekom, J.E.E., van Bennekom, J.A., Tréguer, P., Morvan, J. (1997). Aluminium and silicic acid in water and sediments of the Enderby and Crozet Basins. Deep-Sea Research II, 44, 987-1003.

Van Cappellen, P. (1996). Reactive surface area control of the dissolution kinetics of biogenic silica in deep-sea sediments. Chemical Geology, 132, 125-130.

Van Cappellen, P., Qiu, L. (1997). Biogenic silica dissolution in sediments of the Southern Ocean. II. Kinetics. Deep-Sea Research II, 44, 1129-1149.

Van Weering, T.C.E., Helder, W. and Schalk, P. (1997). Netherlands Indian Ocean Programme 1992-1993, first results and an introduction. Deep-Sea Research II, 44, 6-7, 1177-1193.

Veldhuis, M.J.W., Kraay, G.W., Van Bleijswijk, J.D.L. and Baars, M.A. (1997). Seasonal and spatial variability in phytoplankton biomass, productivity and growth in the northwestern Indian Ocean; the SW and NE monsoon, 1992-1993. Deep-Sea Research I, 44, 425-449.

Warren, B.A. (1987). Ancient and medieval records of the monsoon winds and currents of the Indian Ocean. In: Fein, J.S., Stephens, P.L. (Eds.) Monsoons, Wiley, New York, pp. 137-158.

Webster, P.J. (1987). The elementary monsoon. In: Fein, J.S., Stephens, P.L. (Eds.) Monsoons, Wiley, New York, pp. 3-32.

Xiao, J.L., An, Z.S., Liu, T.S., Inouchi, Y., Kumai, H., Yoshikawa, S., Kondo, Y. (1999). East Asian monsoon variation during the last 130,000 years: evidence from the Loess Plateau of central China and Lake Biwa of Japan, Quaternary Science Reviews, 18, 147-157.

Zimmerman, F. (1987). Monsoon in traditional culture. In: Fein, J.S., Stephens, P.L. (Eds.) Monsoons, Wiley, New York, pp. 51-76.

CHAPTER 2

Simultaneous dissolution of silica and aluminium: an accurate method to analyze biogenic silica in marine sediments.

Erica Koning, Eric Epping and Wim van Raaphorst

ABSTRACT

This study introduces an alkaline leaching technique for the simultaneous analysis of biogenic silica and aluminium in sediments. Measuring aluminium facilitates the discrimination between silica from the biogenic (BSi) and the non-biogenic fraction, because it originates almost solely from the lithogenic phase. The method was tested using fine-grained silicagel, standard clay minerals, artificial sediments, and natural samples ranging from fresh diatoms to aged sediment from different depositional settings. To determine the BSi content, 4 different models each describing the dissolution curves, but of increasing complexity, were applied and for each different type of sample the optimum model was selected on the basis of F-test statistics. For mixtures of silicagel and clay minerals, the contribution of Si from dissolution of the clay was negligible compared to Si from silicagel. For natural samples with high clay content, complex dissolution curves were observed and single-phase first order dissolution was exceptional. This deviation from 'ideal' behavior could only be recognized because of our high-resolution sampling, especially in the first 20 minutes of the experiment. For most of the samples, the distinction between biogenic silica and the silica originating from dissolution of clays could be made on the basis of reactivity constants and the Si/Al ratios of the dissolving phases calculated with the models. The method described here therefore presents an accurate method to analyze biogenic silica in marine sediments even with a relatively high clay mineral content.

This chapter has been submitted to Marine Chemistry

INTRODUCTION

Silicic acid is one of the major nutrients in the marine environment as it is utilized for structural purposes by diatoms, radiolaria, silicoflagellates and sponges to produce skeletal material composed of opal or biogenic silica (BSi). The skeletal remains of these organisms sink to the sediment, often as constituent of fecal pellets (Bathman et al., 1990; Nelson et al., 1996). Because the water column is undersaturated with respect to silicic acid (Hurd, 1973), siliceous particles dissolve during settling and only a small fraction of the original BSi reaches the sediment surface (Brzezinski and Nelson, 1995; Nelson et al., 1995; Tréguer et al., 1995). An additional fraction dissolves at the sediment-water interface and in surficial sediments, leaving only ~2.5% of the original BSi production to be buried in the sediment (Sayles et al, 1994; Koning et al, 1997). Nevertheless, the abundance of biogenic silica in deep-sea sediments reflects the general pattern of productivity of diatoms and other siliceous species in the overlying waters (Lisitzin, 1972; Broecker and Peng, 1982; Thunell et al., 1994). BSi therefore has potential as a proxy for paleoproductivity (Lyle et al., 1988; Mortlock et al., 1991), provided that the mechanisms controlling the cycle of production, dissolution and burial of silica in the modern ocean are understood. A prerequisite for studying the Si-cycle is a reliable method to quantify BSi in the water column, in sediment traps and in the sediment.

Several techniques have been employed to determine BSi, e.g. spectroscopy, X-ray diffraction after transformation to crystallite (Goldberg, 1958; Calvert, 1966), direct X-ray diffraction (Eisma and Van der Gaast, 1971) and normative calculation (Leinen, 1977). All these procedures have their limitations depending on the amount and source of biogenic silica and on the composition of the mineral matrix. Besides the techniques mentioned above, a number of alkaline leaching techniques have been applied (Hurd, 1973; Eggiman et al., 1980; DeMaster, 1981; Krausse et al., 1983; Mortlock and Froelich, 1989; Müller and Schneider, 1993; Gehlen and van Raaphorst, 1993; Ragueneau and Tréguer, 1994; Landén, 1996; Koning et al., 1997; Schlüter and Rickert, 1998; Kamatani and Oku, 2000), which presently are considered to be superior for marine sediments of various composition (DeMaster, 1981; Conley, 1998). Marine sediments, however, consist of a number of reactive silica fractions; a fraction of biogenic origin which is therefore called biogenic silica or biogenic opal, clay minerals, alumino silicates and quartz, which are all more or less susceptible to dissolution in alkaline solutions.

Dissolution of amorphous silica is a surface process that requires the presence of a catalyst. In the case of alkaline leaching, the catalyst is a hydroxyl ion that can be chemisorbed, thereby increasing the coordination number of a silicon atom at the amorphous silica surface to more than four and weakening the oxygen bonds to the underlying oxygen atoms (Iler, 1979). Upon the adsorption of OH, silicon is released into solution as a silicate ion, $Si(OH)_5^-$, which hydrolyzes to soluble silica, $Si(OH)_4$ once the pH falls below 11. In alkaline leaching procedures, either Na_2CO_3 or NaOH is used to supply the hydroxyl ion needed as a catalyst (Iler, 1979).

To distinguish between dissolving biogenic silica and the silica contribution from clay minerals, DeMaster (1981) applied a sequential leaching with samples taken after 1, 2, 3 and 5 hrs. His results showed that the diatoms are quantitatively

dissolved within 2 hr or less and that Si from clay minerals dissolves at a constant rate. DeMaster therefore concluded that the Si-dissolution from clay minerals occurred independently from the dissolution of BSi. Extrapolation of the linear 'clay dissolution line' to time zero would thus correct for the contribution of non-biogenic silica and gives the BSi content of the sample (Fig. 1).

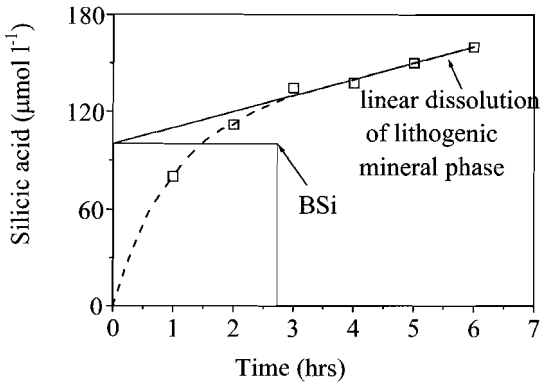

Fig 1: 'Ideal' dissolution curve for biogenic silica in sediments as proposed by DeMaster (1981). Extrapolation of the clay line to time zero would subtract the contribution of silica from the lithogenic fraction and would thus give the BSi content of the sample.

Mortlock and Froelich (1989) showed that for diatom-rich and clay-poor sediments a single 5hr extraction with 2M Na_2CO_3 could be as accurate a measure of biogenic silica as the sequential leaching procedure, although BSi concentrations below 2% were to be regarded with suspicion. In sandy opal-poor sediments from the North Sea, however, the single leach in 2M Na_2CO_3 overestimated the BSi content substantially (Gehlen and van Raaphorst, 1993). In all sequential leaching procedures, correction for the lithogenic mineral phase was made on the basis of a small number of samples, commonly 5 or 6, introducing considerable uncertainties in the intercept determined from extrapolating of the 'clay-line' (Conley, 1998). More importantly, this error is determined solely by the composition and quantity of the clay fraction in the sample and can thus be relatively large at low BSi contents. In 1993, Müller and Schneider applied an auto-analyzer system that allowed for continuous monitoring of the increase of the dissolved silica concentration in a 1M NaOH leaching solution. The almost continuous recording of the 'clay-dissolution line' improved the accuracy of BSi estimated from the extrapolated intercept.

Recently, Kamatani and Oku (2000) described a new approach to correct for the non-biogenic content of the sample. They estimated BSi through linear regression of the extracted SiO_2 plotted against extracted aluminium (Fig. 2).

In the continuous leaching method described in this study, dissolved silica and aluminium are measured simultaneously at 1-second intervals. Of these recorded measurements, a 6-second mean was calculated to reduce noise and to restrict the

number of data points. The remaining number of data points, typically in the order of 600-700, enables the application of analytical models that can adequately describe the often-complex dissolution curves to yield an objective estimate of the biogenic silica content of the sample.

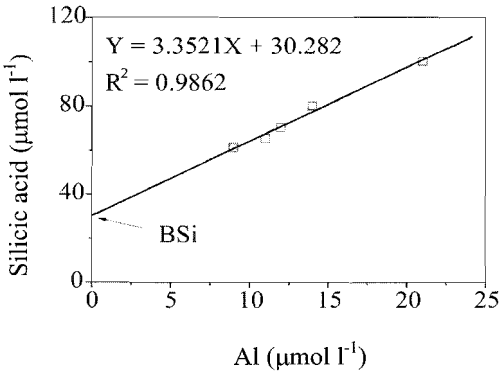

Fig 2: Plot of dissolved silica versus dissolved aluminium. Kamatani and Oku (2000) proposed that all aluminium was associated with the lithogenic fraction of the sample. Silica and aluminium dissolve at a constant ratio and extrapolating their linear relationship to time zero would subtract the contribution of silica from the lithogenic fraction and would thus give the BSi content of the sample.

Using artificial sediments and natural samples, we will evaluate the assumptions on which DeMaster (1981) based his sequential leaching technique, being the independent dissolution of a BSi fraction and a linearly dissolving clay fraction, and test whether the dissolution of Al can be used to better identify the contribution from the lithogenic fraction, as suggested by Kamatani and Oku (2000). We will show that high resolution sampling, especially in the first 20 minutes of an experiment, is essential to give an accurate estimate of BSi in sediments with low biogenic silica content.

MATERIALS AND METHODS

Description of the method

The experimental setup (Fig. 3) used in this study is a modification of the continuous leaching technique for biogenic silica described by Koning et al. (1997), that in turn was adapted from Müller and Schneider (1993). Samples were leached in 0.5M NaOH (pH=13.7) in a stainless steel vessel preheated to 85°C. If the sample was added before the leaching solution reached 85°C, initial dissolution was slow and a

sigmoidal dissolution curve was observed. A sample split was fed into a continuous flow analyzer (Skalar) and analyzed for silicic acid using the spectophotometric molybdate-blue method described by Grasshoff et al. (1983). A second sample was fed into a similar auto-analyzer system, to analyze the simultaneously dissolving aluminium as described by Hydes and Liss (1976). This method was developed for low aluminium concentrations as they occur in natural marine waters, but showed to be excellently suited for the analysis of dissolved aluminium during alkaline leaching. Before entering the auto-analyzer, the sample was acidified with HCl to neutralize the NaOH leaching solution. The neutralized sample stream was segmented by air bubbles to enhance mixing and buffered with a sodium acetate buffer at pH 5. As a final step, Lumogallion was added to form a fluorescence complex with Al^{3+}at 50°C for 5 minutes. Working standard solutions containing 17.8, 178, 356, 534, and 712 µmol Si l^{-1} were prepared for each batch of 0.5M sodium hydroxide leaching solution. Working standards for aluminium contain 10, 20, 30, 60, 100 and 130 µmol Al l^{-1}. Standard curves were measured frequently and showed excellent regressions (>0.999) and little variability in time. Both fluorescence and molybdate-blue adsorption were recorded digitally at one-second sampling resolution, with a typical leaching run-time of 60 to 90 minutes. A silica-aluminium spike was applied to determine the time lag of the Al channel compared to the Si channel.

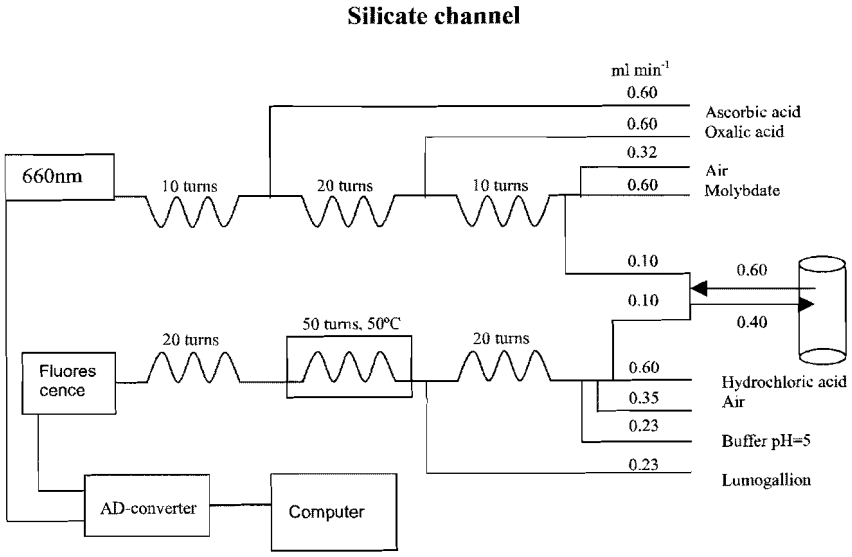

Fig. 3: A schematic view of the autoanalyzer system for the simultaneous measurement of silica and aluminium in solid samples.

Reagents

The reagents for the analysis of dissolved Si analysis were described in Müller and Schneider (1993) and Koning et al (1997). For the aluminium analysis, the following reagents were used.

Hydrochloric acid, 0.05 N. Approximately 82 ml of hydrochloric acid diluted to 5000 ml, with 5 ml of Brij (25% Brij 35 solution) as a surfactant. 0.6 ml min^{-1} of the hydrochloric acid should acidify 0.1ml min^{-1} of leaching solution to a pH of about 5.

Sodium Acetate buffer. For 1000 ml of sodium acetate buffer, 328 g sodium acetate was dissolved in 600 ml of distilled water and acetic acid (96%) added until pH=5.

Lumogallion stock solution contained 50 mg of Lumogallion in 250 ml of distilled water. A Lumogallion working solution was prepared daily by diluting 50 ml of Lumogallion stock solution with 50 ml of distilled water.

Aluminium Standard solutions. To prepare working standard solutions containing 10, 20, 30, 60, 100 and 130 µmol Al l^{-1} a commercial aluminium standard (Merck, concentration 1g l^{-1}) was diluted using the 0,5 N sodium hydroxide leaching solution as diluent.

Samples for testing the method

The combined BSi-Al leaching method was tested using a variety of samples. A fine-grained silicagel (Silicagel 60, 0.063-0,200mm, Merck) was used as an example of a pure silica phase. A range of silicagel weights was analyzed to test the linearity and reproducibility of the method. Since the dissolution of silica is a surface process, insufficient mixing could limit the transport of silicate and hydroxyl ions from and toward the solid surface thereby slowing down the dissolution process. The influence of mixing was studied at two stirring speeds and without stirring at all.

The standard clay minerals kaolinite (Kga-2, Warren County, Georgia, USA), illite (Fithian, Illinois, USA) and Na-montmorillonite (Swy-1, Crook County, Wyoming, USA) were measured to examine the dissolution behavior of pure clay mineral phases of increasing structural complexity. These minerals are primarily crystalline aluminium silicates with stacked-layer structures. Each unit layer in turn is a sandwich of tetrahedral (T) silica sheets, with a silicon atom surrounded by four oxygen atoms and octahedral (O) gibbsite sheets, consisting of two layers of oxygen atoms with aluminium atoms at the octahedral sites (Stumm and Morgan, 1981). Depending on the type of mineral, a unit layer consists of a two- or three-layer structure (T-O or T-O-T). In the three-layer minerals, isomorphous substitution of silicon or aluminium can change the basic Si/Al ratio. Kaolinite is a simple 2-layer clay mineral with a Si: Al ratio of 1. Thus, when kaolinite dissolves, a 1:1 ratio of Si and Al in the leaching solution is to be expected. Illite is a more complex three-layer clay mineral with an overall composition commonly given as $K_{2-x}Si_{6+x}Al_{2-x}$. Depending on x, Si/Al ratios will decrease from >>1, when the outer layers dissolve, to values between 2 and 1, when the contribution from the inner layer becomes important. Montmorillonite is a smectite, a three-layer clay mineral with minor substitutions of Al for Si in the tetrahedron sheet, thus having an overall Si/Al ratio

of 2. Analogous to illite, dissolution of montmorillonite would thus yield a Si/Al ratio that decreases from >>1 when the outer layers dissolve to 2 during the course of the experiment, when the contribution of aluminium from the inner layer becomes important.

Artificial sediments were prepared by mixing silicagel 60 with defined amounts of the standard clay minerals kaolinite, illite and montmorillonite. In addition to these artificial sediments, 12 natural samples were analyzed, including pure diatoms, marine suspended matter, sediment trap material, surface sediments and aged sediments from piston cores (Table 1).

Table 1: Characteristics of the natural marine samples used in this study.

Sample	Location	Characteristics	Reference
Bering Sea	Bering Sea	TPM from 0.1 l sea water	Broerse
Trap B3	Somali slope	Particulate matter	
Balgzand	Dutch Wadden Sea	Benthic diatom sample	
E.rex ooze	Southern Ocean	Diatom ooze	F. Sirocko
NIOP-1238	Somali slope	Sediment, 100,000BP	
Beach sand	Texel, North Sea	Sandy sediment	
AB 13	Angola Basin	Surface sediment	Van Bennekom
AB 19	Angola Basin	Surface sediment	Van Bennekom
AB 25	Angola Basin	Surface sediment	Van Bennekom
IM 99-6	Iberian Margin	Surface sediment	Epping, 2001
IM 99-12	Nazaré canyon	Surface sediment	Epping, 2001
IM 98-12	Iberian Margin	Surface sediment	Epping, 2001

Quantitative analysis of BSi

To allow for an accurate estimate of the reactive silica fraction in the sample, analytical models were used to describe the increase of the dissolved silica concentration during dissolution. The most simple dissolution curve versus time is that of a single reactive silica phase showing first order dissolution. Since the reactive

silica in natural marine samples from the water column and from the sediment is assumed to have a biogenic origin, we will further refer to this reactive silica as biogenic silica, or BSi.
In the case of a single BSi phase, the simultaneous dissolution curves of BSi and aluminium can be described by:

$$\frac{d[BSi]}{dt} = -k[BSi] \quad (1)$$

$$[BSi] = [BSi]_0 e^{-kt} \quad (2)$$

$$Si_{aq} = [BSi]_0 * \left(1 - e^{-kt}\right) \quad (3)$$

Similarly,

$$Al_{aq} = \frac{1}{\beta_1} * [BSi]_0 * \left(1 - e^{-kt}\right) \quad (4)$$

Here, Si_{aq} and Al_{aq} are the concentrations of dissolved silica and aluminium, in μmol l^{-1}, in the reaction vessel at time t (min), $[BSi]_0$ is the initial biogenic silica in μmol l^{-1}present in the vessel, equivalent to the equilibrium concentration of Si_{aq}, k is the reactivity constant (min^{-1}) and β_1 is the atomic Si/Al ratio for the reactive silica fraction.
When dissolving clays (CSi) are present, the dissolution of this fraction can be described as a linear function:

$$\frac{dCSi}{dt} = -b. \quad (5)$$

These rate formulations result in:

Model 1:

$$Si_{aq} = [BSi]_0 * \left(1 - e^{-kt}\right) + bt \quad (6)$$

$$Al_{aq} = \frac{1}{\beta_1} * [BSi]_0 * \left(1 - e^{-kt}\right) + \frac{1}{\beta_{lin}} bt \quad (7)$$

Here, b is the slope of the linear part of the dissolution curve, equivalent to the constant dissolution rate of CSi from the clay minerals (μmol l^{-1} min^{-1}) and β_{lin} is the Si/Al ratio in the lithogenic fraction.
Natural sediment samples may consist of a mixture of types of reactive biogenic silica, deposited at different times and each modified by diagenetic processes.

Assuming that each separate reactive silica fraction shows first order dissolution, the increase of the silicic acid concentration in the reaction vessel with time can be described as the sum of these n first order processes. We have applied this model with n=2 and 3 (models 2 and 3, respectively).

Model 2 and 3:

$$Si_{aq} = \sum_{i=1}^{n} [BSi]_{0,i} \left(1 - e^{-k_i t}\right) + bt \tag{8}$$

$$Al_{aq} = \sum_{i=1}^{n} \frac{1}{\beta_i} [BSi]_{0,i} \left(1 - e^{-k_i t}\right) + \frac{1}{\beta_{lin}} bt \tag{9}$$

$[BSi]_{0,i}$ is the initial biogenic silica present in reactive silica fraction i, k_i is the reactivity constant and β_i is the Si/Al ratio for fraction i.
For an infinite number of fractions i, the time courses of Si and Al with time can be described with a reactive continuum model, based on a γ-distribution of reactivities (Boudreau and Ruddick, 1991; Postma, 1993, as described in Koning et al., 1997).

Model 4:

$$Si_{aq} = [BSi]_0 * \left[1 - \left(\frac{\alpha}{\alpha + t}\right)^{\nu}\right] + bt \tag{10}$$

$$Al_{aq} = \frac{1}{\beta_1} [BSi]_0 * \left[1 - \left(\frac{\alpha}{\alpha + t}\right)^{\nu}\right] + \frac{1}{\beta_{lin}} bt \tag{11}$$

The parameter α measures the average lifetime of the reactive components in the mixture and ν is a non-dimensional parameter solely related to the shape of the Gamma distribution curve. The apparent rate constant K_m for the mixture is given by

$$K_m = \frac{\nu}{\alpha ([BSi]_0)^{1/\nu}} \tag{12}$$

and the apparent order of the reaction is $1+(1/\nu)$ (Postma, 1993). Although this equation is based on the heterogeneity of reactive surfaces, it is equivalent to the power model that may be derived when assuming a decreasing dissolution rate over time (Tarutis, 1993), e.g. due to aging.

For each type of sample, the fit results from the various models were compared in a one-tailed F-test (Sokal and Rohlf, 1995) to evaluate whether the more complex model provided a significantly better description of the data. If adding extra complexity did not significantly improve the fit, the simpler model was applied.

RESULTS

Silicagel

Silicagel 60 showed first order dissolution, with a rapid increase in the concentration of silicic acid during the first 5 minutes of the experiment until the equilibrium concentration, $[BSi]_0$, was reached (Fig. 4).

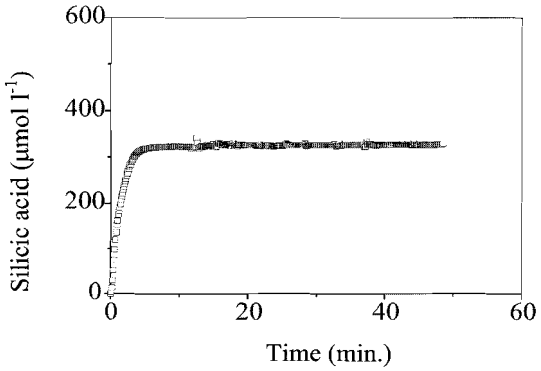

Fig 4: First order dissolution curve as recorded for an artificial fine-grained silicagel.

For pre-dried silicagel samples, 'apparent BSi' yield was 95.3± 3.2%, independent of stirring speed (Fig. 5), but initial dissolution was slower when the solution was not stirred at all.

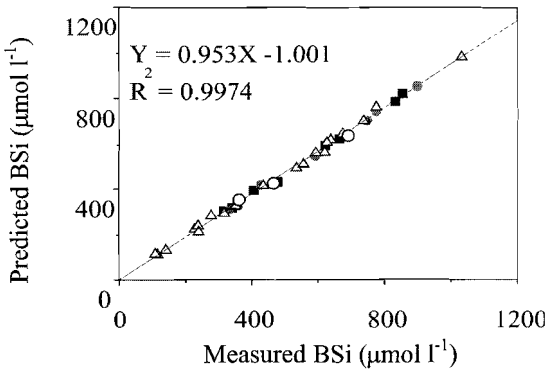

Fig 5: Yield for silicagel measured at different stirring speeds. Open triangles represent samples analyzed at intermediate stirring speed, black squares at high stirring speed and open circles represent samples measured without stirring.

Model 1 proved to be the optimum model to describe the silicagel dissolution curves. The calculated model parameters for the optimum model are given in Table 2. Minor quantities of Al, possibly related to impurities in the silicagel were leached together with the reactive Si (Si/Al = 391).

Clay minerals

The standard clay minerals, kaolinite, illite and montmorillonite, were analyzed as examples of well-defined mineral phases of increasing complexity (Fig. 6).

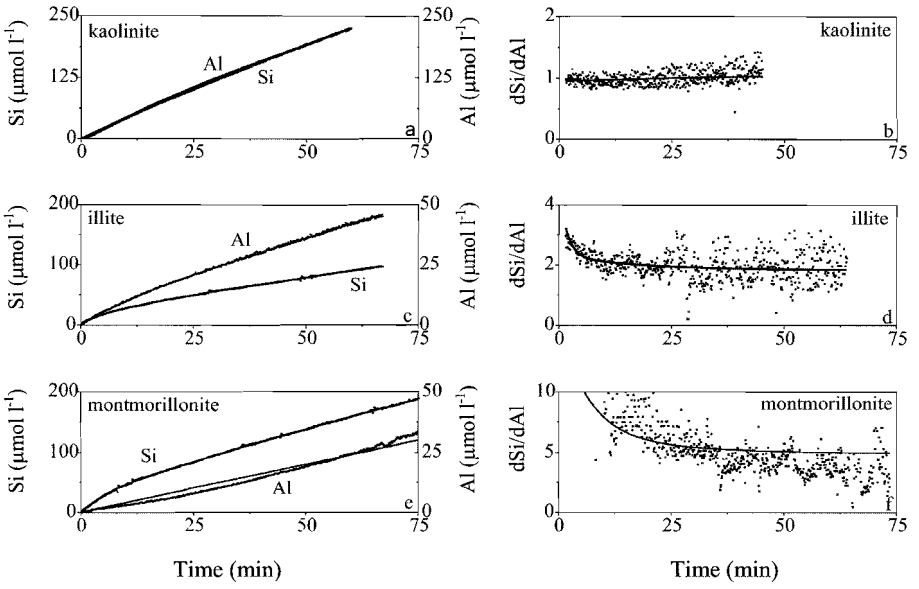

Fig 6: Time courses of the dissolution of silica and aluminium for the standard clay minerals kaolinite, illite and montmorillonite (left panels) and the change of the Si/Al ratio with time for the same clay minerals (right panels). Dots are measured data, solid lines indicate model fits to the dissolution curves.

Of these three clay minerals only the dissolution curves for kaolinite showed a linear increase with time of both silicic acid and dissolved aluminium (Fig. 6a). Fig. 6b shows the dSi/dAl ratio with time, representing the Si/Al ratio of the actually dissolving solid phase. For the kaolinite sample, the dSi/dAl ratio was close to 1 for the entire experiment. Nevertheless, the outcome of model 1 yielded an initial reactive Si fraction with a Si/Al ratio (β_1) of 0.71, suggesting some excess Al compared to Si during the first minutes of leaching, and $\beta_{lin} \approx 1$, the theoretical value for kaolinite (Table 2). The calculated 'apparent BSi' is 0.79% (Table 3), but the β_1 value for this

Table 2: Fit parameters as obtained by modeling of the dissolution curves, using the optimum model for the silicagel, the standard clay minerals and the artificial sediments described in this study.

Sample	Optimum model	BSi_1 ($\mu mol\ l^{-1}$)	BSi_2 ($\mu mol\ l^{-1}$)	k_1 (min^{-1})	K_2 (min^{-1})	b ($\mu mol\ l^{-1}\ min^{-1}$)	β_1	β_2	β_{lin}
Silicagel	1	325	-	0.74	-	0	391	-	-
Kaolinite	1	36.7	-	0.03	-	3.24	0.71	-	1.07
Illite	2	18.7	6.4	0.63	0.081	1.07	28.8	2.7	1.85
Montmorillonite	2	28.3	17.5	0.15	0.028	1.92	>1000	>1000	4.8
Silicagel + kaolinite	1	425	-	0.46	-	3.16	274	-	1.00
Silicagel + illite	2	352	27.7	0.69	0.034	0.98	554	2.33	1.88
Silicagel + montmorillonite	1	426	-	0.51	-	1.66	>1000	-	6.55
Silicagel + kaolinite + montmorillonite	2	128	15.7	0.31	0.02	2.71	384	28	1.98
Silicagel + illite + montmorillonite	2	83	40.4	0.62	0.02	1.17	381	7.42	2.71
Silicagel + illite + montmorillonite	2	66	38.2	0.42	0.02	2.04	392	5.17	4.39

fraction, being almost identical to β_{lin}, confirms the non-biogenic origin (Table 2). For illite and montmorillonite, concentrations of dissolved silica and aluminium did not show a linear increase with time. For these clay minerals, model 2 provided the optimum fit (Table 2). Leaching of excess silica was evident during the first five minutes of the illite dissolution curve (Fig. 6c), illustrated by a β_1 value of 28.8 and dSi/dAl ratios that were > 3 in the early phase of the incubation and slowly decreased to 2 as dissolution continued (Fig. 6d). The β_2 value for illite approximated β_{lin} and BSi_2 could thus be attributed to dissolution of the clay fraction (Table 2). Apparent BSi of the illite calculated from BSi_1 was 0.48% (Table 3). The montmorillonite dissolution curve illustrates the structural complexity of this clay mineral. Considering the theoretical Si/Al ratio of 2, excess Si was released in the first minutes of the experiment whereas in later stages (t >30 min) excess aluminium was released (Fig. 6e). The initial excess of Si is reflected in β_1 and β_2 values >1000 and in the dSi/dAl ratio that decreased from >20 at the start of the experiment to about 3 after 50 minutes and continued to decrease further due to the increasing excess release of aluminium compared to silica (Table 2; Fig. 6f). Apparent BSi for montmorillonite calculated from BSi_1 + BSi_2 was 1.15% (Table 3). For all clay minerals, BSi_1 is >0, indicating an initial apparent BSi phase, but each clay mineral has a distinct signature in β values. For kaolinite, β_1 equaled β_{lin}, indicating that the apparent BSi had a clay origin. For illite, β_1 is 28, and $\beta_2 = \beta_{lin}$. For montmorillonite the very slow initial dissolution of Al was reflected in very high β_1 and β_2 values (>1000). The release of Al during dissolution was kaolinite >> illite >> montmorillonite (Table 3).

Artificial sediments

The time courses of silicic acid and aluminium resulting from the dissolution of the artificial mixtures are presented in Fig 7. For all mixtures, the silica dissolution curves showed a rapid increase in silicic acid concentration during the early phase of the experiment when the silicagel dissolved, followed by a slow increase due to dissolution of the clay mineral. The aluminium dissolution curves were distinct for the three mixtures and similar to those for the pure clay minerals. The silicagel-kaolinite mixture showed a linear increase in dissolved Al with time (Fig. 7a). The dSi/dAl ratio of the dissolving solid phase decreased from 22, when the silicagel dissolved, to 1, the predicted value for pure kaolinite (Fig. 7b). Model 1 gave the optimum fit for the silicagel-kaolinite mixture, indicating that the initial non-linear increase in silicic acid observed in the pure kaolinite sample was obscured in the silicagel-kaolinite mixture. The apparent BSi measured for the silicagel-kaolinite mixture was 11.75%, only 0.32% lower than predicted for this mixture (Table 3). For the silicagel-illite mixture the dissolved aluminium concentration increased rapidly in the first 10 minutes, followed by a slower increase as dissolution continued (Fig. 7c). For this sample, dSi/dAl ratios decreased from values >50 in the first few minutes to 2, the theoretical Si/Al ratio for illite (Fig. 7d). Model 2 provided the optimum fit for the silicagel-illite mixtures. The β values calculated for BSi_1 and BSi_2 reflect the origin of these fractions, β_1=380, as found for pure silicagel, while β_2 (2.33) and β_{lin} (1.88) resemble the β_2 and β_{lin} values found for pure illite (Table 2). The apparent BSi calculated for the silicagel-illite mixture was 8.21%, an insignificant 0.1% higher than

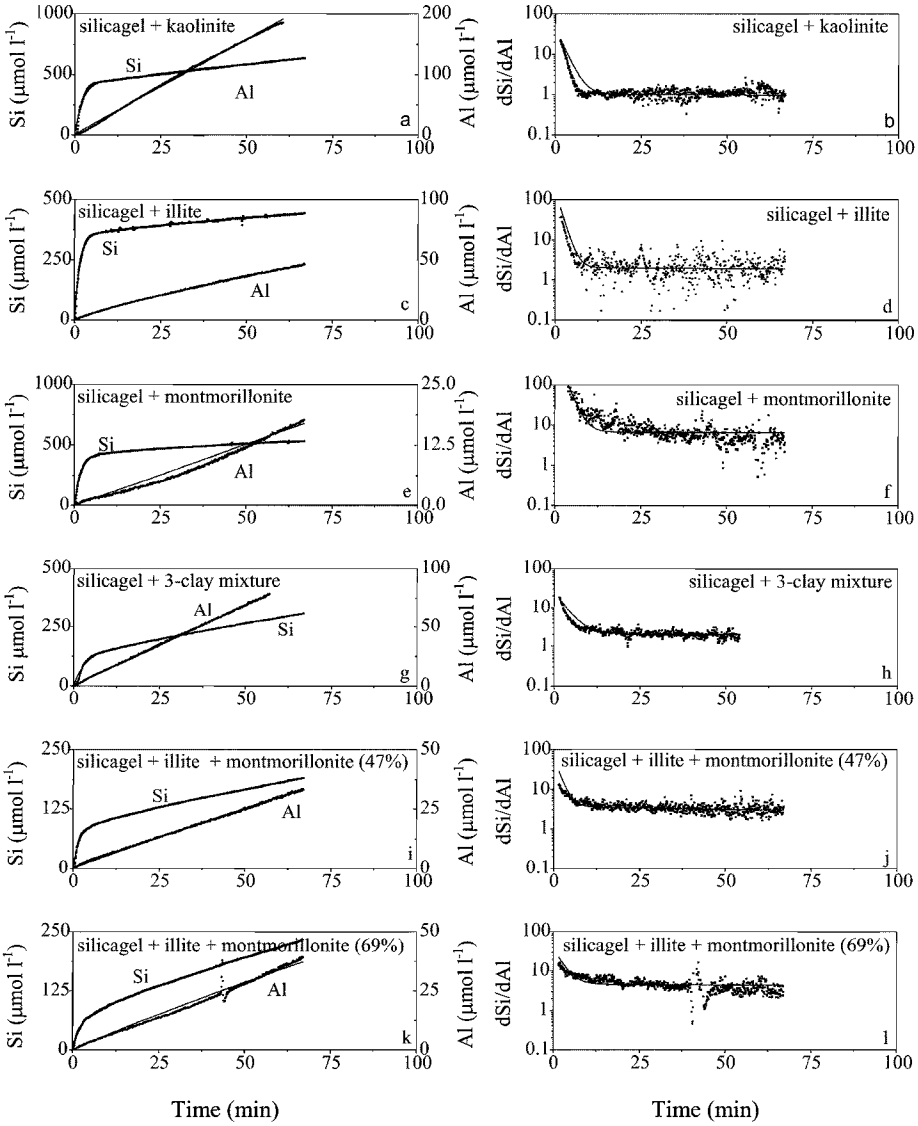

Fig. 7: Time courses of the dissolution of silica and aluminium for mixtures of silicagel with kaolinite, illite and montmorillonite (left panels) and the change of the Si/Al ratio with time for the same clay minerals (right panels). Dots are measured data, solid lines indicate model fits to the dissolution curves.

predicted for this mixture (Table 3). The Al dissolution curve for the silicagel-montmorillonite sample showed an increasing rate of Al release (Fig. 7e) as observed previously for the pure montmorillonite sample. The delayed release of aluminium is reflected in the dSi/dAl ratios that decrease from >100 in the early phase of

Table 3: Contributions of BSi and Al from the separate fractions as calculated from the model parameters (tables 2 and 5).

Sample	Solid-solution Ratio (mg $100ml^{-1}$)	Predicted BSi_1 (%)	BSi_1 (%)	BSi_2 (%)	Al_1 (%)	Al_2 (%)
Silicagel	2	95.3	95.3	-	0.110	-
Kaolinite	27.81	0	0.79	-	0.499	-
Illite	23.64	0	0.48	0.16	0.007	0.027
Montmorillonite	23.88	0	0.71	0.44	0.003	0.0002
Silicagel + Kaolinite	2.75 18.97	12.07	11.75	-	0.122	-
Silicagel + Illite	2.19 23.59	8.10	8.21	0.704	0.079	0.136
Silicagel + Montmorillonite	2.79 20.42	11.46	11.03	-	0.041	-
Silicagel + Kaolinite + Illite + Montmorillonite	0.81 8.78 17.28 12.94	1.94	1.90	0.24	0.111	0.004
Silicagel + Illite + Montmorillonite	0.51 10.36 9.48	2.40	2.44	1.22	0.115	0.074
Silicagel + Illite + Montmorillonite	0.41 8.58 20.2	1.34	1.37	0.80	0.111	0.070
Balgzand	4.1	-	88.4	-	0.040	-
Trap B3	45.3	-	27.1	-	0.162	-
E.rex ooze	6.22	-	87.3	-	0.137	-
NIOP- 1238	21.21	-	6.8	-	0.041	-
Beach sand	215.4	-	0.03	0.01	0.002	0.0005
AB-13	18.5	-	5.2	2.54	0.150	0.248
AB-19	21.0	-	4.8	2.98	0.195	0.267
AB-25	27.8	-	2.1	3.2	0.146	0.684
IM 99-6	44.2	-	0.14	0.41	0.010	0.102
IM 99-12	41.7	-	0.57	0.95	0.049	0.153
IM 98-12	77.0	-	0.04	0.13	0.006	0.038

dissolution, to <5 at the end of the experiment after 65 minutes (Fig. 7f). Although model 1 gave the optimum fit for the silicagel-montmorillonite mixture, the model could not fit to the Al data correctly because of the continuously decreasing dSi/dAl ratio (Fig. 7f). Calculated apparent BSi for the silicagel-montmorillonite mixture was 11.03%, a value close to the predicted apparent BSi (11.46%), despite the poor fit of the Al data (Table 3).

To create an artificial mixture representative of natural sediments, where the lithogenic phase often consists of a mixture of clay minerals, artificial silicagel-kaolinite-illite-montmorillonite and silicagel-illite-montmorillonite mixtures were analyzed (Figs. 7g-j). The release of Al during leaching is higher for the silicagel-3 clay mixture than for the mixture of silicagel-illite-montmorillonite due to the presence of kaolinite (Figs. 7g, i). Constant dSi/dAl ratios were reached after approximately 10 minutes and are consistent with the weighed average of the β_{lin} values observed for the separate clay minerals (Figs. 7h, j). If the sample contained 70% montmorillonite, 29% illite and only 1.4% silicagel, the increasing release of Al during leaching of montmorillonite was evident (Fig. 7k), but even for this sample the difference between measured apparent BSi and predicted apparent BSi was negligible. For these silicagel-clay mixtures, measured apparent BSi equaled predicted apparent BSi (Table 3), indicating that our procedure is suitable to correct for the contribution of BSi from the lithogenic phase even if this phase contains >95% clay.

Silicagel-illite mixtures with a silicagel content ranging from 0.09 to 8.10% were measured to test the applicability of the method for samples with low apparent BSi and high clay content (Fig. 8).

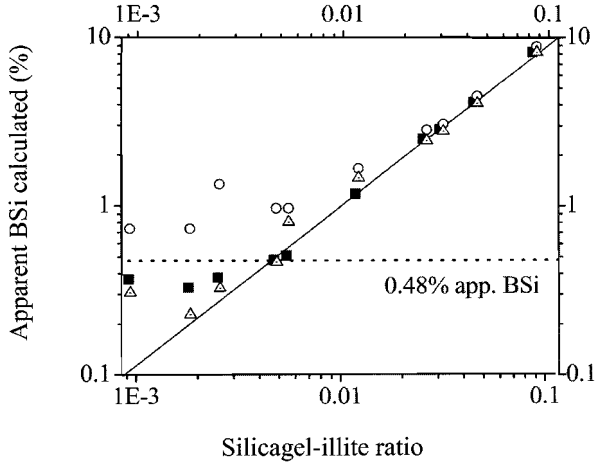

Fig. 8: Calculated BSi versus silicagel content for silicagel-illite mixtures, following the method described in this study (solid squares) and the procedures as proposed by DeMaster (1981, open circles) and Kamatani and Oku (2000, open triangles). The diagonal line represents apparent BSi from the silicagel only. The horizontal dotted line represents the apparent BSi content found for pure illite.

The diagonal line in the plot represents predicted apparent BSi from the silicagel and the horizontal dotted line is 0.48% BSi, the apparent BSi_i of pure illite. For all mixtures model 2 provided the optimum fit and 2 apparent BSi fractions could be recognized (Table 4). For mixtures with a silicagel content >0.48%, measured apparent BSi equaled predicted apparent BSi from the silicagel, but for the silicagel-illite samples with lower silicagel content (0.25, 0.17 and 0.09% silicagel respectively), estimated apparent BSi was too high due the contribution from the clay (Table 4). Accurate estimates of low apparent BSi content (<0.25%) could be obtained for mixtures with an apparent BSi/illite ratio >0.0048 (Table 4).

Natural sediments

Dissolution curves for the natural marine samples are given in Figs. 9 and 10. Sample numbers and characteristics of the sediments are given in Table 1 and calculated model parameters are given in Tables 3 and 5.

Fresh diatoms - For samples consisting mainly of relatively fresh diatoms, like the Bering Sea sample (fig. 9a), Balgzand tidal flat sample (fig. 9b) and the Trap B3 sample (fig. 9c), the equilibrium silicic acid concentrations were reached in less than 20 minutes. For Trap B3 and the Balgzand sample, model 1 gave the optimum fit,

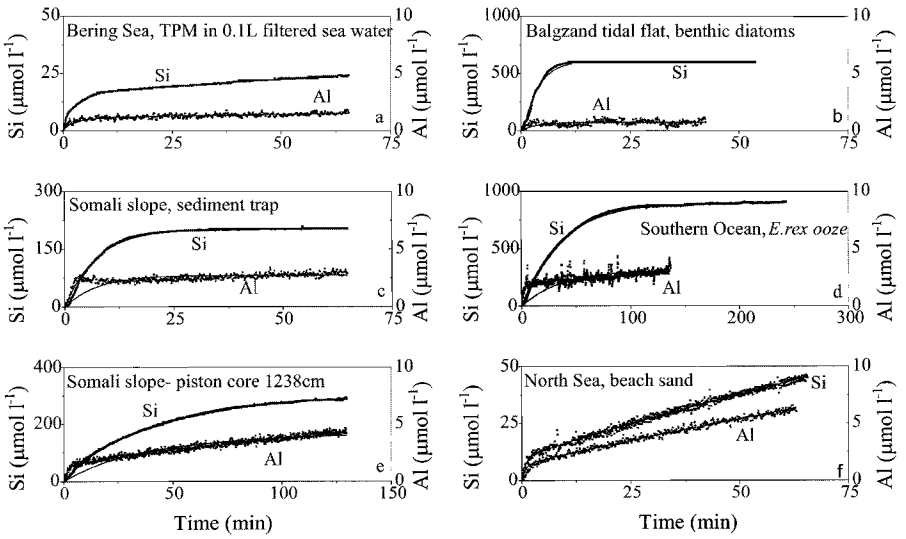

Fig 9: Time courses of the dissolution of silica and aluminium for particulate matter from the Bering Sea (a), a diatom sample from the Balgzand tidal flat (b), sediment trap B3 from the Somali slope (c), *Ethmodiscus rex* diatom ooze from the Southern Ocean (d), piston core sample NIOP-1238 from the Somali slope (e) and a beach sand sample from Texel, North Sea (f). Dots are measured data, solid lines indicate model fits to the dissolution curves.

Table 4: Sample weight, predicted and measured apparent BSi and fit parameters for the silicagel-illite mixtures.

Silicagel (mg)	Illite (mg)	Forams + Sand (mg)	Predicted BSi (%)	Measured BSi (%)	BSi_1 ($\mu mol\ l^{-1}$)	BSi_2 ($\mu mol\ l^{-1}$)	k_1 (min^{-1})	k_2 (min^{-1})	β_1	β_2
2.19	23.59	-	8.10	8.21	352	27.7	0.69	0.03	554	2.33
0.92	19.54	-	4.28	4.13	140.6	12.8	0.71	0.02	76	1.07
0.65	20.18	-	2.97	2.84	98.5	7.61	0.47	0.07	49	2.96
0.41	15.33	-	2.48	2.49	65.3	8.79	0.42	0.03	140	1.18
0.25	20.16	-	1.17	1.18	40.0	16.9	0.76	0.45	341	4.08
0.20	34.93	-	0.54	0.51	30.1	26.5	0.70	0.12	892	5.4
0.15	30.55	-	0.47	0.48	24.5	25.0	0.81	0.09	77	2.39
0.27	101.28	-	0.25	0.39	65.4	163.3	0.35	0.02	60	2.01
0.08	49.35	-	0.17	0.35	28.6	32.4	0.23	0.03	4.7	2.7
0.09	98.05	-	0.09	0.37	60.2	61.4	0.25	0.04	9.6	2.73
0.33	36.46	200.42	0.14	0.17	68.4	255.5	0.35	0.01	30.2	4.1
0.27	45.50	157.78	0.13	0.18	62.1	372.8	0.34	0.01	22.7	3.9

suggesting a single reactive BSi fraction, and b=0, indicating that the samples contained no Si-releasing lithogenic fraction (Table 5). Measured BSi was 27.1% for trap B3 and 88.4% for the Balgzand sample, with negligible amounts of aluminium present in this BSi (Table 3). For the Bering Sea sample, model 2 provided the optimum fit, suggesting two reactive BSi fractions. Both BSi_1 and BSi_2 appear to be of biogenic origin, as indicated by the high k values and the β values that do not support a lithogenic origin (Table 5).

Aged sediments – NIOP-1238, a 100,000 year-old sediment from the Indian Ocean and the Pleistocene *Ethmodiscus rex* ooze from the Southern Ocean are examples of aged BSi and these samples were therefore expected to be less susceptible to dissolution than fresh diatom samples. Indeed, dissolution of these aged sediment samples was considerably slower than dissolution of fresh diatoms, and ~100 minutes were required to dissolve the biogenic fraction completely (Figs. 9 d, e). This difference in reactivity is confirmed by the reactivity constants (k) obtained by modeling of the data curves (Table 5). The reactivity constants k for the fresh samples from the Balgzand tidal flat, trap B3 and the Bering Sea are one order of magnitude higher than those for NIOP-1238 and *E. rex* ooze (Table 5). For the *E.rex* ooze, model 1 gave the optimum fit, suggesting one reactive BSi fraction, and b=0, indicating that this sample contained no Si-releasing lithogenic fraction (Table 5). Measured BSi for the *E.rex* ooze was 87.3% (Table 3). For NIOP-1238 the continuum model (model 4) gave the optimum fit (Table 5). Although a non-biogenic Si-releasing phase was present ($b \neq 0$), this phase most likely did not originate from clays, as indicated by β_{lin} = 48 (Table 5). For NIOP-1238, a BSI content of 6.8% was measured, with minor amounts of aluminium present in the BSi (Table 3). Fig. 9f finally shows a sandy sediment sample from the beach of the island of Texel (North Sea) that represents the lower limit of the method presented in this study (0.04% BSi, Table 3). Model 2 gave the best fit for this beach sand, indicating two reactive BSi fractions and a lithogenic phase, but the similar β values calculated for these fractions suggest that they originate from the same source (Table 5).

Surface sediments - Dissolution curves for 6 sediment samples from the Angola Basin (AB-13, AB-19 and AB-25) and the Iberian Margin (IM 99-6, IM 99-12 and IM 98-12) are given in fig. 10. The samples from the Angola Basin showed a rapid initial increase in both Si and Al (Figs. 10a, c, e), and after 20-40 minutes, a more or less constant dSi/dAl ratio of about 2, representing the lithogenic fraction, was reached (Figs. 10b, d, f). The optimum fit for the samples from the Angola Basin was provided by model 2, suggesting the presence of two different BSi fractions. The β values for samples AB-13 (β_1=15.7; β_2=4.6) and AB-19 (β_1=11; β_2=5) are distinctly higher than the β_{lin} values observed for these samples (1.90 and 1.97 respectively), and the BSi_1 and BSi_2 fractions were therefore both considered to be of biogenic origin. For sample AB-25, $\beta_2 \approx \beta_{lin}$, indicating that this BSi_2 fraction is most likely of lithogenic origin (Table 5). BSi content was 7.7% for AB-13, 7.8% for AB-19 and 2.1% for AB-25 (Table 3).

Samples from the Iberian Margin have a low biogenic silica content that is reflected in the minor initial increase in silicic acid concentration during leaching. The

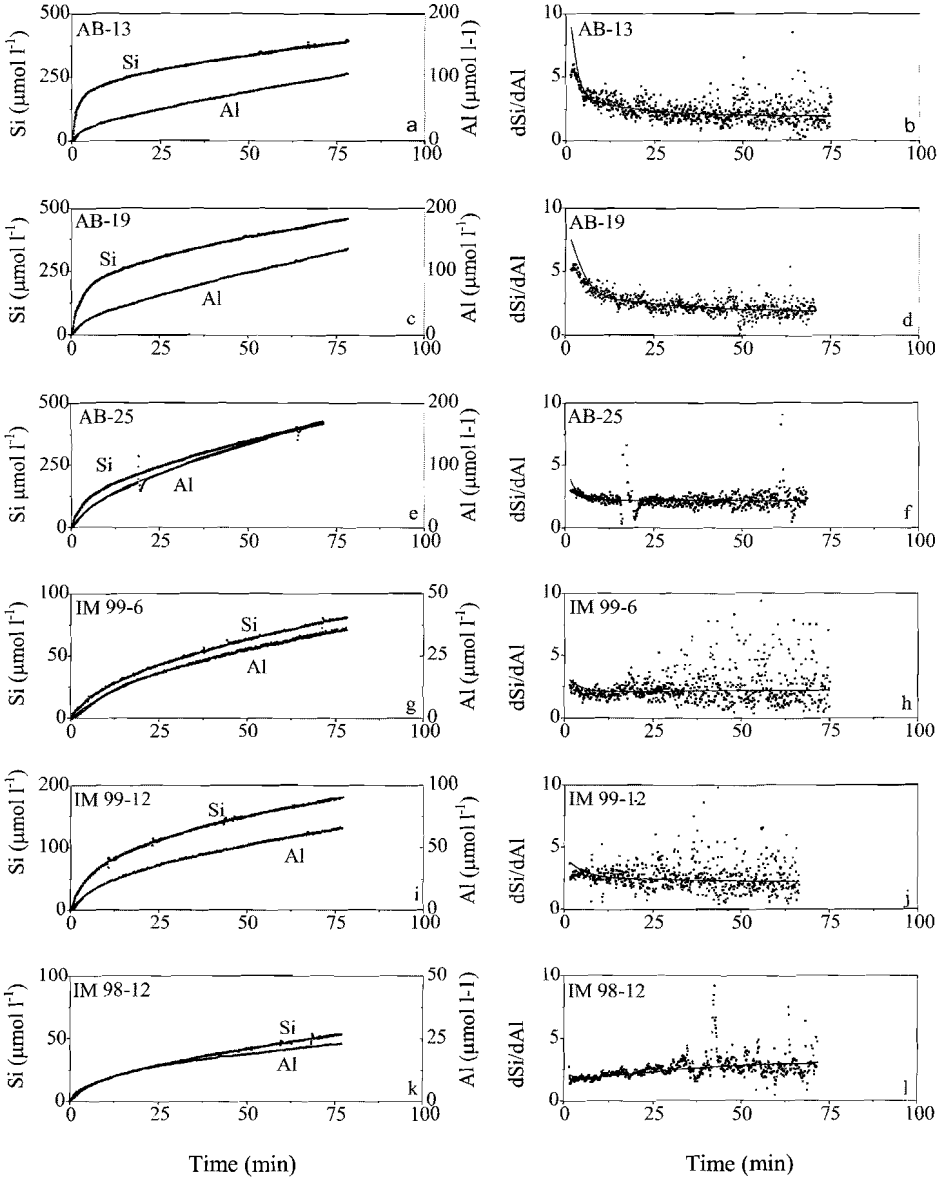

Fig 10: Time courses of the dissolution of silica and aluminium for sediments from the Angola Basin (a, c and e) and the Iberian Margin (g, i and k) and the change of the Si/Al ratio with time for these sediments (right panels). Dots are measured data, solid lines indicate model fits to the dissolution curves.

Table 5: Fit parameters as obtained by modelingof the dissolution curves using the optimum model for the natural marine samples described in this study.

Sample	Optimum model	BSi_1 ($\mu mol\ l^{-1}$)	BSi_2 ($\mu mol\ l^{-1}$)	k_1 (min^{-1})	k_2 (min^{-1})	b ($\mu mol\ l^{-1}\ min^{-1}$)	β_1	β_2	β_{lin}	α	ν	K_m
Bering Sea	2	3.8	12.4	1.99	0.28	0.12	6.97	25.4	16.9	-	-	-
Trap B3	1	204	-	0.133	-	0	75.2	-	-	-	-	-
Balgzand	1	603	-	0.29	-	0	>1000	-	-	-	-	-
NIOP-1238	4	241	-	-	-	0.49	75	-	48	181	6.3	0.008
E.rex ooze	1	904	-	0.027	-	0	287	-	-	-	-	-
Beach sand	2	10	3.5	1.22	0.05	0.49	7.2	9.2	6.9	-	-	-
AB-13	2	161	78.1	0.72	0.08	1.95	15.7	4.6	1.97	-	-	-
AB-19	2	167	104	0.42	0.05	2.41	11	5	1.9	-	-	-
AB-25	2	95	148	0.36	0.03	2.7	6.3	2.1	2.15	-	-	-
IM 99-6	2	10.3	30.1	0.20	0.04	0.54	6.4	1.8	2.34	-	-	-
IM 99-12	2	39.5	66.2	0.33	0.05	0.99	5.2	2.8	2.23	-	-	-
IM 98-12	2	5.2	16.3	0.61	0.07	0.42	2.8	1.5	3.11	-	-	-

dSi/dAl ratios for samples IM 99-6 and IM 99-12 reach constant values after approximately 25 minutes (Figs. 10h, j). For IM 98-12, Si and Al appear to be released at a constant 2:1 ratio during the entire experiment, suggesting that dissolution of clays dominated this sample (Fig. 10L). Model 2 gave the optimum fit for the samples for the Iberian Margin, with β_1 values of 6.4 and 5.2 for samples IM 99-6 and IM 99-12, respectively (Table 3). The values of β_2 and β_{lin} are about equal for these samples, again suggesting that the BSi_2 fraction is of lithogenic origin. For sample IM 98-12, $\beta_1 \approx \beta_2 \approx \beta_{lin}$, confirming that the silicic acid released during leaching is of lithogenic origin. For the samples from the Iberian Margin model 4, the continuum model gave excellent fits, with lower residuals than model 2, but with unrealistically high BSi_0 values of 20% (Fig. 11a).

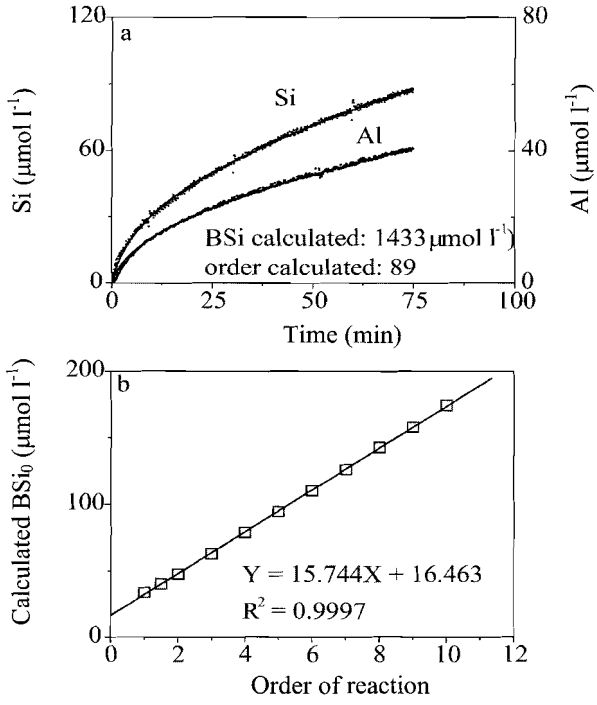

Fig. 11: The unrealistic BSi values calculated when the continuum model (Boudreau and Ruddick, 1991) was applied to the dissolution of sample IM 99-6 from the Iberian Margin (11a) and the relationship between the order of continuum fit with BSi calculated for IM 99-6 (11b).

Using model 4, the values calculated for β_1 and β_{lin} were 2.27 and 2.01, respectively, suggesting that all silicic acid released during leaching originates from the clay fraction of the sample and that a BSi content of 20% is unrealistic.

Apparently, BSi_1 and the order of the reaction could not be estimated independently for the Iberian Margin samples (Fig. 11b), indicating that model 4 could not be used to give an accurate estimate of the BSi content of these samples.

For the samples from the Angola Basin and Iberian Margin, BSi was calculated following our approach and the procedures suggested by DeMaster (1981) and Kamatani (2000). Compared to our approach, DeMaster's procedure gives consistently higher estimates of BSi, while Kamatani's approach underestimates the BSi content (Fig. 12).

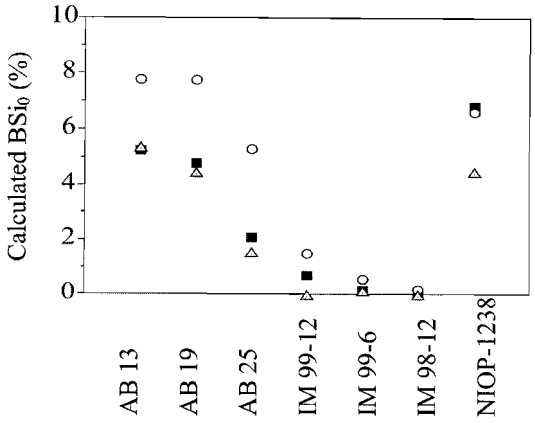

Fig. 12: BSi content for natural samples from the Angola Basin and Iberian Margin, following the method described in this study (solid squares) and the procedures as proposed by DeMaster (1981, open circles) and Kamatani and Oku (2000, open triangles). Note the slightly negative estimates obtained by the method of Kamatani and Oku (2000) for IM 99-12 and IM 98-12.

DISCUSSION

In this study biogenic silica was determined by the continuous measurement of both dissolved silica and aluminium during alkaline leaching. Simultaneously measuring dissolved Si and dissolved Al provides an extra parameter by which the contribution of silica from clays and the biogenic fraction in complex samples, like those from the Iberian Margin and the Angola Basin, could be separated. Since diatoms generally contain virtually no aluminium, almost all aluminium released during the course of a leaching experiment can be attributed to dissolution of the clay fraction (Kamatani and Oku, 2000). The validity of this assumption was tested using fine-grained silicagel as a highly reactive silica phase that contained no aluminium, and the standard clay minerals kaolinite, illite and montmorillonite as 'biogenic silica free' lithogenic alumino-silicates.

Silicagel - The fine-grained silicagel showed perfect first order dissolution with a rapid increase in dissolved silica until the equilibrium concentration was reached. The method showed a linear response in final silicic acid concentrations with increasing sample weights of silicagel, up to a maximum of 1000µmol/l. This is equivalent to 6mg pure SiO_2 in 100ml of leaching solution, concentrations that were never reached in our experiments with natural samples (Fig. 5). Because only one reactive fraction is present in this sample and virtually no aluminium, the sequential leaching as proposed by DeMaster (1981) will give equally accurate results.

Clay minerals - Of the three standard clay minerals, only kaolinite showed dissolution curves with almost no initial excess Si or Al and a constant dSi/dAl ratio as dissolution continued which are consistent with its theoretical crystal structure. The increasing complexity of illite and montmorillonite is illustrated by their dissolution curves. Our results show that illite and montmorillonite do not dissolve at constant Si/Al ratios. Furthermore, montmorillonite samples are notoriously impure, i.e. contaminated with other minerals, and often do not have a homogeneous composition (Dr. K. Nagy, pers. comm.). In all clay minerals, a rapidly dissolving apparent BSi fraction is present. Extrapolating the clay line to time zero or the aluminium versus silica relationship to zero-aluminium concentration for these samples would thus erroneously result in an apparent BSi content of these purely lithogenic phases. However, following our approach part of this apparent BSi can be correctly attributed to the lithogenic phase.

Artificial sediments - Dissolution behavior of the mixtures of silicagel with the clay minerals depended on the type of clay mineral. As expected from the dissolution curves observed for the pure clay minerals, only the mixture of silicagel with kaolinite showed the dissolution curve as hypothesized by DeMaster (1981), with rapid dissolution of the reactive silica fraction and a slow linear dissolution of the mineral phase at a Si/Al ratio of ~1. However, not all clay minerals appeared to dissolve at a constant dSi/dAl ratio, in which case the extrapolation of the aluminium versus silica relationship to zero-aluminium concentration would result in an erroneous estimate of the BSi content of the sample.

For the silicagel-illite mixture two reactive apparent BSi fractions were present that could be distinguished by their distinctly different β_1 and β_2 values (Table 2). Apparently, the BSi fraction and the lithogenic fraction did dissolve independently, as suggested by DeMaster (1981). However, the contribution made by the BSi_2 fraction to the proposed linear extrapolation would result in an overestimate of the true BSi content of this sample. The simultaneous measurement of aluminium, however, provides a tool to correct for the contribution of apparent BSi (BSi_2) from the clay mineral by means of its distinctly different k values and β values (Table 4).

The contribution of apparent BSi from clay minerals would be more substantial for samples with low BSi content. To test the applicability of the method for samples with very low BSi and with high clay content, silicagel-illite mixtures (0.09 to 8.1% silicagel) were measured (Fig. 8). For silicagel-illite mixtures at ratios larger than 1:200, the apparent BSi agreed well with that predicted for silicagel only (Table 5). At lower silicagel ratios, the BSi_1 and BSi_2 fractions can still be distinguished based on their k and β values, but measured BSi increasingly exceeds

the predicted value. For these mixtures, the aluminium versus silica relationship to zero-aluminium concentration (Kamatani and Oku, 2000) would give similar results (Fig. 8), but extrapolating the clay line to time zero (DeMaster, 1989) would result in an overestimate of BSi, because both BSi_1 and BSi_2 would erroneously be attributed to the silicagel (Fig. 8).

To simulate natural sediments that will often consist of a mixture of clay minerals, silicagel-kaolinite-illite-montmorillonite and silicagel-illite-montmorillonite mixtures were analyzed. The β values calculated for BSi_1 and BSi_2 reflected the origin of these fractions and allowed us to separate the contribution of the lithogenic phase from the silicagel, resulting in measured apparent BSi values that agreed excellently with the predicted apparent BSi. At very high montmorillonite contents (>70%) our models could not fit to the aluminium data properly, because of the continuously decreasing dSi/dAl ratios. Yet, the difference between predicted and measured apparent BSi is negligible (Table 4). Sediments with a montmorillonite content >70% are restricted to the Equatorial Pacific (Griffin et al., 1968) and these sediments mostly have BSi contents of more than 10% (Broecker and Peng, 1982).

Natural samples- Natural sediments consist of a mixture of biogenic silica phases with different rates of dissolution and a mixture of mineral phases. In the samples from the water column (Bering Sea, Somali slope), the diatom from the Balgzand tidal flat and the sediments from the Indian and Southern Oceans, the concentration of clay was low, and consequently, the contribution of BSi from non-biogenic fractions was of minor importance. For this type of natural sample, with low aluminium content, a simple 1-point sampling procedure (Mortlock and Froelich, 1989) would give adequate results. High Si/Al ratios are to be expected for fresh BSi, because limited amounts of aluminium, <0.8%, can be incorporated by diatoms during growth (van Beusekom, 1989). In the sediments, however, Si/Al ratios can be lowered during early diagenesis of BSi, due to incorporation of aluminium (van Bennekom et al., 1989; Dixit et al., 2001). Nevertheless, high Si/Al ratios would still be expected for the *E. rex* ooze from the Southern Ocean and NIOP-1238 from the Indian Ocean, areas without major sources of aluminium input. The method proposed by DeMaster (1981) is well suited for this type of sample, but extrapolating Si versus Al to zero aluminium results in an underestimate of BSi, because the dissolving lithogenic phase has a low aluminium content (Fig. 8b). The suspended matter sample from the Bering Sea and the beach sand sample from the North Sea represent the lower limit of the method (0.04%) and illustrate that very low amounts of BSi can be analyzed accurately provided that clay minerals are absent from the sample.

The samples from the Angola Basin and Iberian Margin released considerable amounts of aluminium in the course of the dissolution experiments, indicating that the contribution from the lithogenic phase is important in this type of sediment. Compared to the fresh diatom samples and the aged sediments, β values in BSi from the Angola Basin and the Iberian Margin are low, suggesting a relatively high aluminium content of BSi in these sediments (Table 3). AB-25, collected within the outflow of the aluminium-rich plume of the Congo river, shows the most prominent initial aluminium increase (Fig 9e) and lowest Si/Al ratios (Fig. 9f, table 3) in the initial stage of dissolution. Diatom frustules from the Angola Basin sediments show a relatively high aluminium content upon early diagenesis, with Al/Si ratios up to 0.16

(van Bennekom et al, 1989), which is consistent with the β values observed for our samples (Table 3). Low β values were also found for BSi from the Iberian Margin, but for these samples, we have no information on the aluminium content of the diatom frustules that may confirm our results. The BSi_1 fractions in IM 99-6 and IM 99-12 were attributed to a biogenic origin based on the k1 and β1 values. Although IM 99-6 contained only 0.14% BSi, the BSi/clay ratio is 0.0069, higher than the critical value of 0.0048, suggesting that BSi could be calculated accurately. The β values were about equal for all fractions in IM 98-12, suggesting that this sample contained no BSi of biogenic origin. For the Angola Basin and Iberian Margin sediments, extrapolating the clay dissolution line to time zero as proposed by DeMaster (1981) would however result in an overestimate of BSi, because BSi_2 would erroneously be attributed to the biogenic phase (Fig. 12). Extrapolating the aluminium versus silica relationship to zero-aluminium concentration as proposed by Kamatani and Oku (2000) would yield an underestimate of BSi (Fig. 12), and even negative values for IM 99-12 and IM 98-12, due to the changing dSi/dAl ratios during leaching.

We conclude that for natural sediments with low BSi and high clay content, simultaneous measurement of silicic acid and aluminium is essential because it allows to distinguish between BSi-releasing fractions by their reactivity (k) and Si/Al ratios (β). The method can be applied for very low BSi contents, <0.5%, if the BSi:clay ratio of the sample is larger than 0.005.

CONCLUSIONS

In this study, we have shown that simultaneously measured aluminium can be used to correct for the Si contribution from dissolving clay minerals in silicagel-clay mixtures and in natural sediment samples with low BSi and high clay content. Based on the reactivity constants and Si/Al ratios calculated for the BSi fractions in the sample, fractions of lithogenic origin can be distinguished from the biogenic silica fraction. All standard clay minerals contained an apparent BSi phase and most sediment samples did not dissolve at constant Si/Al ratios, indicating that plotting Si versus Al or extrapolation of a 'linear' clay line to time zero may result in erroneous estimates of the BSi content of samples of unknown lithogenic composition. The method described in this study is suitable both for samples with a very low biogenic silica content, 0.052%, when the clay content of the sample is low, as well as for and for pure diatom samples. For samples with low BSi and high clay content, the k and β values for the BSi fraction in the sample can be used to determine if the BSi is of biogenic or of lithogenic origin.

ACKNOWLEDGEMENTS

The samples analyzed in this study were recovered during cruises with R.V. Tyro (Angola Basin and Somali slope samples) and R.V. Pelagia (Iberian Margin samples). The *Ethmodiscus rex* sample from the Southern Ocean was kindly provided by Dr. F. Sirocko, to Anne de Vreeze. Sandra Broerse (SOC, Southampton) provided the sample from the Bering Sea. We are grateful to Dr. Kathryn Nagy, University of Colorado, Boulder, who informed us on the dissolution behavior of clay minerals.
This is publication number 3619 from the Netherlands Institute for Sea Research.

REFERENCES

Bathman, U.V., Noji, T.T., von Bodungen, B. (1990). Copepod grazing potential in late winter in the Norwegian Sea- a factor in the control of spring bloom development? Marine Ecology Progress Series, 60, 225-233.

Boudreau, B.P., Ruddick, B.R. (1991). On a reactive continuum representation of organic matter diagenesis. American Journal of Science, 291, 507-538.

Brzezinski, M.A., Nelson, D.M. (1995). The annual silica cycle in the Sargasso Sea near Bermuda. Deep-Sea Research I, 42, 1215-1237.

Broecker, W.S., Peng, T.-H. (1982). Tracers in the sea, Eldigio Palisades, New York. 690pp.

Calvert, S.E. (1966). Accumulation of diatomaceous silica in the sediments of the Gulf of California. Geological Society of America Bulletin, 77, 569-596.

Conley, D. J. (1998). An interlaboratory comparison for the measurement of biogenic silica in sediments. Marine Chemistry, 63, 39-48.

DeMaster, D.J. (1981). The supply and accumulation of silica in the marine environment. Geochimica et Cosmochimica Acta, 45, 1715-1732.

Dixit, S., Van Cappellen, P., van Bennekom, A.J. (2001). Processes controlling the solubility of biogenic silica and pore water build-up of silicic acid in marine sediments. Marine Chemistry, 73, 333-352.

Eggimann, D.W., Manheim, F.T., Betzer, P.R. (1980). Dissolution and analysis of amorphous silica in marine sediments. Journal of Sedimentary Petrologists, 50, 215-225.

Eisma, D., van der Gaast, S.J. (1971). Determination of opal on marine sediments by X-ray diffraction. Netherlands Journal of Sea Research, 5, 382—389.

Gehlen, M., van Raaphorst, W. (1993). Early diagenesis of silica in sandy North Sea sediments: quantification of the solid phase. Marine Chemistry, 42, 71-83.

Goldberg, E.D. (1958). Determination of opal in marine sediments. Journal of Marine Research, 17, 178-182.

Grasshoff, K., Ehrhardt, M. Kremling, K. (Eds), (1983). Methods of seawater analysis. 2nd edition, Verlag Chemie, Winheim. 417pp.

Griffin, J.J., Windom, H., Goldberg, E.D. (1968). The distribution of clay minerals in the World Ocean. Deep-Sea Research I, 15, 433-459.

Hurd, D.C. (1973). Interactions of Biogenic opal sediment and sea water in the central equatorial Pacific. Geochimica et Cosmochimica Acta, 37, 2257-2282.

Hydes, D.J., Liss, P.S. (1976). Fluorimetric method for the determination of low concentrations of dissolved Aluminium in natural waters. Analyst, 10: 922-931.

Iler, R.K. (1979). The chemistry of silica. Wiley-Interscience, New York. 866 pp.

Kamatani, A., Oku, O. (2000). Measuring biogenic silica in marine sediments. Marine Chemistry, 68, 183-264.

Koning, E., Brummer, G.J.A., van Raaphorst, W., van Bennekom, A.J., Helder, W. van Iperen, J.M. (1997). Settling, dissolution and burial of biogenic silica in the sediments off Somalia (northwestern Indian Ocean). Deep-Sea Research II, 44, 1341-1360.

Krausse, G.L., Schelske, C.L. Davis, C.O. (1983). Comparison of three wet-alkaline methods of digestion of biogenic silica in water. Freshwater Biology, 13, 73-81.

Landén, A., Holby, O., Hall, P.O.J. (1996). Determination of biogenic silica in marine sediments- selection of pretreatment method and effect of sample size. Vatten, 52, 85-92.

Leinen, M. (1977). A normative calculation technique for determining opal in deep-sea sediments. Geochimica et Cosmochimica Acta, 41, 671-676.

Lisitzin, A.P. (1972). Sedimentation in the world ocean. Society of Economical Paleontologists and Mineralogists Special Publication, 17, 218p.

Lyle, M., Murray, D.W., Finney, B.P., Dymond, J., Robbins, J.M., Brooksforce, K. (1998). The record of late Pleistocene biogenic sedimentation in the eastern tropical Pacific Ocean. Paleoceanography, 3, 39-59.

Mortlock, R.A., Froelich, P.N. (1989). A simple method for the rapid determination of Biogenic opal in marine sediments. Deep-Sea Research I, 36, 1415-1426.

Mortlock, R.A., Charles, C.D., Froelich, P.N., Zibello, M.A., Saltzman, J., Hays, J.D., Burckle, L.H. (1991). Evidence for lower productivity in the Antarctic Ocean during the last glaciation. Nature, 351, 220-223.

Müller, P.J., Schneider, R. (1993). An automated method for the determination of opal in sediments and particulate matter. Deep Sea Research I, 40, 425-444.

Nelson, D.M., Tréguer, P., Brzezinski, M.A., Leynaert A., Quéguiner, B. (1995). Production and dissolution of biogenic silica in the ocean: Revised global estimates, comparison with regional data and relationship to biogenic silica sedimentation. Global Biogeochemical Cycles, 9, 359-372.

Ragueneau, O., Tréguer, P. (1994). Determination of biogenic silica in coastal waters: applicability and limits of the alkaline digestion method. Marine Chemistry, 45, 43-51.

Schlüter, M., Rickert, D. (1998). Effect of pH on the measurement of biogenic silica. Marine Chemistry, 63, 81-92.

Sokal, R., Rohlf, F.J. (1995). Biometry, the principals and practice of statistics in biological research, 3rd edition. Freeman, New York, 887 pp.

Stumm, W., Morgan, J.J. (1981). Aquatic chemistry, 3rd edition. Wiley-Interscience, New York, 780 pp.

Tarutis, W.J. (1993). On the equivalence of the power and reactive continuum models of organic matter diagenesis. Geochimica et Cosmochimica Acta, 57, 1349-1350.

Thunell, R.C., Pride, C.J., Tappa, E., Muller-Karger, F.E. (1994). Biogenic Silica fluxes and accumulation rates in the Gulf of California. Geology, 22, 303-306.

Tréguer, P., Nelson, D.M., van Bennekom, A.J., DeMaster, D.J., Leynaert, A., Quéguiner, B. (1995). The silica cycle in the world ocean: A reestimate. Science, 268, 375-379.

Van Bennekom, A.J., Jansen, J.H.F., van der Gaast, S.J., van Iperen, J.M., Pieters, J. (1989). Aluminium-rich opal: an intermediate in the preservation of biogenic silica in the Zaire (Congo) deep-sea fan. Deep-Sea Research I, 36, 173-190.

Van Beusekom, J.E.E. (1989). Wechselwirkungen zwischen gelöstem Aluminium und Phytoplankton in marinen Gewässern. PhD Thesis, University of Hamburg, Germany. 164p.

CHAPTER 3

Settling, dissolution and burial of biogenic silica in the sediments off Somalia (northwestern Indian Ocean).

Erica Koning, Geert-Jan A. Brummer, Wim van Raaphorst,
A. Johan van Bennekom, Willem Helder and Jolanda M. van Iperen

ABSTRACT

Particle fluxes of biogenic silica through the water column, silica burial fluxes into the sediments and the flux of dissolved silica across the sediment-water interface estimated from pore water profiles are used to assess the behavior of biogenic silica at two stations 80 and 270 kilometers offshore along a transect off the Somali coast in the north-western Indian Ocean. Particulate biogenic silica fluxes varied from 0.3 mmol m^{-2} day^{-1} in the non-upwelling season to 6 mmol m^{-2} day^{-1} during upwelling in the trap on the Somali slope. Fluxes were lower in the trap in the Somali basin; from 0.2 to 2.3 mmol m^{-2} day^{-1}. Evaluation of the dissolution curves derived by wet chemical leaching in sediment trap and sediment samples shows that the K_m values, the apparent reactivity rates in alkaline medium, are higher for the shallow sediment traps than for the deep trap and the boxcore sediments. Modeling of pore water profiles shows that in the sediment most dissolution occurs in the top half cm, and pore water effluxes are in close agreement with those from in-situ benthic incubations. Our results show that less than 10% of the biogenic silica arriving on the Somali Margin is buried in the sediments, giving a burial efficiency lower than the ~20% reported from the open Arabian Sea.

INTRODUCTION

The abundance of biogenic silica in deep-sea sediments reflects, in general, the pattern of productivity of diatoms and other siliceous species in the overlying

This chapter has been published in Deep-Sea Research II, 44, 1341-1360.

waters (Lisitzin, 1972; Thunell et al., 1994; Broecker and Peng, 1982). Sediments with a high biogenic silica content are found around the Antarctic continent, along the equatorial belt in the Pacific, off the African coast in the Atlantic and the coast of Peru in the Pacific, and in the northernmost Pacific. In all these regions, surface waters are characterized by high nutrient concentrations maintained by intense upwelling, causing high primary production (Broecker and Peng, 1982). However, since all ocean waters are undersaturated with respect to silica (Hurd, 1983), silica dissolves in the water column during settling of siliceous particles and only a small fraction of the initial production of biogenic silica is deposited and buried (Wollast and Mackenzie; 1983). About 75% of this dissolution is believed to take place in the upper water column above 1000m (Nelson et al., 1995; Brzezinski and Nelson, 1995; Tréguer et al., 1995; Gersonde and Wefer, 1987).

In the north-western Indian Ocean a situation similar to the coastal upwelling systems off West Africa and Peru is present during boreal summer when strong SW monsoon winds are generated by the formation of low atmospheric pressure over the Asian Plateau and high atmospheric pressure over the relatively cold southern subtropical Indian Ocean (Clemens et al., 1991; Brock et al., 1992). In contrast to the areas with high biogenic silica in the Atlantic, Pacific and Southern Oceans, where a large number of studies have been carried out on the fate of biogenic silica (DeMaster, 1981; Hurd, 1973; DeMaster et al., 1991; Jansen and van der Gaast, 1988; Bareille et al., 1991; Sayles et al., 1996), the north-western Indian Ocean, so far, has not been studied extensively. Although productivity is high in the Somali area, little biogenic silica is found in the sediments (Sirocko, 1989). As said before, the main part of the biogenic silica produced in the euphotic zone dissolves in the upper water column. Those particles that escape dissolution in the water column reach the sediment, where another part dissolves before the remainder is eventually buried. After burial, dissolution continues, giving rise to pore water silicic acid concentrations well above those in the overlying water. This concentration gradient results in an efflux of silicic acid across the sediment-water interface, thereby returning dissolved silica to the water column. For budget considerations, burial fluxes of biogenic silica in the sediment and pore water effluxes should balance the particulate flux that arrives at the sediment.

The aim of this study was to construct this budget for biogenic silica based on particle fluxes, sediment accumulation rates, pore water dissolution profiles and biogenic silica contents of the sediments for two sites on the Somali continental margin and to estimate the burial efficiency of biogenic silica to evaluate its use as an indicator for past siliceous productivity.

HYDROGRAPHIC SETTINGS

The Somali region of the northwestern Indian Ocean is strongly influenced by the SW monsoon, which blows from May to October. In May, when the monsoon starts, the strengthening of the northward current south of the equator and along the Somali coast results in the formation of 2 anticyclonic gyres, the southern gyre and

the Great Whirl, each bounded by a wedge of cold upwelled water. This two-gyre system, with strong upwelling at 5°N and 10°N, remains about stationary to mid-August (Fischer et al., 1996). In winter, the air over the Asian continent cools and the wind blows from NE to SW, the NE monsoon, and the Somali Current flows to the southeast. The seasonal reversal in the surface circulation of the Indian Ocean (Nair et al., 1989) results in strong differences between the oligotrophic period during the NE monsoon, when productivity is almost as low as that of the Sargasso Sea (Smith and Codispoti, 1980), and the SW monsoon, when upwelling of nutrient-rich waters induces high rates of primary production and makes the area one of the most productive of the world's oceans (Burkill et al., 1993). The intensity and extent of the monsoonal upwelling may vary widely on an annual basis (Smith, 1984; Smith and Codispoti, 1980; Hitchcock and Olson, 1992).

MATERIALS AND METHODS

All samples were obtained during the Netherlands Indian Ocean Program (NIOP, 1992-1993) at a transect off the Somali coast at 10°N (figs.1 and 2). The choice for the location of the transect was made based on a literature review, which a.o. showed relatively low current velocities at depth >800m suitable for deploying time-series sediment traps. Along the transect, two arrays of sediment traps were moored from June 1992 to February 1993. Array MST-8 was deployed on the Somali slope to record the sedimentation associated with coastal upwelling and sediment redistribution, whereas MST-9 was deployed in the deep Somali Basin outside the zone of coastal upwelling proper, as a pelagic reference site. Furthermore, 9 boxcores were taken along the transect and benthic landers were deployed at the sediment water interface below the traps (table 1).

Sediment traps

Particulate fluxes of biogenic silica settling towards the sea floor were intercepted by time-series sediment traps moored on the mid slope (MST-8B) and in the deep basin (MST-9G) at bottom depths of 1533m and 4047m, respectively (fig. 2). Array MST-8 included a Salzgitter/HDW "Kiel"-type trap with a baffled collecting area of 0.5 m^2 at 1265m depth (MST-8B), whereas array MST-9 contained a Technicap-PPS5 trap (MST-9G) with a baffled collecting area of 1.0 m^2 at 3047 m depth, i.e. 268 m and 1000 m above the sea floor, respectively. Both traps started sampling on June 7, 1992, in synchronized one- or two-week intervals until completion on February 14, 1993. Measured current velocities were lower than 15 cm sec^{-1}, although up to 20 cm sec^{-1} in rare instances, and inclinations were within 9° of the vertical, indicating that particle flux sampling was not seriously biased by hydromechanic interference throughout the deployment period (Brummer, 1995).

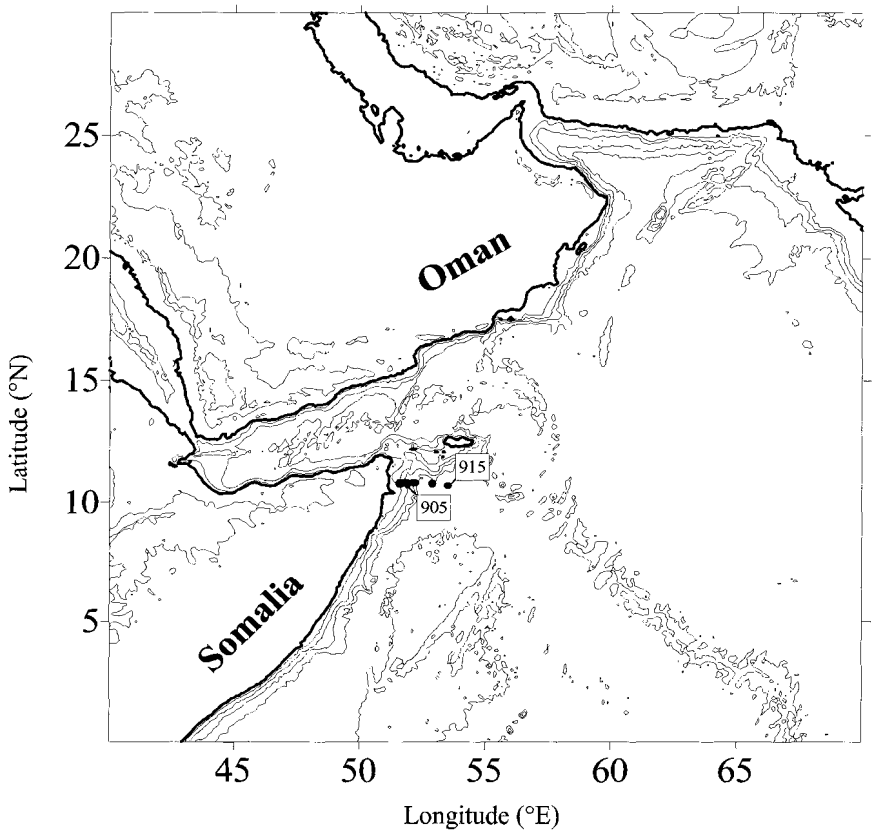

Fig. 1: The research area in the NW Indian Ocean with the location of the Somali transect.

Prior to deployment, the collecting cups were filled with a solution of 1.0 g l^{-1} of $HgCl_2$ (as a biocide), 9 g l^{-1} of $Na_2B_2O_7$ $(H2O)_{10}$ (to buffer at a pH of 8.8-8.9) and 0.05 g l^{-1} of CsCl (as a diffusion tracer) on sea water collected from the actual site and depth of deployment. After recovery, the supernatant solution of each cup was sampled for analysis of dissolved silica, and samples were stored at 4°C in the dark until further processing in the laboratory (for details, see Brummer, 1995). In the laboratory, the particulate residues were "swimmer"-picked and Folsom-splitted (average accuracy ±3.5%) using the original supernatant solution. Aliquots of the particulate residue were retained on pre-weighed 0.45µm cellulose acetate filters under a low vacuum, shortly rinsed with a small, known amount of cold milli-Q, and oven-dried at 55°C. After back-weighing, the retentate was separated from the filters and coarsely ground for biogenic silica analysis as outlined below. Particulate fluxes of biogenic silica were calculated from the concentrations of excess dissolved silica in the supernatant, the air humidity corrected total weights of multiple aliquots and the

weight percent biogenic silica. To cover the season not sampled by the traps (March to May), fluxes were interpolated between the first (mid June) and last (mid February) sampling periods. These interpolated fluxes were added to the measured fluxes to obtain estimates of the annual flux for each site.

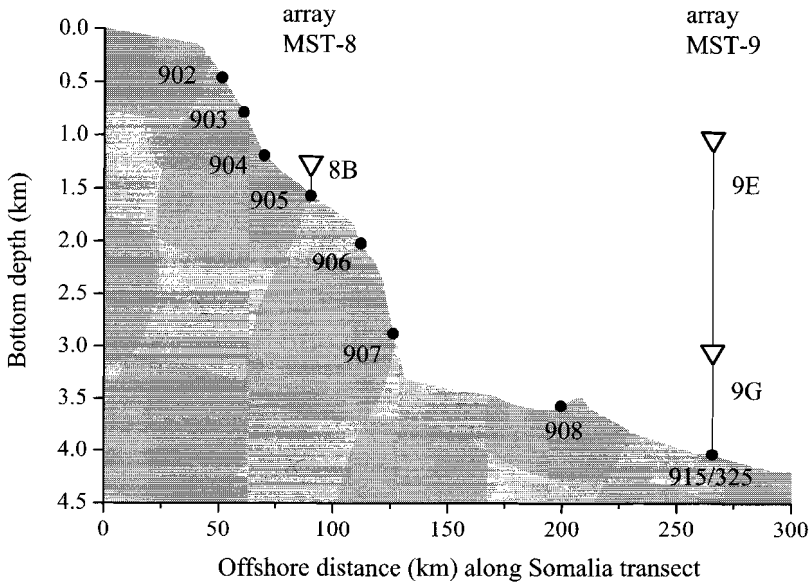

Fig. 2: Topography of the Somali transect and position of the sampling stations.

Boxcores

A 50 cm diameter cylindrical box corer was used which allowed for simultaneous, undisturbed sampling of bottom water and sediment. Immediately after retrieval the boxcores were sub- sampled on deck. Plastic liners of 6 cm diameter were inserted smoothly into the sediment, capped and immediately transported to the cold van maintained at bottom water temperature. From these subcores, pore water was obtained by extruding 0.5 - 2.0 cm sections in Reeburgh type squeezers under 2 - 3 bar of N_2- gas (Helder et al., 1995). Pore water samples were analyzed within 12 hours after retrieval of the boxcores for dissolved silica according to Strickland and Parsons on a Technicon TRAACS Auto-Analyzer. Coretop samples (0 - 0.25 cm) from all boxcores on the Somali transect were analyzed for biogenic silica. In addition, boxcores 905 and 915 were analyzed at regular downcore intervals for biogenic silica and $CaCO_3$.

Table 1: Station numbers, positions, water depth and station activities at the sampling site. For the sediment traps the deployment time in days is given.

station	latitude	longitude	depth (m)	boxcore	trap [days]	lander
902	10°46.8'N	51°34.6'E	565	X		
903	10°47.1'N	51°39.4'E	797	X		
904	10°47.6'N	51°46.3'E	1197	X		
905	10°46.9'N	51°56.4'E	1580	X	252	X
906	10°47.5'N	52°07.6'E	2171	X		
907	10°48.0'N	52°14.7'E	2896	X		
908	10°45.5'N	52°54.8'E	3596	X		
915	10°41.7'N	53°32.7'E	4059	X	252	X
325	10°41.0'N	53°32.7'E	4065	X		

For ^{14}C AMS dating of the boxcores, between 150 and 350 (0.07g.) large, well preserved shells of planktonic foraminifera were picked from the fraction >250μm. From the relative age difference between the top, 10cm and 25cm samples, the sediment accumulation rate was calculated. The sediment accumulation rate multiplied by the dry bulk density (dry weight/wet volume) gives the mass accumulation rate (MAR).

In-situ Benthic Chamber incubations

Both at stations 905 and 915, silicic acid fluxes across the sediment-water interface were measured on shipboard incubated cores and in-situ. For in-situ measurements a free-falling benthic bottom lander (BOLAS) was used (for a detailed description see Duineveld et al., in press; Tahey et al., 1995). Nutrient concentrations measured in water samples taken from the benthic chamber were used to calculate fluxes. For shipboard incubations, 31 cm diameter acrylic cores were inserted into a boxcore which still had the in-situ water on top. The incubations were sealed on top and incubated at in-situ temperature. At regular intervals (1 - 2 hours) water samples were taken from the overlying water to determine nutrient concentrations, which were used to calculate nutrient fluxes over the sediment-water interface .

Diatoms

Relative (% of autochthonous species) and absolute diatom abundances (ADA) and fluxes of autochthonous diatom species were calculated for all samples of sediment trap 8B, for selected samples of traps 9E and 9G, for coretop samples of boxcores 902, 905 and 915, and for samples 5, 10, 15, 20 and 25 cm downcore in

boxcore 905. For detailed description of the analytical methods see van Iperen et al. (1993).

Determination of biogenic silica

All sediment trap and sediment samples were analyzed for biogenic silica using a modified version of the automated wet chemical leaching method of Müller and Schneider (1993). In their procedure, biogenic silica is dissolved in 1 M NaOH in a stainless steel vessel at 85°C. The leaching solution is continuously fed into a Skalar Continuous Flow analyzer, chemicals are added and finally the solution is passed through a photocell where absorptions at 660 nm are recorded. In our modified version, 0.5 M NaOH is used to minimize dissolution of clay minerals. To improve the sensitivity of the silicic acid analysis, the Sulfuric acid and Molybdate solutions added separately by Müller and Schneider (1993) were replaced by one combined Sulfuric acid- Molybdate mixture, acidifying 0.5M NaOH to a pH of 2 at the time of the reaction of silicic acid with Molybdate instead of pH = 1.04 in the original procedure. This change in pH gave a two- to three-fold increase in absorptions, which is useful considering the low biogenic silica concentrations in sediments from our study area. Sample size was generally between 5 and 50 mg, depending on the biogenic silica content of the sample, and never exceeded 100mg. Measured biogenic

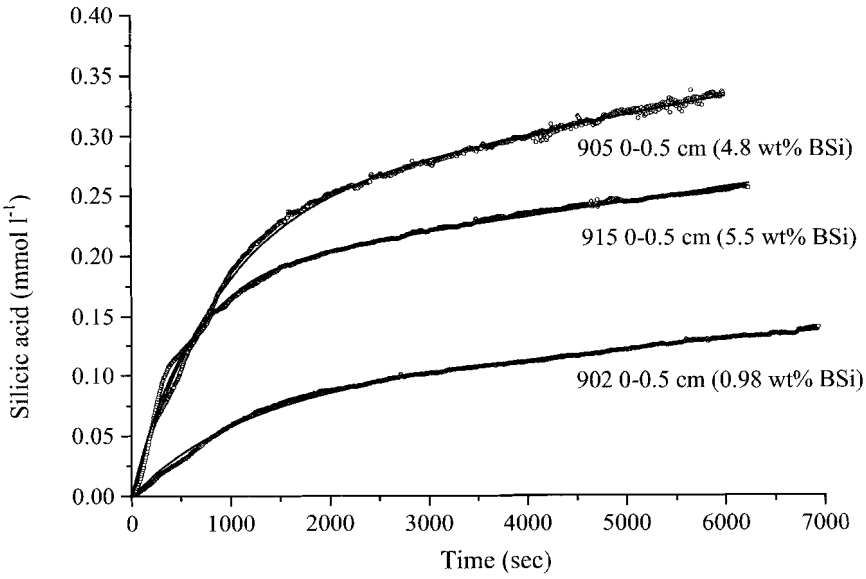

Fig. 3: Leaching curves for boxcores 902, 905 and 915. Open circles indicate measured data points, solid lines indicate fitted curves.

silica content of the sample was independent of sample size. To improve the data acquisition, the analyzer output was recorded digitally every second, with a typical sample run lasting for 1.5 to 2 hours. A six-second average was used for further calculations to reduce the number of datapoints and to dampen the influence of outliers and noise. A four-standard calibration curve was measured daily, and showed little or no change in slope over time.

Dissolution of biogenic silica from natural sediments in high pH leaching solutions normally slows down considerably after the first 15 minutes or so, which may be due to heterogeneity of the reactive sites or to aging of reactive surfaces during leaching (Van Cappellen, 1996). As a result, the slope of the curve representing the silica concentration in the leaching reagent decreases as leaching proceeds, until a more or less straight line is encountered, representing the slow dissolution of alumino silicates in the sample (DeMaster, 1981). To account for these processes, we applied the reactive continuum model of Boudreau and Ruddick (1991) to the non-linear part of the leaching curve. The model was originally developed for the degradation of organic matter, but has also been applied successfully to the dissolution of ferric oxides (Postma, 1993). Based on a Gamma distribution of surface reactivities the reactive continuum describes the total amount of biogenic silica left in the sample as a function of time:

$$BSi_{(t)} = BSi_{(0)} * \left[\frac{\alpha}{\alpha + t}\right]^{\nu} \qquad (1)$$

where $BSi_{(t)}$ is the amount of biogenic silica in the sample at time t in $mmol.l^{-1}$, $BSi_{(0)}$ is the amount of biogenic silica in the sample at time zero in $mmol.l^{-1}$, the parameter α measures the average lifetime of the more reactive components in the mixture and ν is a non-dimensional parameter solely related to the shape of the Gamma distribution curve. Although this equation is based on the heterogeneity of reactive surfaces, it is equivalent to the power model that may be derived when assuming a decreasing dissolution rate over time (Middelburg, 1989), e.g. due to aging. The rate of dissolution of the total biogenic silica is the derivative of eq (1) with respect to time,

$$\frac{dBSi}{dt} = -K_m (BSi_{(t)})^{1+1/\nu} \qquad (2)$$

The parameter K_m is apparent rate constant for the decay of the mixture and is equal to

$$K_m = \frac{\nu}{\alpha \left(BSi_{(0)}\right)^{\frac{1}{\nu}}} \qquad (3)$$

Taking into account the slow dissolution of silicic acid from clay minerals as a constant simultaneous and independent process (DeMaster, 1981), the reactive continuum model predicts that the concentration of silicic acid in the leaching solution changes according to:

$$M_{(t)} = BSi_{(0)} * \Gamma\left[1-\left(\frac{\alpha}{\alpha+t}\right)^{\nu}\right] + b * t \qquad \text{(model I)} \qquad (4)$$

Here, $M_{(t)}$ is the concentration of silicic acid present in the leaching solution at time t (mmol l^{-1}), $BSi_{(0)}$ the biogenic silica present in the sediment sample (%), Γ is the solid-solution ratio and b is the slope of linear part of the leaching curve that is attributed to the dissolution of clay minerals.
The order of the reaction is given by: 1+1/ ν. At high values of ν, 1/ ν approaches zero and the reaction is first order. In those cases, model I can be simplified to:

$$M_{(t)} = BSi_{(0)} * \Gamma\left[1-e^{-K_m t}\right] + b * t \qquad \text{(model II)} \qquad (5)$$

To calculate $BSi_{(0)}$, models I and II were fitted to the experimental data with the Microsoft Excel Solver routine, that minimizes the sum of the squares of residuals. Normally, between 600 and 1200 datapoints were fitted while changing 4 (model I) or 3 (model II) parameters. Examples of sediment leaching curves are given in Fig. 3.
From the measured biogenic silica weight percentages, the accumulation of biogenic silica in the sediment (BSi-AR) can be calculated by multiplying the mass accumulation rate with the biogenic silica weight percentage: BSi-AR = MAR * BSi wt% / 100.

Pore water fluxes

Pore water profiles were described with the steady state diffusion-first order dissolution model (e.g. Aller and Benninger, 1981; Schink et al., 1975):

$$0 = D_s \frac{\partial^2 C}{\partial z^2} + K_d (C_a - C) \qquad (6)$$

D_S is the molecular diffusion coefficient for silicic acid corrected for tortuosity according to Andrews and Bennett (1981):

$$D_s = \frac{D_0}{\phi F} \qquad (7)$$

D_0, the free solution molecular diffusion coefficient (Wollast and Garrels, 1971), was corrected for temperature using the Stokes-Einstein relation (Li and Gregory, 1974). ϕ is porosity and F the resistivity formation factor; z denotes depth in meters, K_d is the apparent first order rate constant for dissolution (d^{-1}) and C_a is the apparent saturation silicic acid concentration reached at depth in mmol.l^{-1}.

With boundary conditions $C_{(0)}= C_0$ and $C_{(\infty)} = C_a$, the solution for Equation 6 is:

$$C_{(z)} = (C_0 - C_a)e^{-\delta z} + C_a \tag{8}$$

where C_0 is the concentration of silicic acid at z=0 in mmol.l^{-1} and δ is $\sqrt{K_{Si} / D_{Si}}$ (m^{-1}).
Fluxes from the sediment follow from Fick's first law of diffusion:

$$J_{(sed)} = -\phi D_s \frac{\partial C}{\partial z} \tag{9}$$

Near the sediment-water interface, sediments are affected by physical processes occurring in the overlying water, like resuspension of particles by sudden increases in near-bottom flow velocity. Close to the sediment surface, velocity fluctuations, which give rise to turbulent diffusion, approach zero and molecular processes become quantitatively more important than turbulence. If rates of diagenetic reaction within the sediment are high, concentrations of dissolved species near the sediment-water interface may build up and bring about a rise in concentration within the diffusive sublayer above the value found for the overlying, well mixed water (Berner, 1980). In the deep ocean, the thickness of the diffusive boundary layer is about 1 mm; in shallow waters, it may be almost an order of magnitude smaller (Boudreau and Guinasso, 1980).
Although the diffusive sublayer (DBL) at the seafloor is very thin, it cannot be ignored when considering exchange of dissolved material between seawater and the sediment-pore water system. Silicic acid fluxes across the DBL can be described by:

$$J_{(dbl)} = -D_0 \frac{C_0 - C_w}{Z_{dbl}} \tag{10}$$

Here, C_W is the silicic acid concentration in the water overlying the sediment in mmol.l^{-1} and Z_{dbl} is the thickness of the Diffusive Boundary Layer in m. At z=0, assuming continuity, the flux across the DBL must be equal to the flux from the sediment. From this constraint, the concentration C_0 in equations 8 and 9 can be calculated as:

$$C_0 = \frac{C_b \phi \sqrt{K_d D_{Si}}\, e^{-\delta z} + C_w \frac{D_0}{Z_{dbl}}}{\frac{D_0}{Z_{dbl}} + \phi \sqrt{K_d D_{Si}}\, e^{-\delta z}} \tag{11}$$

Equations 8 and 11 were used to model all pore water profiles. Since the thickness of the DBL was unknown, a range of values for Z_{dbl} between 0 and 1 mm was used. For calculation of fluxes used for the mass balance, Z_{dbl} was fixed at 400 μm.

RESULTS

Sediment traps

Particulate fluxes were up to 6 mmol m^{-2} day^{-1} on the Somali slope during the SW Monsoon from June-October when coastal upwelling was intense and down to 0.3 mmol m^{-2} day^{-1} during the non-upwelling periods (fig. 4a). Substantially lower fluxes ranging from 2.5 to 0.2 mmol m^{-2} day^{-1}, respectively, were intercepted in the deep Somali basin further offshore (fig. 4b). Weight percentages of biogenic SiO_2 over the time series ranged from 9 to 33% on both trap sites, with highest values recorded during the SW Monsoon. The average K_m values, the reactivity rate constants in alkaline medium found when modeling the dissolution curves, were considerably higher for the relatively shallow trap on the slope than for the deeper trap in the basin (fig. 5). On an annual basis, the estimated particulate biogenic silica flux amounts to 0.85 mol m^{-2} $year^{-1}$ on the Somali slope and 0.32 mol m^{-2} $year^{-1}$ in the Somali basin which amounts to 16.4wt% and 20.8wt% of the total particulate flux respectively.

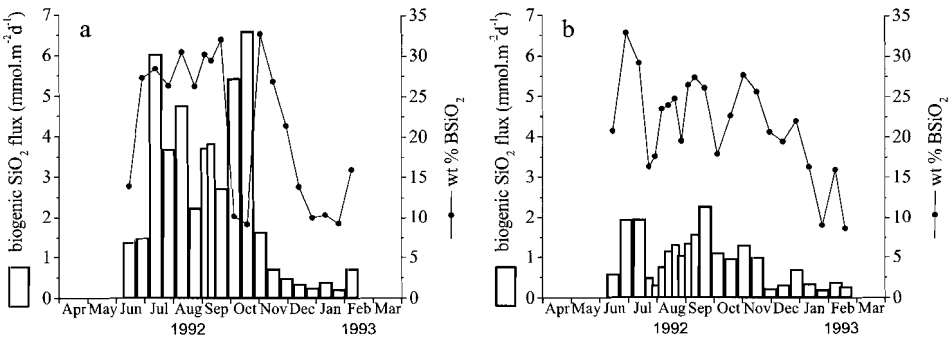

Fig. 4: Particulate biogenic silica fluxes and $BsiO_2$ wt% for sediment trap 8B (4a) and particulate biogenic silica fluxes and $BsiO_2$ wt% for sediment trap 9G (4b).

Diatoms

Diatom fluxes of autochthonous species were ten times higher during the SW monsoon than during the NE monsoon and five times higher on the slope than in the basin. Highest fluxes were reached in October. A pronounced species succession was evident and could be divided in 5 groups, but only part of the species record is preserved in the sediment. The dominant groups and their characteristics are listed in table 2.

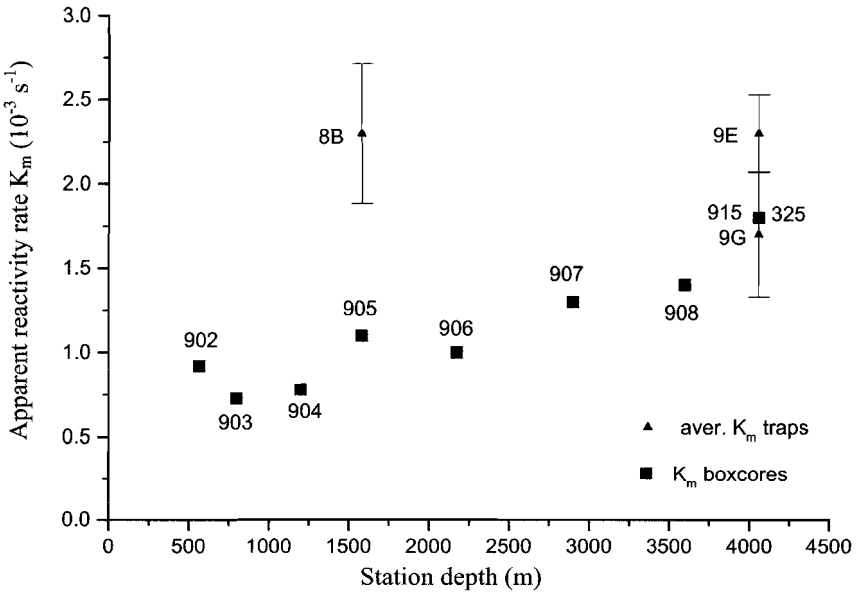

Fig. 5: K_m ,apparent reactivity rates in 0.5M NaOH, for boxcore tops and sediment traps.

Table 2: Dominating diatom species in the sediment traps with their characteristics, the period of dominance and their preservation in the sediment.

	dominance	preservation
small, weakly silicified species a.o. Rhizosolenia imbricata	June	no
well silicified, mainly Thalassionema nitzschioides	July-August	good
small, fragile species, a.o. Nitzschia bicapitata and Nitzschia bifurcata	September	no
thick, well silicified Chaetoceros resting spores	October	good
non-upwellers: diverse assemblage with a high input of oceanic species, well silicified	Present year-round, dominating outside the upwelling	good

Sediments

Biogenic silica weight percentages in the boxcores tops ranged from 0.98% for boxcore 902 near the Somali coast to 6.6% for boxcore 915 in the basin (table 3). In general, K_m, the apparent leaching rate constants in the boxcore tops also increased with station depth. A distinct change in biogenic silica wt% and K_m values was evident between boxcores 904 and 905. The downcore profile for boxcore 905 showed a minimum wt% at 1.75cm depth. A similar feature, but not as pronounced, could be recognized in boxcore 915. Downcore BSi profiles, $CaCO_3$ profiles and profiles showing the K_m values for boxcores 905 and 915 are given in fig. 6.

Table 3: Water depth, BSi weight percentages (total sediment and carbonate free), K_m values (the apparent reactivity rate constants in alkaline medium) and silicic acid pore water effluxes for the boxcores on the Somali transect.

Water depth (m)	coretop BSi (wt%)	Coretop BSi (wt% $CaCO_3$ free)	K_m (10^{-3} s^{-1})	J(pore water) (mol.m^{-2} .$year^{-1}$)
565	0.98	4.0	0.92	3.00
797	1.35	5.1	0.73	1.36
1197	0.90	3.1	0.78	0.025
1580	4.8	11.8	1.1	0.61
2171	4.3	11.6	1.0	0.37
2896	6.6	17.2	1.3	--
3596	4.9	13.2	1.4	0.28
4059	5.5	13.2	1.8	0.28
4065	5.2	13.9	1.8	0.34

Pore waters

Pore water silicic acid profiles from all boxcores on the Somali transect were modeled to calculate the dissolution fluxes across the sediment-water interface. In general, the difference between the silicic acid concentration in the boxcore water and from the CTD at 5m above the sediment was less than 1%, except for station 325. Here, the boxcore water concentration was lower, probably due to an analytical error and the silicic acid concentration from the CTD has been used to calculate the pore water efflux at this station. In general, pore water effluxes decreased with water depth, from 3.00 mol m^{-2} $year^{-1}$ for boxcore 902 near the coast to 0.28 mol m^{-2} $year^{-1}$ for boxcore 915 in the basin, all taken in February outside the upwelling season. Boxcore 325, taken at the same site as 915 but during the upwelling season, shows a higher pore water efflux than boxcore 915, 0.34 mol m^{-2} $year^{-1}$ (table 3). All pore water profiles were modeled using a Z_{dbl} of 400μm. To evaluate the influence of Z_{dbl} on the pore water effluxes, profiles 905 and 915 were modeled with Z_{dbl} ranging from 0 to 1mm, which gave pore water effluxes of 0.61 ± 0.04 mol m^{-2} $year^{-1}$ for station 905

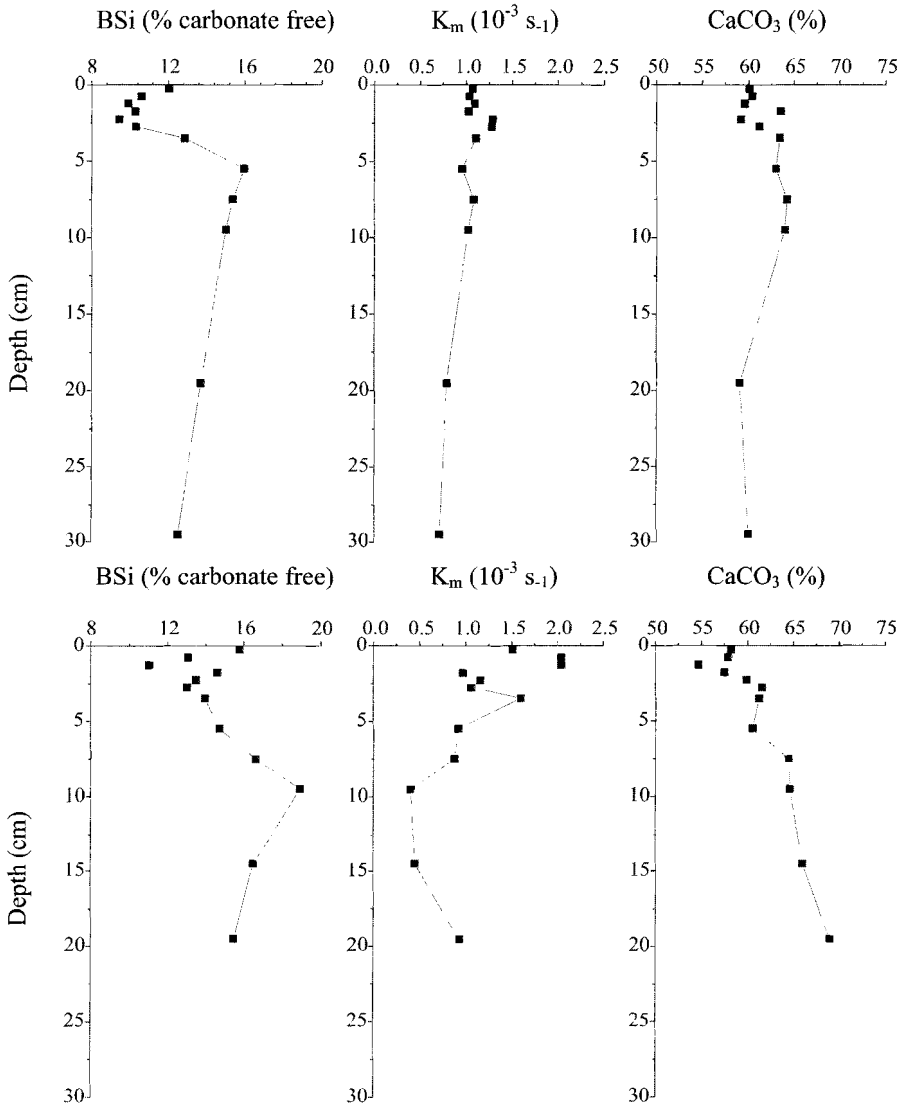

Fig. 6: Biogenic silica wt%, K_m and $CaCO_3$ profiles for boxcores 905 (top row) and 915 (bottom row).

and 0.28 ± 0.01 mol m^{-2} $year^{-1}$ for station 915. Best fits to the profiles gave a DBL thickness of 4mm for 905 and 4.5mm for 915. Pore water profiles, with insets showing the enlarged sediment-water interface, for boxcores 905 and 915 are given in fig. 7.

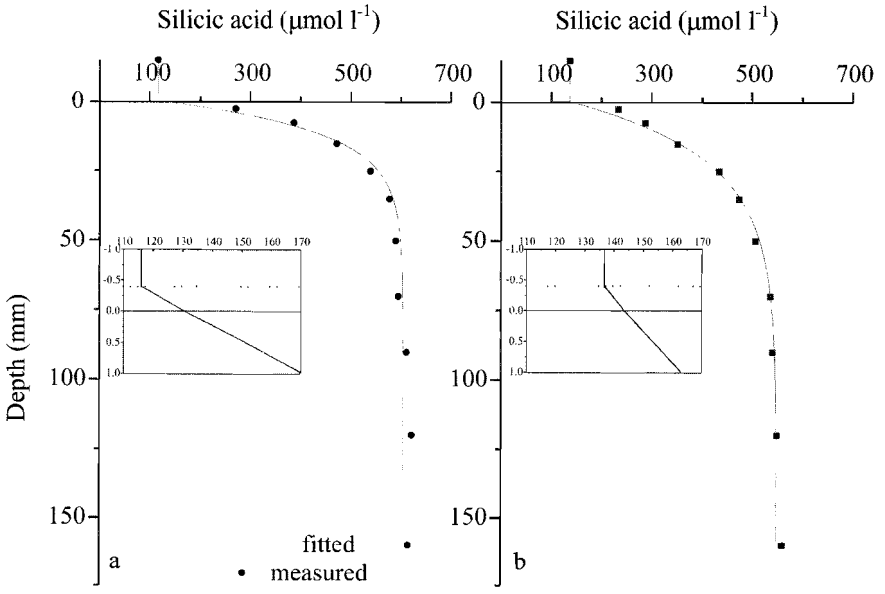

Fig. 7: Pore water profiles, with insets showing the enlarged sediment-water interface, for boxcores 905 (7a) and 915 (7b).

In-Situ Benthic chamber incubations

Diffusive fluxes across the sediment-water interface were measured at stations 905 and 915. At station 905, both in-situ and shipboard incubations were performed. At station 915, the bottom lander was not deployed and results are from shipboard incubations only. For station 905, silicic acid fluxes found with the lander were slightly lower (0.87 mol m^{-2} $year^{-1}$) than those found with the shipboard incubations (1.05 mol m^{-2} $year^{-1}$), but both methods give comparable values, with an average of 0.96 mol m^{-2} $year^{-1}$. The fluxes found with the shipboard incubations at station 915 are lower at 0.26 mol m^{-2} $year^{-1}$.

DISCUSSION

Annual fluxes of particulate biogenic silica on the Somali slope and in the Somali basin appear to be largely determined by coastal upwelling and associated offshore transport generated during the SW monsoon (fig. 4a and b). Satellite images from late May 1992 already show the appearance of colder water along the coast with a distinct gyre at 10°N and another one at 5°N, which merge into one large system when the monsoon progresses (de Bruin, 1995). In response, particle fluxes on the

slope increase by an order of magnitude from typical non-upwelling values of 0.2 - 0.7 mmol m^{-2} $day^{-1}$to 2 - 6 mmol m^{-2} day^{-1} and biogenic silica weight percentages increase from 10 - 15% to about 30%. In October, the trap on the slope shows peak fluxes up to 6.6 mmol m^{-2} day^{-1} despite the biogenic silica content of only 9 %. No increased input of lithogenic material, no phytoliths nor fresh-water diatoms were found that would indicate atmospheric or riverine input, neither did the flux of benthic diatoms change which would have been the case if the material had originated from the coast. Other evidence, a.o. from benthic foraminifera (S. Conan, pers. comm.) is consistent with a sedimentary source around the shelf break from where a carbonate-rich mass was transported laterally, diluting the pelagic biogenic silica settling in the trap cups with resuspended sediment. Fluxes to the trap in the Somali basin show the same overall pattern as found on the slope, with fluxes increasing from 0.02-0.5 mmol m^{-2} day^{-1} in the non-upwelling period to 1.0 -2.2 mmol m^{-2} day^{-1} in the upwelling, but with distinctly lower annual fluxes of 0.32 mol m^{-2} $year^{-1}$, which we interpret as reflecting the decreased influence of upwelling away from the coast. This interpretation agrees well with the 0.21 mol.m^{-2} $year^{-1}$ found by Haake et al. (1993) and Nair et al. (1992) in the western Arabian Basin at the same depth further away from the actual upwelling, who also show high fluxes during the SW monsoon and very low fluxes during the NE monsoon.

Satellite images from the monsoon period of 1992 show that the two-gyre system mentioned before is not constant in space and time, which results in the patchy occurrence of diatom blooms (Veldhuis et al., 1997). No measurements of primary productivity have been made year-round and it is therefore hard to make an estimate of the diatom production. From CTD-Rosette casts and surface water samples taken in June, July, August and February, biogenic silica production was estimated at 1.35 to 2.4 mol m^{-2} $year^{-1}$at the site on the slope (MST-8). Given the sediment trap derived biogenic silica flux of 0.85 mol m^{-2} $year^{-1}$, this means that between 40 and 65% dissolves in the upper water column. The only other diatom productivity data available for this area give values of 4-8 mol m^{-2} $year^{-1}$ (Lisitzin, 1972), but this is presently considered to be an overestimate because subsequent research has shown that the Si/C ratio in the diatoms is in the order of 0.13 (Brzezinski, 1985) rather than the 0.4 as used by Lisitzin (1972).

In the sediment traps, a pronounced diatom species succession with 5 distinct groups could be recognized during the upwelling period (Table 2), but not much of this species record is preserved in the sediments. The diverse non-upwelling assemblage is present year-round, but its relative abundance is low during the SW monsoon, due to the very high fluxes of typical upwelling species. The small, weakly silicified species of diatoms which dominate the assemblage in June and September generate a large part of the high BSi fluxes intercepted by the traps but dissolve prior to burial. The two well silicified upwelling species, *T. nitzschioides* and the solution-resistant *Chaetoceros* resting spores make up about 60% of the sediment, and dominate the sediment both in the coretops and downcore, thereby preserving a residual upwelling signal. Preferential dissolution of upwelling species may also account for the much lower biogenic silica weight percentages in the boxcores, of up to 6.6%, i.e. a factor 3 lower than in the sediment traps.

Averages of the apparent reactivity rate constant K_m, obtained from fitting the leaching curves, are higher for the shallow sediment traps than for the deep trap and

all boxcore sediments (fig. 7), which indicates that the more reactive fraction of the biogenic silica dissolves easily during settling and upon reaching the sediment. The average K_m value of 2.3 10^{-3} s^{-1} for trap 8B at 1265m water depth in the upwelling area on the slope is about the same as that for trap 9E at 1000m in the basin, while the reactivity at 3000m is lower (1.67 10^{-3} s^{-1}) for trap 9G, which probably reflects the dissolution of reactive diatom species in the water column. The sediment at station 915, 1000m below trap 9G, has a K_m value equal to that of trap 9G, while a lower reactivity would be expected due to continued dissolution during particle settling and the preferential dissolution of reactive species at the sediment-water interface. This increased reactivity in the sediments below trap 9G may be caused by lateral or downslope transport of more reactive material.

On the Somali transect, biogenic silica wt% and K_m values of coretop sediments generally increase with water depth while pore water effluxes of silicic acid decrease. The high efflux at station 902 indicates that highly reactive silica was deposited here, but the low K_m value and the very low wt% of biogenic silica show that this reactive material has already been dissolved. There are still some problems in explaining the changes in K_m values along the Somali transect, because K_m represents the reactivity of the mixture as a whole and will be influenced by the relative amounts of the different siliceous species in this mixture. Since it is not possible to make a distinction between diatoms, radiolarians and other siliceous species in the leaching curves, the influence of the species composition on the K_m values can not be ruled out. Biogenic silica profiles in boxcores 905 and 915 show minima of respectively 3.75% and 5% (9.4% and 11% carbonate free, Fig. 6) at approximately 1.5 to 2cm depth, and K_m values show maxima of 1.28 and 2.04 10^{-3} s^{-1} in the same depth interval, indicating that this biogenic silica minimum may be caused by high reactivity rates of the dissolving material. In general, the downcore K_m value in the sediment decreases to approximately 0.6 10^{-3} s^{-1} at 25cm depth which is about equal to the K_m value in the core top sediments on the slope and may represent the K_m value of the less reactive residual biogenic silica. ^{210}Pb profiles show that bioturbation depth is approximately 10cm, with a submaximum at 5cm in both boxcores 905 and 915, indicating non-local mixing (W. Boer, pers. comm.). The observed biogenic silica maximum in boxcore 905 at 5cm depth may therefore be due to bioturbation. In boxcore 915, this biogenic silica maximum is found at 9cm depth, where ^{210}Pb profiles indicate non-local mixing at 5cm, but all leaching curves from this boxcore show a distinct change in slope after 5 minutes, indicating the presence of two separate fractions of biogenic silica. Apparently, bioturbation causes a redistribution of surface sediment with a higher biogenic silica content to depths around 10cm.

Pore water silicic acid effluxes range from 8.2 mmol m^{-2} day^{-1} for station 902 on the slope to 0.7 mmol m^{-2} day^{-1} for station 915 in the Somali Basin. All pore water effluxes were fitted using a diffusive boundary layer thickness of 400μm. The model uses a constant K_d and can not fit the datapoint just below the sediment-water interface. When the silicic acid concentration in the water above the sediment is not taken into account, it is possible to fit through all the datapoints but this leaves an additional 100μmol silicic acid to be accounted for in the diffusive boundary layer, thereby stretching this layer to 4mm. Since a diffusive boundary layer thicker than

1mm is not considered realistic (Boudreau and Guinasso, 1980) there must be a thin, extremely reactive layer present at the sediment-water interface. The sampling resolution in our profiles is not high enough to detect this layer and fluxes calculated from the profiles are therefore underestimated, which may explain the difference between modeled pore water fluxes and diffusive fluxes from the in-situ incubations. Again bioturbation can not be ruled out. The rapid exchange between pore water and overlying water due to bioturbation may give lower pore water silica concentrations, which causes underestimation of pore water effluxes and may be another explanation for the observed difference between modeled and diffusive fluxes. Fluxes similar to those found on the Somali transect, (0.5-2.7 mmol m^{-2} day^{-1}) were found in other highly productive areas like the Polar Front (van Bennekom et al., 1988), the SE Pacific (Wakefield, 1982) and the Equatorial Pacific (McManus et al., 1995).

Mass Balances

For stations 905 and 915, particulate biogenic silica fluxes, diffusive fluxes from the sediment and burial fluxes are compared to calculate a mass balance at these sites (Figs.8a and b). For this purpose, pore water effluxes are recalculated to mol m^{-2} $year^{-1}$ for comparison with the sediment trap fluxes. At station 905, particulate fluxes show that 0.85 mol m^{-2} $year^{-1}$ arrives on the mid slope, of which only 0.063 mol m^{-2} $year^{-1}$ or 7.5% is eventually buried. The measured effluxes of

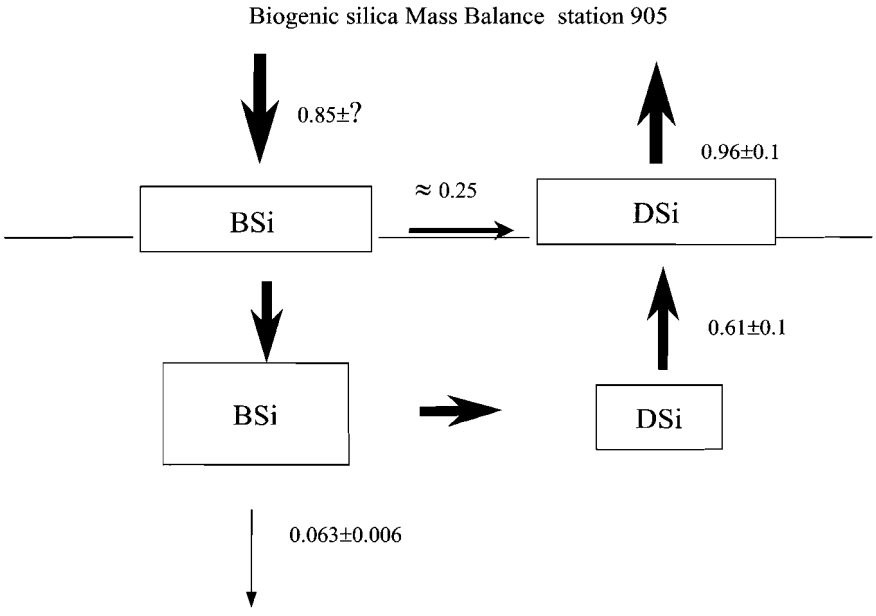

Fig. 8a: Mass balance for station 905. BSi indicated biogenic silica, DSi indicates dissolved silica. All fluxes are given in mol $m^{-2}year^{-1}$.

dissolved silica from the sediment amount to 0.61 and 0.96 mol m^{-2} $year^{-1}$ based on pore water modeling and in-situ benthic incubations, respectively (fig. 8a). Pore water efflux and burial flux together do not completely balance the particle fluxes from the trap. The excess 0.25 mol m^{-2} $year^{-1}$ that can not be accounted for may represent the flux of dissolution prone diatom species present in the traps but lacking in the core tops, and/or the additional efflux from the thin, extremely reactive layer just below the sediment-water interface not sampled in the profiles or may be due to bioturbation.

Input fluxes to the deep Somali Basin at site 915 are much lower at 0.32 mol m^{-2} $year^{-1}$ and about balanced by sedimentary dissolution and burial (fig. 8b). At the deep site in the Somali Basin 0.018 mol m^{-2} $year^{-1}$ of biogenic silica accumulates in the sediment, giving a burial efficiency of 6%. These burial fluxes are compared with data from other studies (table 4). Burial efficiencies found in the Somali area are lower than those found in the Arabian Basin (Haake et al., 1993), which is also influenced by the Indian Ocean summer monsoon, but compare well with other areas throughout the world. Unfortunately, most of the papers that present sediment trap studies do not include sediment samples and no data are available from the extensively studied circumpolar silica belt in the Antarctic Ocean, other than budget calculations based on global estimates (Nelson et al., 1995; Treguer et al., 1995). So far, available data from studies combining particle fluxes and sediment show no relation between particulate biogenic silica fluxes and burial efficiency, but give comparable burial efficiencies for sediments under areas of high production like the Somali area and areas of low production like the BATS site near Bermuda.

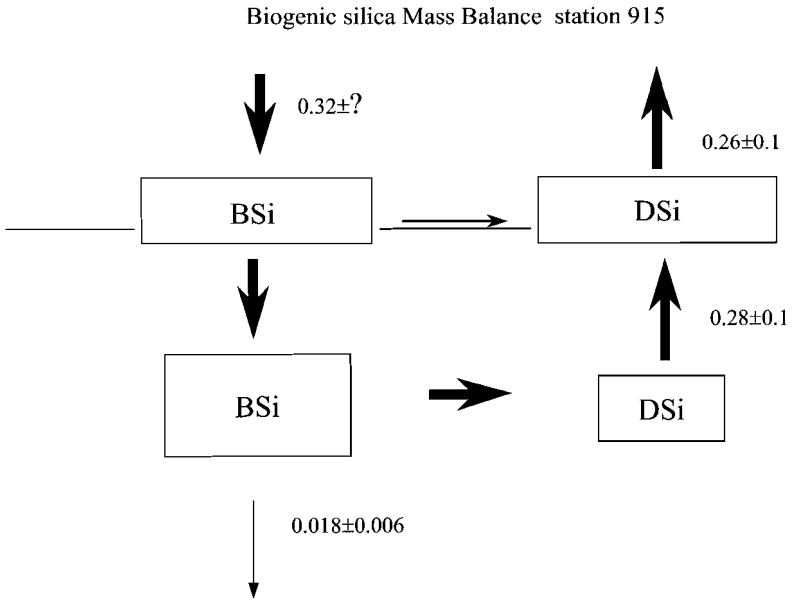

Fig. 8b: Mass balance for station 915. BSi indicated biogenic silica, DSi indicates dissolved silica. All fluxes are given in mol $m^{-2}year^{-1}$.

Table 4. Literature data of sediment trap fluxes and burial efficiencies.

Station site	particulate flux ($g\ m^{-2}\ year^{-1}$)	burial efficiency (%)	Reference
BATS W. Atlantic	1.28	6	Sayles et al., 1996
E. Pacific Rise E. Pacific	3.56	3-4	Dymond & Lyle, 1985
Guatemala Basin	6.59	4-8	
Galapagos	10.1	20	Cobler & Dymond, 1980
N Bengal Indian Ocean	8.6	2.3	Rameswamy & Nair, 1994
C Bengal	9	0.33	
S Bengal	7.3	0.55	
Cap Blanc E.South Atl.	2.6	2	Fischer & Wefer, 1996
Guinee Basin N	4.7	10	
Guinee Basin S	5.4	9	
Walvis Ridge	3.7	3	
Somali Slope NW Indian	57.2	8	this study
Somali Basin	21.5	6	this study
W Arabian Basin	14.1	15	Haake et al., 1993
C Arabian Basin	3.6	25	
E Arabian Basin	5.6	21	

CONCLUSIONS

Particulate fluxes of biogenic silica collected by the sediment traps on the Somali slope and in the Somali Basin show a distinct seasonal pattern with high fluxes during the SW monsoon and low fluxes during the NE monsoon. Particulate fluxes are higher on the slope than in the basin, and are about balanced by pore water effluxes and sediment burial fluxes, with low burial efficiencies (6-8%). Although most of the typical upwelling species of diatoms that are abundant in the traps are dissolved prior to sediment burial, two well silicified upwelling indicators dominate the sediments both in the core tops and downcore, thereby preserving a residual upwelling signal.

ACKNOWLEDGEMENTS

We thank captain and crew of the RV Tyro, the NIOZ technicians for coring and for handling the moorings. Jan van Ooyen, Annette van Koutrik and Evaline van Weerlee (Department of Marine Chemistry and Geology) are thanked for the shipboard nutrient analyses. We acknowledge Ralph Schneider for his assistance in developing the analytical equipment and Tjeerd van Weering as well as Eric Epping for fruitful discussion. The Netherlands Indian Ocean Programme was funded and co-ordinated by the Netherlands Marine Research Foundation (SOZ) of the Netherlands Organization for Scientific Research (NOW). This is publication no. 3180 of the Netherlands Institute for Sea Research.

REFERENCES

Aller, R.C., Benninger, L.K. (1981). Spatial and temporal patterns of dissolved ammonium, manganese, and silica fluxes from bottom sediments of Long Island Sound, U.S.A. Journal of Marine Research, 39, 295-314.

Andrews, D., Bennett, A. (1981). Measurements of diffusivity near the sediment-water interface with a fine-scale resistivity probe. Geochimica et Cosmochimica Acta 45, 2157-2169.

Bareille, G., Labracherie, M, Labeyrie, L., Pichon, J.-J., Turon, J.-L. (1991). Biogenic silica accumulation rate during the Holocene in the Southeastern Indian Ocean. Marine Chemistry, 35, 537-551.

Berner, R.A. (1980) Early diagenesis, a theoretical approach. Princeton University Press, Princeton, New Jersey, 241pp.

Boudreau, B.P., Guinasso, N.L. (1980) The influence of a diffusive sublayer on accretion, dissolution and diagenesis on the sea floor. In: Fanning K.A. and F.T. Manheim (eds.) The dynamic environment of the ocean floor

Boudreau, B.P., Ruddick, B.R. (1991). On a reactive continuum representation of organic matter diagenesis. American Journal of Science, 291, 507-538.

Brock, J.C., McClain, C.R., Hay, W.W. (1992). A southwest monsoon hydrographic climatology for the northwestern Arabian Sea. Journal of Geophysical Research, 97, 9455-9465.

Brzezinski, M.A. (1985). The Si:C:N ratio of marine diatoms: Interspecific variability and the effect of some environmental variables. Journal of Phycology, 21, 382-389.

Brzezinski, M.A., Nelson, D.M. (1995). The annual silica cycle in the Sargasso Sea near Bermuda. Deep-Sea Research, 42, 1215-1237.

Broecker, W.S., Peng, T.-H. (1982). Tracers in the sea, Eldigio Palisades, New York. 690pp.

Brummer, G.-J.A. (1995). Sediment traps and particle dynamics. In: van Hinte J.E., Tj.C.E. van Weering and S.R. Troelstra (eds.) (1995) Tracing a seasonal upwelling. Cruise reports Netherlands Indian Ocean Programme, Vol. 4, National Museum of Natural History, Leiden, 146p.

Burkill, P.H., Mantoura, R.F.C., Owens, N.J.P. (1993). Biogeochemical cycling in the northwestern Indian Ocean: a brief overview. Deep Sea Research II, 40, 643-649.

Clemens, S., Prell, W., Murray, D., Shimmield, G., Weedon, G. (1991). Forcing mechanisms of the Indian Ocean monsoon. Nature, 353, 720-725.

Cobler, R., Dymond, J. (1980). Sediment trap experiments on the Galapagos Spreading Center, Equatorial Pacific. Science, 209, 801-803.

de Bruin, T.F. (1995). Remote sensing. In: Baars M.A. (ed.) (1995) Monsoons and pelagic systems. Cruise reports Netherlands Indian Ocean Programme, Vol. 1, National Museum of Natural History, Leiden, 143p.

DeMaster, D.J., Nelson, T.M., Harden, S.L., Nittrouer, C.A. (1991). The cycling and accumulation of biogenic silica and organic carbon in Antarctic deep-sea and continental margin environments. Marine Chemistry, 35, 489-502.

DeMaster, D.J. (1981) The supply and accumulation of silica in the marine environment. Geochimica et Cosmochimica Acta, 45, 1715-1732.

Duineveld, G.C.A., de Wilde, P.A.W.J., Berghuis, E.M., Kok, A., Tahey, T., Kromkamp, J. (1997). Benthic respiration and standing stock on two contrasting continental margins in the western Indian Ocean: The Yemen/ Somali upwelling region and the margin off Kenya. Deep-Sea Research II, 44, 1293-1318.

Dymond, J., Lyle, M. (1985) Flux comparisons between sediments and sediment traps in the eastern tropical Pacific: Implications for atmospheric CO_2 variations during the Pleistocene. Limnology and Oceanography, 30, 699-712.

Fischer, J., Schott, F., Stramma, L. (1996). Current and transports of the Great Whirl-Socotra Gyre system during the summer monsoon, August 1993. Journal of Geophysical Research, 101, 3573-3587.

Fischer, G., Wefer, G. (1996). Long-term observations of particle fluxes in the eastern Atlantic: Seasonality, changes of flux with depth and comparison with the sediment record. In: Wefer G., W.H. Berger, G. Siedler and D.J. Webb (eds.) The South Atlantic: Present and Past Circulation. Springer-Verlag Berlin Heidelberg, 325-344.

Gersonde, R., Wefer, G. (1987). Sedimentation of biogenic siliceous particles in Antarctic waters from the Atlantic sector. Marine Micropaleontology, 11, 311-332.

Haake, B., Ittekot, V., Ramaswamy, V., Nair, R.R., Curry, W.B.(1993). Seasonality and interannual variability of particle fluxes to the deep Arabian Sea. Deep Sea research , 40, 1323-1344.

Helder, W., Kloosterhuis, R.T., Nolting, R.F. (1995). Early diagenesis in sediments from the oxygen minimum zone off Yemen In: van Hinte J.E., Tj.C.E. van Weering and S.R. Troelstra (eds.) (1995) Tracing a seasonal upwelling. Cruise reports Netherlands Indian Ocean Programme, Vol. 4, National Museum of Natural History, Leiden, 146p.

Hitchcock, G.L., Olsen, D.B. (1992). NE and SW monsoon conditions along the Somali coast during 1987. In: B.N. Desai (Ed.) Oceanography of the Indian Ocean. Oxford & IBH, New Delhi, 583-593.

Hurd, D.C. (1973). Interactions of biogenic opal sediment and sea water in the central equatorial Pacific. Geochimica et Cosmochimica Acta, 37, 2257-2282.

Jansen, J.H.F., van der Gaast, S.J. (1988) Accumulation and dissolution of opal in Quaternary sediments of the Zaire deep-sea fan (northeastern Angola Basin). Marine Geology, 83, 1-7.

Li, Y.-H., Gregory, S. (1974). Diffusion of ions in sea water and in deep-sea sediments. Geochimica et Cosmochimica Acta, 38, 703-714.

Lisitzin, A.P. (1972). Sedimentation in the world ocean. Society of Economic Paleontologists and Mineralogists Special Publication, 17, 218p.

McManus, J., Hammond, D.E., Berelson, W.M., Kilgore, T.E., DeMaster, D.J., Ragueneau, O.G., Collier, R.W. (1995). Early diagenesis of biogenic opal: Dissolution rates, kinetics and paleoceanographic implications. Deep-Sea research II, 42, 871-903.

Middelburg, J.J. (1989). A simple rate model for organic matter decomposition in marine sediments. Geochimica et Cosmochimica Acta, 53, 1577-1588.

Müller, P.J., Schneider, R. (1993). An automated method for the determination of opal in sediments and particulate matter. Deep Sea Research I, 40, 425-444.

Nair, R.R., Ittekot, V., Managanin, S.J., Ramaswamy, V., Haake, B., Degens, E.T., Desai, B.N., Honjo, S. (1989). Increased particle flux to the deep ocean related to monsoons. Nature, 338, 749-751.

Nelson, D.M., Tréguer, P., Brzezinski, M.A., Leynaert A., Quéguiner, B. (1995). Production and dissolution of biogenic silica in the ocean: Revised global estimates, comparison with regional data and relationship to biogenic silica sedimentation. Global Biogeochemical Cycles, 9, 359-372.

Postma, D. (1993). The reactivity of iron oxides in sediments: A kinetic approach. Geochimica et Cosmochimica Acta, 57, 5027-5034.

Ramaswamy, V., Nair, R.R. (1994). Fluxes of material in the Arabian Sea and Bay of Bengal – Sediment trap studies. In: Lal D. (ed.), Biogeochemistry of the Arabian Sea, Indian Academy of Sciences, Bangalore, 91-112.

Sayles, F.L., Deuser, W.G., Goudreau, J.E., Dickinson, W.H., Jickells, T.D., King, P. (1996) The benthic cycle of biogenic opal at the Bermuda Atlantic Time Series site. Deep Sea Research I, 43, 383-409.

Schink, D.R., Guinasso, N.L., Fanning, K.A. (1975). Processes affecting the concentration of silica at the sediment-water interface of the Atlantic Ocean. Journal of Geophysical Research, 80, 3013-3031.

Sirocko, F. (1989). Zur akkumulation von Staubsedimenten im nördlichen Indischen Ozean; Anzeiger der Klimageschichte Arabiens und Indiens. Dissertation, Christian-Albrechts-Universität Kiel. Berichte, Geologisch-Paläontologisch Institut, Universität Kiel, 27, 185pp.

Smith, S.L., Codispoti, L.A. (1980). Southwest monsoon of 1979: chemical and biological response of Somali coastal waters. Science, 209, 597-600.

Smith, S.L. (1984). Biological indications of active upwelling in the northwestern Indian Ocean in 1964 and 1979, and a comparison with Peru and northwest Africa. Deep-Sea Research, 31, 951-967.

Strickland, J.D.H., Parsons, T.R. (1968). A practical handbook of seawater analysis. Fisheries Research Board of Canada, Bulletin 167, 1-311.

Tahey, T., Belgers, J., Kok, A. (1995). Oxygen uptake, nutrient fluxes, phytopigments and fauna in the sediment. In: van Hinte J.E., Tj.C.E. van Weering and S.R. Troelstra (eds.) (1995) Tracing a seasonal upwelling. Cruise reports Netherlands Indian Ocean Programme, Vol. 4, National Museum of Natural History, Leiden, 146p.

Thunell, R.C., Pride, C.J., Tappa, E., Muller-Karger, F.E.(1994). Biogenic Silica fluxes and accumulation rates in the Gulf of California. Geology, 22, 303-306.

Tréguer, P., Nelson, D.M., van Bennekom, A.J., DeMaster, D.J., Leynaert, A., Quéguiner, B. (1995). The silica cycle in the world ocean: a reestimate. Science, 268, 375-379.

van Bennekom, A.J., Berger, G.W., van der Gaast, S.J., de Vries, R.T.P.(1988). Primary productivity and the silica cycle in the Southern Ocean (Atlantic sector). Palaeogeography, Palaeoclimatology, Palaeoecology, 67, 19-30.

Van Cappellen, P. (1996). Reactive surface area control of the dissolution kinetics of biogenic silica in deep-sea sediments. Chemical Geology, 132, 125-130.

van Iperen, J.M., van Bennekom, A.J., van Weering, T.C.E.(1993). Diatoms in surface sediments of the Indonesian Archipelago and their relation to hydrography. Hydrobiologia, 269/270, 113-128.

Veldhuis, M.J.W., Kraay, G.W., Van Bleijswijk, J.D.L., Baars, M.A.(1997). Seasonal and spatial variability in phytoplankton biomass, productivity and growth in the northwestern Indian Ocean; the SW and NE monsoon, 1992-1993. Deep-Sea Research I, 44, 425-449.

Wakefield, S.J. (1982). Silica distribution in interstitial waters and sediments from the southeastern Pacific. Sedimentary Geology, 31, 13-31.

Wollast, R., Garrels, R.M. (1971). Diffusion coefficient of silica in sea water. Nature Physical Science, 229, 94.

Wollast, R., Mackenzie, R.M. (1983). Sedimentary geochemistry of Silicon. In: S.R. Alston (ed.), Silicon geochemistry and biogeochemistry, Academic Press, San Diego, 39-73.

CHAPTER 4

Selective preservation of upwelling-indicating diatoms in sediments off Somalia, NW Indian Ocean.

Erica Koning, Jolanda M. van Iperen, Wim van Raaphorst, Willem Helder, Geert-Jan A. Brummer and Tjeerd C.E. van Weering.

ABSTRACT

The diatom species composition of settling biogenic silica particles collected in sediment traps was compared with the underlying sediment to determine the preservation of the various diatom species and to investigate the potential of biogenic silica as an indicator for changes in paleo-upwelling intensity. During the Netherlands Indian Ocean Programme (NIOP), settling particles were collected at two sampling sites off Somalia (NW Indian Ocean) for nine months, from June 1992 to February 1993. One sediment trap array was deployed on the Somali slope directly below one of the main upwelling gyres and a second array, meant as a reference site to reflect pelagic sedimentation, was moored in the Somali Basin away from direct coastal upwelling influence. At both sites diatoms represented over 90% of the total opal microorganisms. On the Somali slope, total annual diatom flux was 12.6 10^9 valves m^{-2}, 76% of which was collected during the 112 days of the southwest monsoon, with peak fluxes in October, the end of the upwelling season. In the Somali Basin, the total annual flux was lower, 4.8 10^9 valves m^{-2}, and only 39% was collected during the SW monsoon period (98 days). At both sampling sites, a distinct seasonal diatom species succession of 'pre-upwellers', 'upwellers' and 'oceanic species' was apparent. Although only a small part of the diatom assemblage escaped dissolution at the sediment-water interface, two species, *Thalassionema nitzschioides* and *Chaetoceros* resting spores, were preserved in the boxcore sediment, indicating that they are resistant to dissolution at the sediment-water interface. Eighty one percent of the deposition of *Thalassionema nitzschioides* and 78% of the deposition of *Chaetoceros* occurred during the upwelling period. Since these two species are the dominant component of the diatom assemblage in the sediments, and thus determine the biogenic silica content, we conclude that this preserved biogenic silica reflects the upwelling in the surface layer of the water column. On the Somali Margin, variations

This chapter has been published in Deep-Sea research I, 48, 2473-2495.

in biogenic silica flux as inferred from sedimentary records can therefore be used as an indicator for changes in paleo-upwelling intensity.

INTRODUCTION

The productivity pattern of diatoms and other siliceous organisms in surface waters is reflected in their abundance in deep-sea sediments (Lisitzin, 1972; Broecker and Peng, 1982; Thunell et al., 1994). Sediments with a high biogenic silica content are found along the margins of West Africa, Peru and the North Pacific, around the Antarctic continent, and along the equatorial belt in the Pacific, areas where upwelling of nutrient-rich waters causes high primary production. In contrast, the northwestern Indian Ocean, which is considered to be one of the most productive regions in the world, does not show a high biogenic silica content in the sediments (Smith and Codispoti, 1980; Smith, 1984; Nair et al., 1989; Hitchcock and Olsen, 1992). On the Somali Margin, diatoms are a major component of the export flux from the productive surface layer, with biogenic silica percentages of up to 40% measured in sediment traps. However, biogenic silica content of the sediment is low, around 6% (Koning et al. 1997). As all ocean waters are undersaturated with respect to silica (Hurd, 1973), dissolution of diatom frustules takes place during settling and only a small fraction of the biogenic silica produced in the surface layer of the water column is deposited and buried. A major part of the initial siliceous production, up to 75%, is believed to dissolve in the upper 1000m of the water column (Brzezinski and Nelson, 1995; Gersonde and Wefer, 1987; Nelson et al., 1995; Tréguer et al., 1995). In a previous paper we have shown that on the Somali Margin, biogenic silica burial efficiencies are low and a further ~90% of the residual siliceous particle flux deposited on the bottom dissolves on the sediment-water interface prior to burial (Koning et al. 1997).

In this study, detailed qualitative and quantitative diatom analyses were carried out on particulate material from moored sediment traps and on surface sediments collected at 2 sampling sites (Fig. 1a) to obtain information about the seasonal and spatial variability of the diatom assemblage in relation to upwelling intensity. The diatom assemblage from the sinking particles collected in the sediment trap was compared with the underlying sediment, to study the preservation of distinct diatom species, and to assess the possible use of biogenic silica as an indicator for paleo-upwelling.

HYDROGRAPHY

The surface currents in the northwestern Indian Ocean show strong seasonal variations, caused by the alternating NE and SW monsoonal winds. From November to April, atmospheric pressure above the cold Tibetan Plateau is relatively high, resulting in NE monsoonal winds which force a Somali Current that flows from north to south. In early spring, heating of the Indian subcontinent causes the formation of an

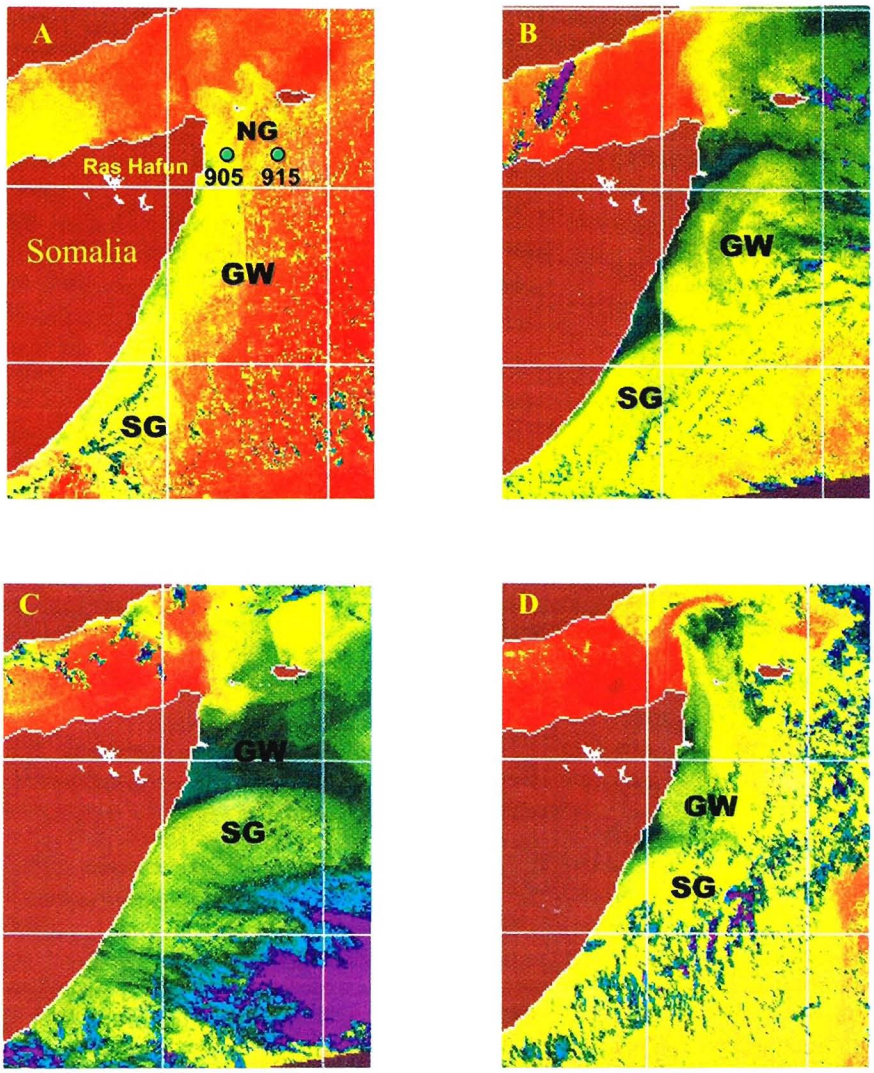

Fig. 1: Satellite pictures showing the progression of the monsoon and the position of the upwelling wedges during the SW monsoon. A: May 28, B: July 6, C: August 1 and D: September 21. Colors indicate water temperature: Blue-green is cold, 16°C, red is warm, 30 °C. Light blue and purple colors indicate clouds. Circles (in A) indicate the position of sampling stations 905 (Somali slope, with sediment trap MST-8B and boxcore 905) and 915 (Somali basin, with sediment trap MST-9G and boxcore 915). The approximate positions of the major gyres are given. NG: Northern Gyre; GW: Great Whirl; SG: Southern Gyre.

area of low atmospheric pressure above the Himalayas, while pressure above the relatively cold Southern Indian Ocean is high. Because of this pressure gradient, southwesterly winds rapidly gain strength along Somalia and persist at high velocities during the entire SW monsoon until late September (Prell, 1984; Webster, 1987). In response, coastal upwelling is generated and a succession of large, anti-cyclonic eddies develops, each bound by wedges of cold, upwelled water. The eddies migrate northward, along with the Somali current (Brock et al., 1992; Fischer et al., 1996; Schott, 1983; Schott et al., 1990; Rixen et al., 1996). Off Ras Hafun (Fig. 1a), such a wedge of cold upwelled water remains almost continuously present during the SW monsoon, a feature generally shown off prominent capes in the Arabian Sea and elsewhere. Further offshore, the wedge merges into a filament or jet curving along the eddy margin, advecting high concentrations of upwelled nutrients into the Somali Basin.

Different water masses influence Indian Ocean hydrography. Below approximately 3800m depth Antarctic Bottom Water (AABW) fills the Indian Ocean. This water leaves the Circumpolar Current and flows northward through the Somali Basin into the Arabian Sea, where it disappears through gradual upwelling into the overlying Deep Water. The depth range from above 3500m to about 1500m and shallower is occupied by Indian Deep Water (IDW), a water mass that originates from North Atlantic Deep Water (NADW). Indian Deep Water is not formed in the Southern Ocean, but represents that fraction of NADW carried along into the Indian Ocean with the upper Circumpolar Current. IDW penetrates northward into the western boundary current and spreads further northward into the Arabian Sea, its properties being modified along the way by mixing with thermocline waters from above, upwelling of AADW from below and by injections of Persian Gulf and Red Sea Water (Tchernia, 1980; Tomczak and Godfrey, 1994).

In May 1992, at the start of the Netherlands Indian Ocean Programme (van Weering et al., 1997), the onset of the SW monsoon was marked by thermal doming along coastal Somalia and offshore transport from Cape Ras Hafun in the frontal zone between the Northern Gyre and the Great Whirl (Fig. 1a). Shipboard measurements above the slope on June 2, 1992, show a core of advected coastal waters, with surface temperatures of about 26°C (Fig. 2a), depleted in SiO_4 and with a primary production of 1.4 gC m^{-2} day^{-1} (Baars et al., 1994; Veldhuis et al., 1997). On June 6, slightly colder water was advected to the slope site (Fig. 1b). Meanwhile, the basin site remained well within the oligotrophic, nutrient exhausted and warm water of the Great Whirl. By mid June, coastal upwelling and eddy circulation had intensified. In early July, the Great Whirl front extended over the slope site. By late July, the Southern Gyre approached from the south and nearly merged with he Great Whirl (Fig. 1c), causing massive advection of coastally upwelled water across both mooring sites. These waters were characterized by temperatures as low as 17°C and SiO_4 concentrations of up to 10 μM at the surface (Fig. 2b), but primary production remained moderately low, 0.7 – 0.9 gC m^{-2} day^{-1} because of vertical mixing to well below the photic zone (Baars et al., 1994; Veldhuis et al., 1997). From late July to mid August, surface water circulation changed rapidly, small-scale eddies and associated fronts were formed, warm Gulf of Aden water approached the slope site and cold frontal waters from the Southern Gyre were advected to the Basin site. Around mid August, when the Southern Gyre retreated southward, a deep mixed layer

rich in silicate (15 µM) and with temperatures of 24°C was found at both mooring sites. From early September on, surface waters showed a rapid warming to about 26°C, first over the deep basin site and by the end of September also over the slope site, while coastal upwelling diminished and the associated fronts retreated to the coast, away from the slope. Winds abated at the end of September, signaling the end of the SW monsoon.

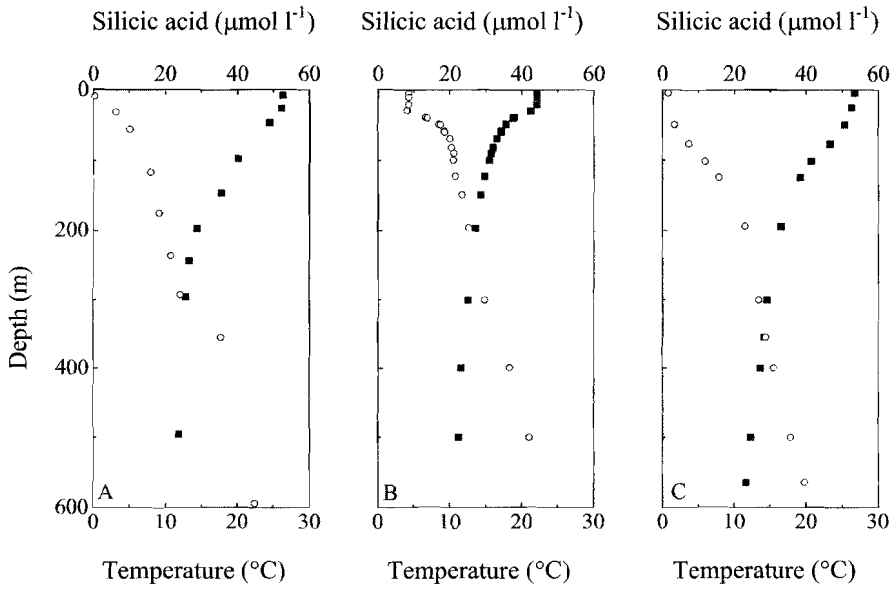

Fig. 2: CTD water column profiles for temperature and H_4SiO_4 sampled in the vicinity of the Somali slope site at different sampling dates. A: June 2, B: July 21, and C: February 13. Circles indicate silicic acid, squares indicate temperature.

There are no data available for the intermonsoon period. However, mixed layer temperatures derived from foraminiferal $\delta^{18}O$ in the sediment traps (S. M.-Th. Conan, personal communication) indicate an increasing surface mixed layer temperature, which peaked in November. Winter cooling lowered the sea surface temperature, and strong NE monsoonal winds followed in mid December. Shipboard measurements from the peak of the NE monsoon in mid February at the slope station (905) show a deep mixed layer with a temperature of 26°C, SiO_4 concentrations of 2µM (Fig. 2c), and primary productivity values of around 0.7 gC m^{-2} day^{-1} (Baars et al., 1994; Veldhuis et al., 1997).

MATERIALS AND METHODS

Sediment traps

The two arrays of moored sediment traps were deployed along a transect off Somalia for a period of nine months, from June 7, 1992 to February 14, 1993 (Fig. 1). Array MST-8 was deployed within the region of active coastal upwelling on the Somali continental slope (10°45.444´N / 51° 56.655´E) at a bottom depth of 1533m with sediment trap B at 1265m depth, i.e. 268m above the sea floor. Array MST-9 was moored outside the region of direct coastal upwelling, in the deep Somali Basin south of Socotra (10° 43.068´N / 53 ° 34.422´E) at a bottom depth of 4047m with trap G at 3047m depth, i.e. at 1000m above the sea floor. Samples correspond to 1- or 2-week-intervals. In order to study the seasonal pattern, all samples of the MST-8 B and MST-9 G series were analyzed for diatoms. For relating particle fluxes collected in the sediment trap cups to the actual hydrographic conditions at the surface at the time of production, all sample closing dates were corrected to depth zero, assuming a settling velocity of 150m d^{-1} (Knappertsbusch and Brummer, 1995). For a detailed description of the sediment trap arrays, see Koning et al., 1997.

Cores

Cylindrical cores, with a 50 cm diameter, were taken along a transect off Somalia (Fig. 1a). From boxcores 905 and 915, underlying the sediment traps MST-8 and MST-9, samples taken from the fluff layer and at the 0-1, 5-6, 10-11, 15-16, 20-21 and 25-26 cm intervals were analyzed for diatom species composition. Sedimentation rates were calculated from ^{14}C-AMS dating (Dr. K. van der Borg, R.J. van de Graaff Laboratory, Utrecht University, Table 1).

Table 1: ^{14}C AMS dating results, Sedimentation Rates (SR), Dry Bulk Densities (DBD) and Mass Accumulation Rates (MAR) for boxcore sediments from stations 905 and 915 on the Somali Margin.

Depth (cm)	Age (cal yr)	SR (cm kyr^{-1})	DBD (g cm^{-3})	MAR (g cm^{-2} kyr^{-1})
Station 905				
0	0	19.1	0.41	8.2
10	520	19.1	0.56	11.2
26	1290	20.8	0.62	12
Station 915				
0	0	3.6	0.53	1.9
10	2745	3.6	0.68	2.4
24	5497	5.1	0.69	3.5

Diatoms

To minimize silica dissolution, some modifications were needed with respect to the standard acid cleaning method of Schrader (1974). An excess amount of 12% H_2O_2 and 1N HCl was added to circa 200 mg of dried homogenized material and the mixture was heated for 2½-h at 60°C (instead of 80°C) to remove organic and calcareous material. To minimize sample loss, four gentle centrifugation steps (7 min. at 1200 rpm) were introduced to remove the residual chemicals and to concentrate the diatoms. The supernatant was now free of diatoms, while fragmentation of the valves in the residue had not increased significantly.

Quantitative slides were prepared in evaporation trays (∅ 96 mm) following Batterbee (1973) with three circular LM cover slips (∅ 19 mm) and one SEM slip (∅ 10 mm). The LM slips were embedded in Naphrax (r.i. = 1.72) and subsequently examined with a Leitz Laborlux 12 POL microscope at 1000x magnification. For each slide at least 200 individuals were counted along non-overlapping traverses. Specimens representing more than one half of the valve were counted as one and for long pennate diatoms such as *Lioloma* spp., *Thalassiothrix* spp., *Thalassionema* spp. and *Alveolus marina* each pole was counted as one half specimen. Other fragments were not counted.

Diatom density, DD, is given as the number of diatom valves per gram dry weight and is derived from:

$$DD = \frac{N * \left(A/a\right) * \left(V/v\right)}{G} \qquad (1)$$

where N is the number of autochthonous specimens (marine pelagic species) counted along an area (a) of traverses as a fraction of the total area of the evaporation tray (A) and v is the subvolume of the total suspension volume (V) used in the tray. The denominator (G) expresses the dry weight of the material. Diatom fluxes (DF) in the traps and diatom burial fluxes (DBF) in the sediments were calculated as follows:

DF = DD * particulate mass fluxes

DBF = DD at depth z * sediment mass accumulation rates (Table 1)

Particulate mass fluxes were taken from van Weering et al., 1997. Here, z is depth of the sample in the sediment. Results are expressed as valves m^{-2} d^{-1}. The annual diatom flux in the sediment traps was estimated by assuming the missing three months (March to June) to have mean non-upwelling values (Koning et al., 1997). As an example, the annual diatom flux for the slope trap (MST-8) is

$$\text{Annual DF (1992-1993)} = \sum_{B4}^{B12} DF + \left(\sum_{B2}^{B3} DF + \sum_{B13}^{B20} DF \right) * \frac{253}{140} \qquad (2)$$

Where B4-B20 indicate trap sample numbers.

Burial efficiencies (BE) of diatom species groups, and burial efficiencies of single species, indicate which part of the diatom assemblage collected in the lower trap is resistant to dissolution and will be buried in the sediment. Burial efficiencies were calculated from:

$$BE = \frac{\text{DBF at Zbm}}{\text{annual DF in sediment trap}} * 100\% \quad (3)$$

where DBF and annual DF can be based on either diatom species group flux or on single diatom species flux and Zbm is below the mixing depth in the sediment. Here, the diatom burial flux is the average diatom flux of all samples below the sediment mixing depth (~5cm, as derived from ^{210}Pb profiles).

Taxonomic analyses

In each slide specimens were identified to the species level. In a few cases, difficulties arose in distinguishing between two or more species. These species were combined in one counting group. Relative diatom abundances of individual taxa were given as percentage (%) of the total marine diatom assemblage. Allochthonous species (littoral benthic, epibiontic and continental species) were counted separately, as they originate from the shelf, and were expressed as percentage of the autochthonous assemblage. Diatom species fluxes were calculated by multiplying the species percentages with the daily total diatom flux and dividing by 100.

Principal Component Analysis

To investigate the covariability between the different diatom species, as observed in the species composition plots, a Principal Component Analysis (PCA) was carried out by means of SYSTAT (Wilkinson, 1988). Out of approximately 100 species and species groups recognized in the sediment traps, the statistical analysis covered the 22 most numerous diatom species, all with abundances of more than 0.5% of the annual flux, or with an abundance of more than 4% in any single sample. As a first step in the analysis in order to increase normality of the dataset, diatom density data were logtransformed and standardized to mean zero and standard deviation one for each species (Tabachnick and Fidell, 1996). As the result of standardization, all diatom species had a similar weight, and their variance could thus be compared successfully. The PCA results were visualized in a biplot showing the correlation between the species. Long vectors, which are pointing in the same direction, indicate a high positive correlation between diatom species abundances, while orthogonal vectors indicate a zero correlation.

RESULTS

Sediment traps

On the Somali slope, (MST-8, trap B), three distinct periods could be recognized, pre-upwelling, upwelling and post-upwelling (Fig. 3b). Highest fluxes of autochthonous diatoms were recorded from July to October 1992, which coincides with the period of the SW monsoon (Fig. 3b). Peak fluxes (201 10^6 valves m^{-2} d^{-1})

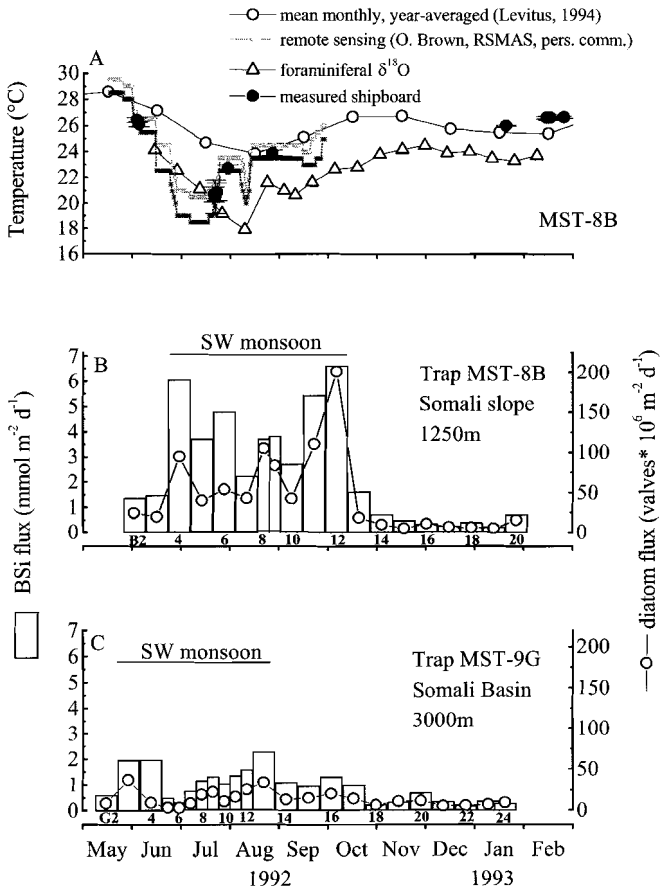

Fig. 3: Temperature fluctuations for 1992-1993 at sampling site MST-8B (top) and biogenic silica fluxes and total diatom fluxes for sediment traps MST-8B on the Somali slope (middle) and MST-9G in the Somali Basin (bottom). Sample numbers of the traps are given below the biogenic silica flux bars. Black horizontal bars indicate the duration of the SW monsoon period.

were reached at the end of the upwelling period, in October. The total diatom flux for 1992 was 12.6 10^9 valves m^{-2}, 76% of which was intercepted during the 112 d of the SW monsoon period. Diatom fluxes in trap MST-9G in the Somali Basin showed a similar pattern, with a pre-upwelling, upwelling and post-upwelling period, but fluxes were an order of magnitude lower. At this site, the total diatom flux for 1992 was 4.8 10^9 valves m^{-2}, of which only 39% was recorded during the SW monsoon period, which lasted 98 d at this site (Fig. 3c). At both sites, the contribution of allochthonous species to the flux recorded in the sediment traps was low, always less than 6% of the total diatom count. On the Somali slope, average contribution of allochthonous species was 2.1%, with the highest numbers, 6% and 6.9 10^6 valves m^{-2} d^{-1}, found in early July (sample B4). For the sediment trap in the Somali Basin the average contribution of allochthonous species to the total diatom count was 1.4%, with a maximum of 4% and 0.5 10^6 valves m^{-2} d^{-1} (sample G8) in mid July. In the slope trap, *Rhizosolenia* species dominated the pre-upwelling period in June. During the upwelling period from July to October a distinct succession of dominant species could be recognized (Fig. 4a), with *Thalassionema nitzschioides* in July followed by *Nitzschia bicapitata* in September and finally a peak flux of *Chaetoceros* resting spores in early October at the end of the upwelling season. The assemblage in the post-upwelling period was more diverse and consisted of oceanic species. In the Somali Basin trap, the same species contributed to the assemblage as in the Somali slope trap, but without a clear successive dominance of single species during the SW monsoon (Fig. 4b). In both sediment traps, most minor species in the assemblage did not show a distinct seasonal pattern (Figs. 4c and d).

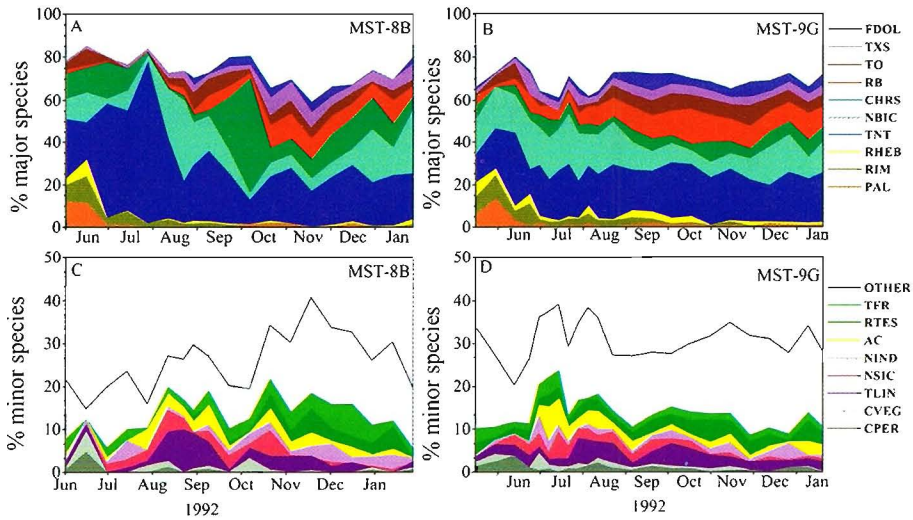

Fig. 4: Cumulative relative abundances of diatom species on the Somali slope (left panels; A, C) and in the Somali Basin (right panels; B, D). Species codes are explained in Table 2.

Table 2: Diatom species codes as used in the principle component analysis.

	pre-upwelling species
CPER	*Chaetoceros peruvianus* Brightwell
CVEG	*Chaetoceros* Ehrenberg vegetative cells
PAL	*Proboscia alata* (Brightwell) Sundström
	Proboscia indica (Peragallo) Hernández-Becerril
RHEB	*Rhizosolenia hebetata* f. *semispina* (Hensen) Gran
	Rhizosolenia styliformis Brightwell
RIM	*Rhizosolenia imbricata* Brightwell
	Rhizosolenia fallax Sundström
	Rhizosolenia ostenfeldii Sundström
	Upwelling species
AC	*Actinocyclus curvatulus* Janisch
	Actinocyclus vestigulus Watkins
CHRS	*Chaetoceros* Ehrenberg resting spores
NBIC	*Nitzschia bicapitata* Cleve
	Nitzschia bifurcata Kaczmarska & Licea
NIND	*Neodelphineis indica* (Taylor) Tanimura
NSIC	*Nitzschia sicula* (Castracane) Hustedt
TFR	*Thalassionema frauenfeldii* (Grunow) Hallegraeff
	Thalassionema bacillare (Heiden) Kolbe
TLIN	*Thalassiosira lineata* Jousé
	*Thalassio*sira *lineoides* Herzig & Fryxell
TNT	*Thalassionema nitzschioides* Grunow in van Heurck
	Thalassionema nitzschioides var. *parva* Heiden & Kolbe
	Thalassionema pseudonitzschioides Schuette & Schrader
	Thalassionema synedriforme (Greville) Hasle
	Oceanic species
AN	*Azpeitia nodulifer* (Schmidt) Fryxell & Sims
	Azpeitia barronii Fryxell & Watkins
ANEO	*Azpeitia neocrenulata* (van Landingham) Fryxell & Watkins
	Azpeitia tabularis var. *egregius* (Rattray) Hustedt
CRAD	*Coscinodiscus radiatus* Ehrenberg
FDOL	*Fragilariopsis doliolus* (Wallich) Medlin & Sims
RB	*Rhizosolenia bergonii* Peragallo
RTES	*Roperia tesselata* (Roper) Grunow in van Heurck
TO	*Thalassiosira oestrupii* (Ostenfeld) Proshkina-Lavrenko
	Thalassiosira oestrupii var. *venrickae* Fryxell & Hasle
TXS	*Thalassiothrix spathulata* Hasle
	Thalassiothrix gibberula Hasle
	Lioloma pacificum (Cupp) Hasle
	Other species
RCR	*Rhizosolenia crassispina* Schröder

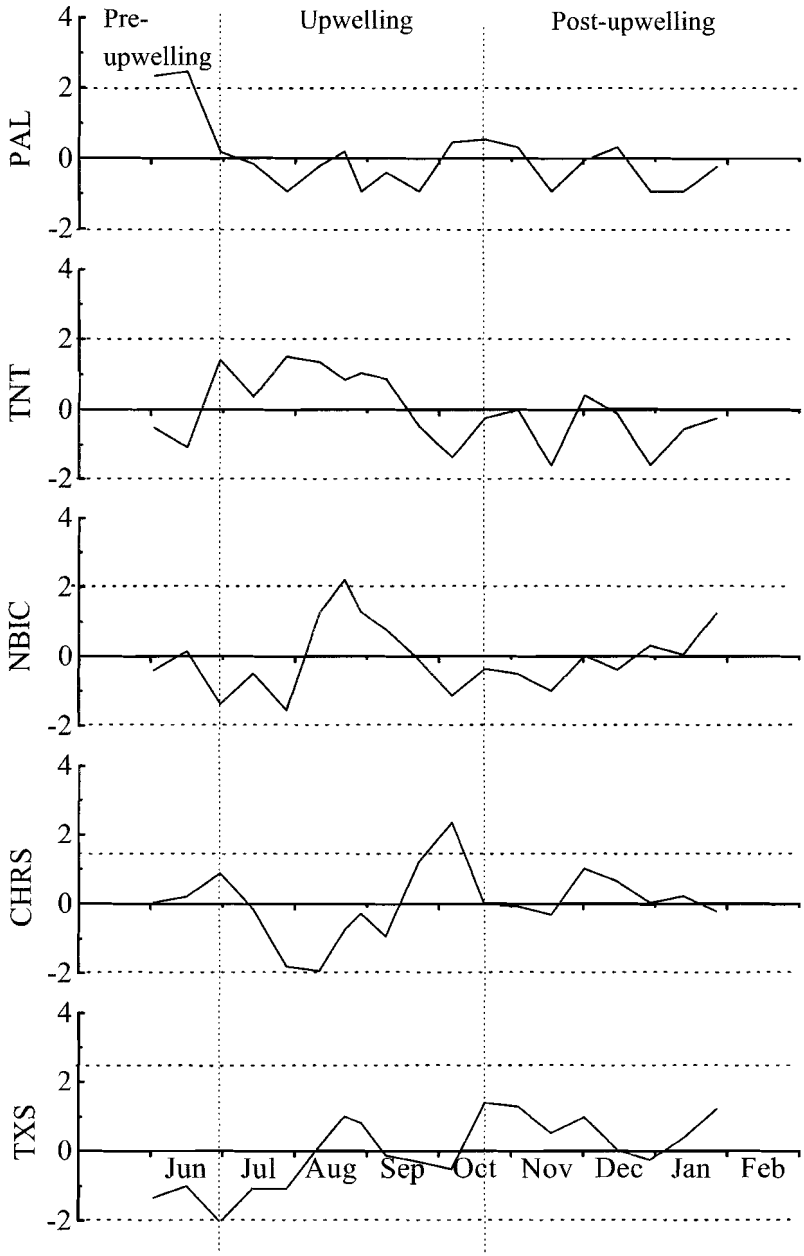

Fig 5: Logtransformed and standardized diatom densities (mean zero, standard deviation 1) of 5 major species in the sediment trap on the Somali slope. Dotted lines indicate 2* standard deviation. Species codes are explained in Table 2.

PCA

From Figs. 3b and 4a, the first order relationships between the major diatom species in the slope trap were evident and a clear succession of dominant diatom species could be recognized. No such dominance is evident at the basin trap (Fig. 4b) or for most minor species at both sites (Figs. 4c and 4d). However, the dominance of a species as seen in Fig. 4 is a relative dominance and could thus be caused either by an increase of the species itself or by a decrease of other species in the assemblage. Fig. 5 shows the absolute variance of 5 species (log-transformed and standardized). Because of standardization, those species that appeared in a few samples only (e.g. *Chaetoceros*) showed high relative changes, with peaks of more than 2 times their standard deviation, while for species that are present year-round (e.g. *Thalassionema nitzschioides*) relative changes were smaller. The standardized plots confirm that the species succession as indicated by Fig. 4 is realistic. It further shows that bloom events of *N. bicapitata* and *Chaetoceros* resting spores are restricted to distinct and short intervals within the upwelling season, and that the upwelling period is not characterized by a homogeneous group of species. This becomes more evident from the PCA biplot (Fig. 6) where the species belonging to the oceanic group have high scores on PC1 and the species from the pre-upweller group have high species on PC2 (PC1 and PC2 together explain 37.5% of variance). The other species however do not group together on one common axis, but have high scores on one of the axes PC3-6 (explaining another 37.5%).

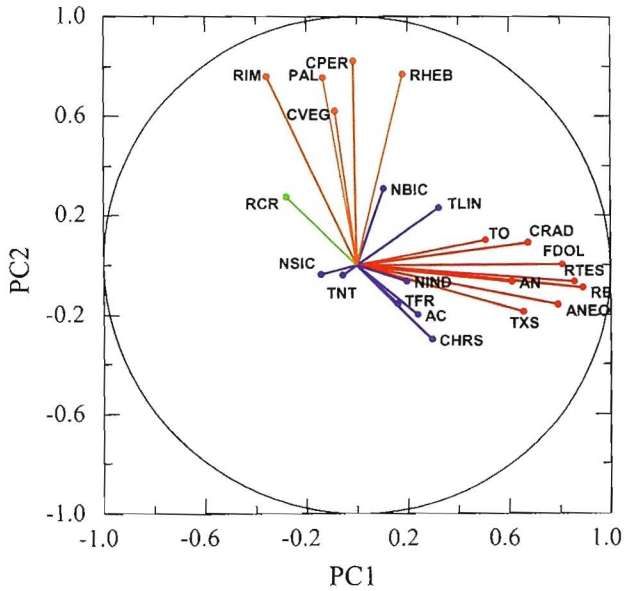

Fig. 6: Diatom species scores for the first two principal components of standardized diatom densities of the 22 most abundant diatom species from sediment traps MST-8B and MST-9G. Diatom species are represented by vectors. S pecies codes are explained in Table 2. Orange: pre-upwellers, blue: upwelling-species, red: post-upwellers (oceanics), green: other species.

Sediments

In the sediments, burial fluxes of autochthonous diatoms were an order of magnitude lower than the sediment trap fluxes, and also the species assemblage in the sediment differed significantly from the assemblage in the traps. Burial fluxes for most species belonging to the pre-upweller group are low and an important upwelling species like *N. bicapitata* is absent from the boxcore assemblage (Table 3).

Burial efficiencies, relative to the trap fluxes (Eq. 2), based on single diatom species were calculated for all species used in the Principle Component Analysis (Table 4). Almost all diatoms belonging to the pre-upweller group and some of the upwelling species had very low or zero burial efficiencies, thus indicating that they dissolve before burial. Highest burial efficiencies are found for the species from the oceanic group. In the sediment, fluxes are more or less constant with depth, with exception of the surface fluff layer. Mass accumulation rates are hard to determine in the fluff layer. The high diatom flux in there reflects the high diatom densities in the sample relative to deeper layers. Burial efficiency based on total diatom fluxes was 8.7% for the Somali slope and 6.7% for the Somali Basin (Table 5).

DISCUSSION

Sediment traps

The production of diatoms depends mainly on the availability of nutrients. In the upwelling area of the Indian Ocean along the coast of Somalia, high loads of dissolved silicate and other nutrients become available when the upwelling starts in early summer (Fig. 2a). Satellite images from late May 1992 showed the appearance of colder water along the coast, with distinct upwelling gyres at 5°N and 10°N, which merged into one large system as the monsoon progressed (Fig. 1). In response, particulate mass fluxes and biogenic silica fluxes on the slope increased by an order of magnitude (Conan and Brummer, 2000; Koning et al., 1997). Like these particulate mass fluxes, diatom fluxes on the Somali slope were largely determined by coastal upwelling, and 76% of the total annual diatom flux was intercepted during the 112 days of the upwelling season from July to October (Fig. 3b). The high diatom fluxes from July to October were in concordance with the lower temperatures, higher nutrient contents and higher primary production rates measured during the summer period (Baars et al., 1994; Veldhuis et al., 1997). Offshore, in the Somali Basin, coastal upwelling influence was less important and shorter in time. Here, only 39% of the total annual diatom flux occurred within the 98 days of the upwelling season (Fig. 3c).

Diatom fluxes in the sediment traps increased tenfold when the monsoon started. On the Somali slope, typical diatom fluxes during the winter months were in the order of 5–10 10^6 valves m^{-2} d^{-1}, increased to 50-100 10^6 valves m^{-2} d^{-1} in July, August, and September, and peaked at 201 10^6 valves m^{-2} d^{-1} at the end of the monsoon in October. The very high particulate mass flux in October (Fig. 3b) was probably caused by lateral transport of a resuspended carbonate mass originating from

Table 3: Diatom species fluxes in the boxcore samples for boxcore 905, Somali slope, and boxcore 915, Somali Basin. Species codes are explained in Table 2. All diatom fluxes are given in valves 10^6 m^{-2} y^{-1}.

	Pre-upwelling group					Upwelling species					
species	CPER	CVEG	PAL	RHEB	RIM	AC	NBIC	NIND	NSIC	TFR	TLIN
BX905/ fluff	0.00	0.00	0.00	0.00	0.00	20.67	31.00	0.00	20.67	5.17	10.33
BX905/ 0-1cm	0.00	0.00	0.00	10.05	0.00	0.00	0.00	0.00	0.00	10.05	15.08
BX905/ 5cm	0.00	0.00	0.00	0.00	0.00	0.00	0.00	4.50	0.00	2.25	0.00
BX905/ 10cm	0.00	0.00	0.00	0.00	0.00	4.60	0.00	0.00	0.00	2.57	4.60
BX905/ 15cm	0.00	24.57	0.00	5.17	0.00	5.17	0.00	0.00	0.00	0.00	5.17
BX905/ 20cm	0.00	0.00	0.00	5.69	0.00	5.69	0.00	0.00	0.00	2.72	5.69
BX905/ 25cm	0.00	0.00	0.00	5.30	0.00	0.00	0.00	0.00	0.00	0.00	0.00
burial flux 905 (10-25cm)	0.00	3.51	0.00	4.04	0.00	3.87	0.00	0.00	0.00	1.32	3.87
BX915/ fluff	0.00	0.00	1.33	5.31	0.00	5.31	0.00	1.33	2.66	2.66	5.31
BX915/ 0-1cm	0.00	2.46	0.00	5.27	1.41	5.27	1.41	0.00	2.46	0.70	3.87
BX915/ 5cm	0.00	0.00	1.87	0.00	0.93	0.00	0.00	0.00	0.00	0.47	2.80
BX915/ 10cm	0.00	0.00	2.11	2.11	1.06	1.06	0.00	0.00	1.06	1.06	3.17
BX915/ 15cm	0.00	1.12	1.12	1.12	1.12	2.23	0.00	0.00	0.00	0.00	1.12
BX915/ 20cm	0.00	0.00	0.00	1.58	0.00	1.58	0.00	0.00	1.58	0.00	2.37
burial flux 915 (10-20cm)	0.00	0.37	1.08	1.60	0.72	1.62	0.00	0.00	0.88	0.35	2.22

	Oceanic species group										Other
species	TNT	CHRS	AN	ANEO	CRAD	FDOL	RB	RTES	TO	TXS	RCR
BX905/ fluff	676.82	986.82	113.66	10.33	51.67	90.25	134.33	72.33	31.00	90.25	10.33
BX905/ 0-1cm	227.79	366.92	84.44	10.05	39.21	0.00	44.23	15.08	15.08	42.22	5.03
BX905/ 5cm	304.88	375.76	68.63	4.50	64.13	22.91	68.63	18.00	4.50	27.50	9.00
BX905/ 10cm	169.50	498.20	77.09	10.36	81.69	31.07	77.09	4.60	9.20	48.80	4.60
BX905/ 15cm	293.50	513.31	103.44	0.00	60.77	18.10	98.27	5.17	20.69	42.79	0.00
BX905/ 20cm	297.26	441.90	43.28	0.00	70.61	5.69	64.92	11.39	11.39	38.15	27.33
BX905/ 25cm	114.22	345.63	74.25	5.30	74.25	0.00	89.28	0.00	5.30	59.59	19.45
burial flux 905 (10-25cm)	218.62	449.76	74.51	3.91	71.83	13.72	82.39	5.29	11.65	47.33	10.82
BX915/ fluff	104.29	94.32	26.57	10.63	14.61	20.59	55.80	6.64	11.96	34.54	1.33
BX915/ 0-1cm	61.16	65.73	34.10	13.01	14.41	10.55	31.64	9.14	6.68	20.39	0.00
BX915/ 5cm	77.46	66.26	32.66	9.33	5.60	13.07	41.06	4.67	11.20	21.47	1.87
BX915/ 10cm	68.20	74.01	32.78	5.29	10.57	17.97	38.06	6.34	15.86	23.79	1.06
BX915/ 15cm	100.93	63.57	42.38	7.81	10.04	12.83	41.27	2.23	13.38	30.11	4.46
BX915/ 20cm	65.98	40.30	32.40	10.27	10.27	14.62	46.62	6.32	7.90	16.59	3.16
burial flux 915 (10-20cm)	78.37	59.29	35.85	7.79	10.29	15.14	41.98	4.97	12.38	23.50	2.89

Table 4: Burial efficiencies calculated for the single diatom species. Sediment trap diatom fluxes are total diatom fluxes for the year 1992-93 in valves 10^6 m^{-2}. Diatom burial fluxes are average fluxes for the sediment samples below the mixing depth and are given in valves 10^6 m^{-2} y^{-1} Species codes are explained in Table 2.

Species	DF trap B	DBF bc905	BE 905	DF trap G	DBF bc915	BE 915
Pre-upwellers						
CPER	41.8	0.0	0.0	48.2	0.0	0.0
CVEG	154.3	3.51	2.3	39.8	0.4	0.9
PAL	212.3	0.0	0.0	120.0	1.0	0.8
RHEB	101.9	4.0	4.0	106.7	1.6	1.5
RIM	276.7	0.0	0.0	157.3	0.7	0.4
Upwelling species						
AC	191.6	3.8	2.0	77.8	1.6	2.1
NBIC	1412.8	0.0	0.0	725.3	0.0	0.0
NIND	176.7	0.0	0.0	54.6	0.0	0.0
NSIC	247.4	0.0	0.0	75.7	0.9	1.2
TFR	317.9	1.3	0.4	87.6	0.3	0.4
TLIN	343.7	3.9	1.1	153.2	2.2	1.4
TNT	3777.0	218.6	5.8	1110.9	78.4	7.1
CHRS	2633.2	449.8	17.1	226.3	59.3	26.2
Post-upwelling oceanic species						
AN	65.1	74.5	114.4	69.7	35.8	51.4
ANEO	63.0	3.9	6.2	57.2	7.8	13.6
CRAD	38.4	71.8	187.0	54.4	10.3	18.9
FDOL	267.4	13.7	5.1	186.6	15.1	8.1
RB	438.2	82.4	18.8	457.3	42.0	9.2
RTES	93.1	5.3	5.7	126.7	5.0	4.0
TO	487.4	11.6	2.4	278.5	12.4	4.5
TXS	348.5	47.3	13.6	177.2	23.5	13.3
Other species						
RCR	124.1	10.82	8.7	19.8	1.0	5.0

the shelf break, which is indicated by the increased amounts of benthic foraminifera in the sediment trap sample of the same period (Koning et al., 1997; Conan and Brummer, 2000). The massive flux of *Chaetoceros* resting spores in the same period, however, does not seem to have the same origin since no surface sediments with a *Chaetoceros* content high enough to have caused this massive diatom flux were found and the biogenic silica content of the upper shelf sediments is very low, less than 1% (Koning et. al., 1997). Furthermore, the preservational state of the spores was excellent, as they showed no physical damage and often still contained protoplasm, which does not support a sedimentary origin. Trap MST-9G in the Somali Basin showed a species pattern similar to the slope trap, but with distinctly lower fluxes that

Table 5: Diatom burial efficiencies for the pre-upweller and oceanic diatom species groups, for the major upwelling species and for the total diatom assemblage. All diatom fluxes are given in valves $10^6 m^{-2} y^{-1}$

	DF trap B	DBF bc905	BE	DF trap G	DBF bc915	BE
pre-upweller group	787.0	6.0	0.8	472.0	3.7	0.8
Upwelling species						
TNT	3777.0	218.6	5.8	1110.9	78.4	7.1
NBIC	1412.8	0.0	0.0	725.3	0.0	0.0
CHRS	2633.2	449.8	17.1	226.3	59.3	26.2
Rest upwellers	1277.3	9	0.7	449	5	1.1
Oceanic group	1801.0	310.6	17.2	1407.6	151.9	10.8
Total Trap B	12623.0	1100.2	8.7			
Total Trap G				4853.2	325.7	6.7

reflect the decreased upwelling influence offshore. Apparently, for most of the 1992 monsoonal season, the area of intense coastal upwelling did not extend as far as the Somali Basin. Indeed, satellite images confirm that the two-gyre upwelling system was not constant in space and time, resulting in subsequent advances and retreats of the upwelling gyre over the Somali Basin site and thus in a sporadic occurrence of diatom blooms over the basin site (Veldhuis et al., 1997).

Annual diatom settling fluxes and biogenic silica settling fluxes on the Somali slope (12.6 10^9 valves m^{-2}) are comparable to those from coastal California (Sauter and Sancetta, 1992; Thunell et al., 1994; Thunell, 1998) but higher than fluxes found in areas of the Eastern Atlantic influenced by coastal upwelling, where diatom fluxes range from 0.5 to 5 10^9 valves m^{-2} (Lange et al., 1994; Jickells et al., 1996; Treppke et al., 1996a; Treppke et al., 1996b; Lange et al., 1998; Romero et al., 1999).

In the Somali slope region, three periods can be distinguished, pre-upwelling, upwelling and post-upwelling (Fig. 3b). These periods were characterized by a succession of distinct diatom species assemblages in the traps (Fig. 4a and b). The pre-upwelling period (samples b2 and b3) was characterized by high concentrations of small, weakly silicified species such as *Proboscia alata*, *Rhizosolenia imbricata, R. hebetata* and *R. crassispina*. The dominance of these pre-upwellers before the onset of the upwelling season was probably caused by their ability to adjust their buoyancy, which allows them to migrate to deeper levels below the euphotic zone to obtain the nutrients trapped there before the actual upwelling starts. (Villareal, 1988).

The upwelling period was characterized by the successive dominance of three diatom species, *Thalassionema nitzschioides, Nitzschia bicapitata* and *Chaetoceros* resting spores. *T. nitzschioides* (samples b4-b6), dominated the assemblage in July, when the two-gyre upwelling system was firmly established, temperatures were the lowest (17.3°C, Baars et. al., 1994) and H_4SiO_4 concentrations in the surface waters were high (Fig. 2). *T. nitzschioides* tolerates variable conditions but is usually recorded from upwelling regions with increased nutrient supply (Hasle and Mendiola,

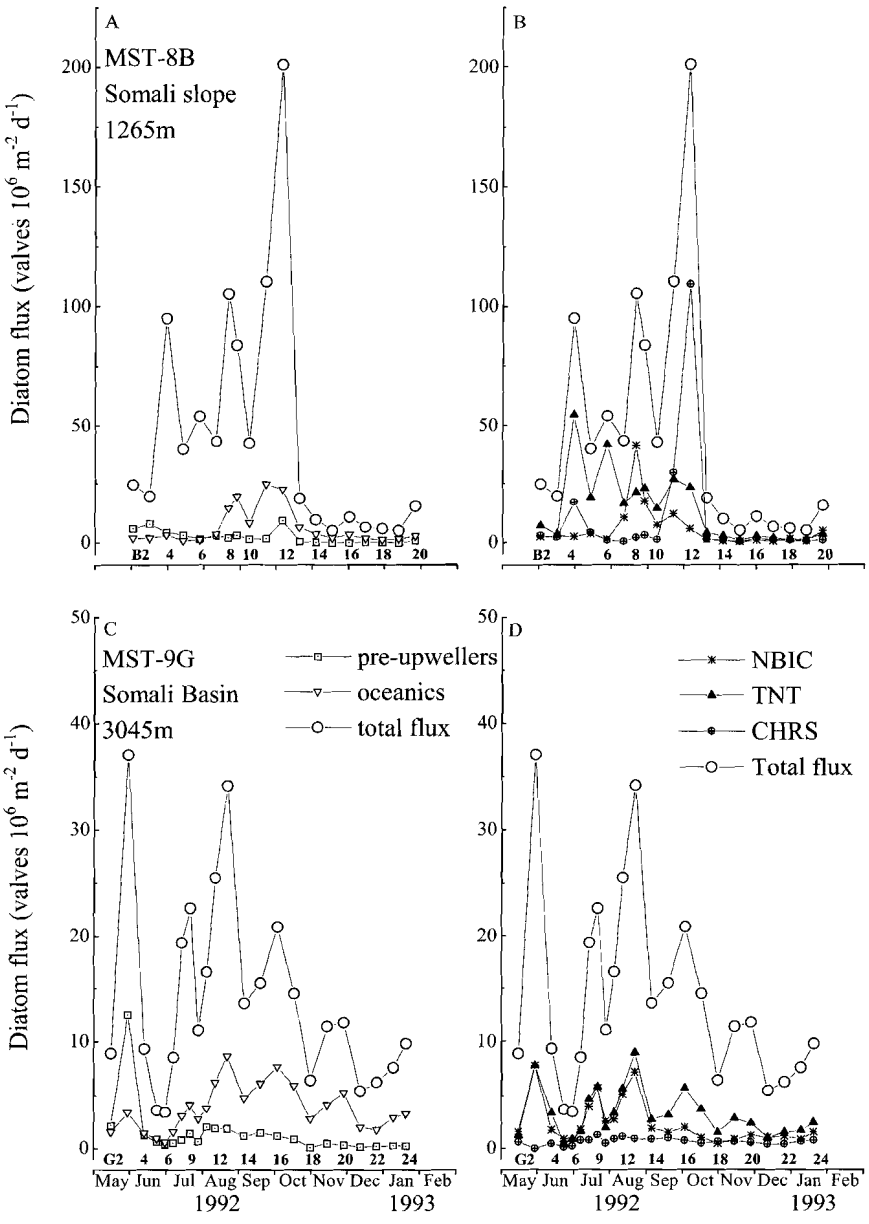

Fig. 7: Diatom fluxes when species are grouped as pre-upwellers, upwellers species and post-upwelling oceanics (species codes and clusters are explained in Table 2). MST-8B, Somali slope (top) and MST-9G, Somali Basin (bottom).

1967; Margalef, 1978; Schuette and Schrader, 1981; Sancetta, 1982; Abrantes, 1988; Lange et al.,1998; Romero et al., 1999). In sediment traps in the eastern Equatorial and North Atlantic, *T. nitzschioides* showed peak fluxes during spring and summer coastal upwelling (Lange et al., 1998; Romero et al., 1999). From Figs. 4a and 7, the dominance of *T. nitzschioides* in the July assemblage is evident (80% (Fig. 4a) and a species flux of up to 55 10^6 m^{-2} d^{-1}). The low values found for the diversity index h′ confirm the presence of a bloom assemblage with a low diversity and an important contribution of a single upwelling species, in this case *T. nitzschioides* (Fig. 4a).

In August, the diatom assemblage shifted towards high concentrations of a second important diatom in the upwelling period, the small, fragile diatom *N. bicapitata*, which is considered to indicate oceanic upwelling conditions (Lange et al., 1994; Treppke et al., 1996a; Lange et al., 1998; Romero et al., 1999). As seen in satellite images, by September the upwelling gyre had already retreated to the Somali slope site (Fig. 1). We therefore interpret the massive appearance of *N. bicapitata* in August and September as a result of the retreat of the upwelling system from the Somali Basin.

Chaetoceros resting spores, which dominated the diatom assemblage in October, (b11-b12) is known from coastal areas with high nutrient levels (Hargraves and French, 1975; Garrison, 1981; Pitcher, 1990) and forms resting spores to survive nutrient deficient conditions (Pitcher, 1986). In October, at the end of the SW monsoon, nutrients were nearly assimilated to exhaustion, what could have initialized the massive formation of *Chaetoceros* resting spores.

The post-upwelling assemblage, present year-round but dominant during the intermonsoon and NE monsoon periods (samples b13-b20) was more diverse, due to the contribution of tropical, oligotrophic species. Important taxa in this oceanic species group were *Rhizosolenia bergonii, Thalassiothrix spathulata* and *Thalassiosira oestrupii*. On the Somali slope, highest fluxes of oceanic species were found at the end of the upwelling period, in August to October, when the upwelling gyre had already retreated from the Somali Basin (Fig. 7). In the Somali Basin, fluxes of oceanic species were more or less constant throughout the sampled period.

Although the relations between the individual diatom species appear to be evident from their successive dominance in the slope trap, this dominance is based on the relative abundance of a species in the assemblage. In the pre-upwelling and post-upwelling periods, when species fluxes are low, the importance of a species could be overestimated because of the absence of the upwelling species that generate the massive diatom fluxes during the SW monsoon. To confirm the observed covariability between the diatom species, a Principal Component Analysis was carried out. The species scores extracted from the analysis indicate that two distinct diatom groups can be recognized, the group of pre-upwelling species, with high scores on PC2 and the group of post-upwelling species, with high scores on PC1. The orthogonal species vectors for the diatom species (Fig. 6) indicate that no correlation exists between the two species groups. The upwelling assemblage, however, shows a diffuse and heterogeneous pattern on PC1 and PC2 (Fig. 6). The major upwelling species have high scores on different principal components, but not on one common principal component associated with upwelling. This indicates that the upwelling species do not form one coherent group, but rather a succession of dominating species (Figs. 4 and 5).

In the sediment traps on the Somali slope and in the Somali Basin, benthic diatoms that originate from a water depth of less than 200m, were never abundant. In the Somali slope trap, fluxes of benthic diatoms showed an increase only at the beginning and at the end of the upwelling period, probably due to increased energetic conditions and resuspension on the shelf caused by the changing monsoonal circulation patterns. As expected, no periods of increased benthic diatom influx were found in the trap in the Somali Basin, proving that resuspension is not of importance at this deep ocean site, 250km off the coast.

Sediments

The diatom assemblage in the sediment below the sediment traps differed significantly from the assemblage found in the traps. To interpret these differences, diatom group burial efficiencies and single species burial efficiencies were calculated for the 22 most abundant species (Tables 4 and 5). Burial efficiencies for the weakly silicified pre-upwellers and the upweller *Nitzschia bicapitata* are very low or zero and these species are no longer present in the sediment assemblage. Apparently these species dissolve at the sediment-water interface before being buried. We can exclude their disappearance due to dissolution in the water column below the traps, because these same species are still present in the MST-9G trap, 1500m deeper than trap MST-8B. At the Somali slope site, a significant decrease in diatom flux was observed between the fluff sample and the 0-1cm sample (Table 3, Fig. 8), but the downcore percentages of the 3 diatom species groups are about constant. This again confirms that most dissolution and, as a consequence, the major shift in diatom species assemblage takes place at the sediment water interface.

Of the upwelling species, *Thalassionema nitzschioides* and *Chaetoceros* resting spores have high fluxes and relatively high species burial efficiencies. In the sediment below the slope trap, these species are present in significant amounts, about 60% of the total diatom flux, and they thereby preserve the upwelling signal recorded in the sediment trap. At the Somali Basin site, where upwelling is less important, the flux of *Chaetoceros* resting spores is lower and the burial flux of upwellers is also lower, around 40%. As suggested by the species burial efficiencies (Table 3), several diatom species in the oceanic group appear dissolution resistant resulting in sediment enrichment in taxa such as *Azpeitia nodulifer* and *Coscinodiscus radiatus*. The oceanic species group has a high burial efficiency, comparable to the burial efficiency of *Chaetoceros* resting spores and is higher on the Somali slope than in the basin.

All burial efficiencies compare a 1-year sediment trap record and a particulate diatom flux representative only for the season 1992-1993, with a time-integrated burial flux of >750 years for the Somali slope sediment and >3000 years for the Somali Basin sediment (Table 1). As mentioned before, particulate fluxes may vary widely on an annual basis, and the resulting calculated burial fluxes would fluctuate accordingly. Burial efficiencies at the Somali slope could have been overestimated, if particulate diatom fluxes for 1992-1993 were below average. Indeed, satellite images show that temperatures during the monsoon of 1992 were relatively high, which may indicate less intense coastal upwelling (Rixen et al. 1996). Burial efficiencies must be interpreted with caution, but some general patterns are evident. The weakly silicified

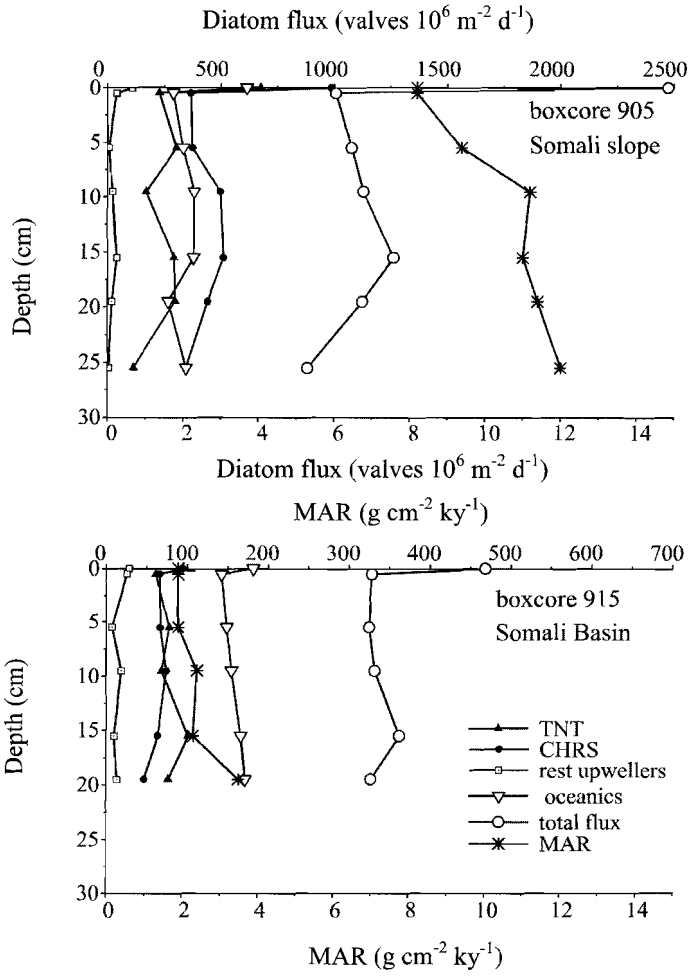

Fig. 8: Downcore profiles of total diatom fluxes and fluxes in boxcores 905 (Somali slope) and 915 (Somali Basin) for the same diatom species groups as in Fig. 7.

species in the pre-upweller group and upwelling species like *Nitzschia bicapitata*, *Nitzschia sicula* and *Neodelphineis indica* have burial efficiencies that are close to zero. Well preserved species, with high particulate fluxes and relatively high burial efficiencies, are the upwellers *Thalassionema nitzschioides* and *Chaetoceros* resting spores, as well as the oceanic species *Rhizosolenia bergonii*, *Roperia tesselata* and *Thalassiothrix spathulata*. Most of the weakly silicified pre-upwelling and upwelling species have lower burial efficiencies in the Somali Basin than on the Somali slope, which could be caused by prolonged residence at the sediment-water interface, due to the lower sedimentation rates at the deep basin site. For the more resistant species, burial efficiencies are about equal at both sites.

Based on total fluxes from sediment traps and surface sediments, total diatom burial efficiency is 8.7% for the Somali slope and 6.8% for the Somali Basin. These values are somewhat higher than the burial efficiency of 1% found by Treppke et al. (1996a), for their trap site in the Guinea Basin in the Eastern Equatorial Atlantic, at a water depth of 4481m.

ACKNOWLEDGMENTS

The cruises with R.V. Tyro to the NW Indian Ocean (1992/1993) were financially supported by The Netherlands Marine Research Foundation and by NIOZ. We thank Captain J. de Jong, officers and crew of R.V. Tyro for their assistance, as well as the technicians of NIOZ who participated in the cruises and preparations. We thank Rineke Gieles for $CaCO_3$ measurements. We are grateful to Katja Philippart for an introduction in the secrets of PCA analyses. Martien Baars surveyed the 1992 NOAA archive at the Rosenstiel School of Marine and Atmospheric Sciences (RSMAS), Miami, and transferred a selection to NIOZ. Don Olson and Sharon Smith at RSMAS are thanked for help and financial support regarding the satellite pictures. The helpful comments of two anonymous reviewers helped us to structure our thoughts and greatly improved the manuscript.
This is publication number 3491 of the Netherlands Institute for Sea Research.

REFERENCES

Abrantes, F. (1988). Diatom assemblages as upwelling indicators in surface sediments off Portugal. Marine Geology, 85, 15-39.

Baars, M.A., Bakker, K.M.J., De Bruin, T.F., Van Couwelaar, M., Hiehle, M.A., Kraaij, G.W., Oosterhuis, S.S., Schalk, P.H., Sprong, I., Veldhuis, M.J.W., Wiebinga, C.J., Witte, J.IJ. (1994). Seasonal fluctuations in plankton biomass and productivity in the ecosystems of the Somali Current, Gulf of Aden and southern Red Sea. In Monsoons and pelagic systems; Cruise Reports Netherlands Indian Ocean Programme, ed. M. Baars, Vol. 1, pp. 45-54. National Museum of Natural History.

Batterbee, R.W. (1973). A new method for the estimation of absolute microfossil numbers, with reference especially to diatoms. Limnology and Oceanography, 18, 647-653.

Brock, J.C., McClain, C.R., Hay, W.W. (1992). A southwest monsoon hydrographic climatology for the northwestern Arabian Sea. Journal of Geophysical Research, 97, 9455-9465.

Broecker, W.S., Peng, T.-H. (1982). Tracers in the Sea. Eldigio, Palisades, NY, 690pp.

Brzezinski, M.A., Nelson, D.M. (1995). The annual silica cycle in the Sargasso Sea near Bermuda. Deep-Sea Research I, 42, 1215-1237.

Conan, S.M.-H., Brummer, G.-J.A. (2000). Fluxes of planktic foraminifera in response to monsoonal upwelling on the Somalia Basin margin. Deep-Sea Research II, 47, 2207-2227.

Fischer, J., Schott, F., Stramma, L. (1996). Current and transports of the Great Whirl-Socotra Gyre system during the summer monsoon, August 1993. Journal of Geophysical Research, 101, 3573-3587.

Garrison, D.L. (1981). Monterey Bay phytoplankton II. Resting spore cycles in coastal diatom populations. Journal of Plankton Research, 3, 137-156.

Gersonde, R., Wefer, G. (1987). Sedimentation of biogenic siliceous particles in Antarctic waters from the Atlantic sector. Marine Micropaleontology, 11, 311-332.

Hargraves, P.E., French, F. (1975). Observations on the survival of diatom resting spores. Nova Hedwigia Beiheft, 53, 229-240.

Hasle, G.R., Mendiola, B.R. (1967). The fine structure of some *Thalassionema* and *Thalassiothrix* species. Phycologia, 6, 107-125.

Hitchcock, G.L., Olsen, D.B. (1992). NE and SW monsoon conditions along the Somali coast during 1987. In: B.N. Desai (Ed.) Oceanography of the Indian Ocean. Oxford & IBH, New Delhi, 583-593.

Hurd, D.C. (1973). Interactions of biogenic opal sediment and sea water in the central equatorial Pacific. Geochimica et Cosmochimica Acta, 37, 2257-2282.

Jickells, T.D., Newton, P.P., King, P., Lampitt, R.S., Boule, C. (1996). A comparison of sediment trap records of particle fluxes from 19 to 48 °N in the Northeast Atlantic and their relation to surface water productivity. Deep-Sea Research I, 43, 7, 971-986.

Knappertsbusch, M., Brummer, G.-J. A. (1995). A sediment trap investigation of sinking coccolithophorids in the North Atlantic. Deep-Sea Research I, 42, 1083-1109.

Koning, E., Brummer, G.J.A., Van Raaphorst, W., Van Bennekom, A.J., Helder, W., van Iperen, J.M. (1997). Settling, dissolution and burial of biogenic silica in the sediments off Somalia (northwestern Indian Ocean). Deep-Sea Research II, 44, 1341-1360.

Lange, C.B., Treppke, U.F., Fischer, G. (1994). Seasonal diatom fluxes in the Guinea Basin and their relationships to trade winds, ITCZ migrations and upwelling events . Deep-Sea Research I, 41, 859-878.

Lange, C.B., Romero, O.E., Wefer, G., Gabric, A.J. (1998). Offshore influence of coastal upwelling off Mauritania, NW Africa, as recorded by diatoms in sediment traps at 2195m water depth. Deep-Sea Research I, 45, 985-1013.

Lisitzin, A.P. (1972). Sedimentation in the world ocean, Society of Economic Paleontologists and Mineralogists Special Publication, 17, 218pp.

Margalef, R. (1978). Size of centric diatoms as an ecological indicator. Mitteilungen internationale Verein fur theoretische angewendete Limnologie, 17, 202-210.

Nair, R.R., Ittekot, V., Managanin, S.J., Ramaswamy, V., Haake, B., Degens, E.T., Desai, B.N., Honjo, S. (1989). Increased particle flux to the deep ocean related to monsoons. Nature, 338, 749-751.

Nelson, D.M., Tréguer, P., Brzezinski, M.A., Leynaert, A., Quéguiner, B. (1995). Production and dissolution of biogenic silica in the ocean: Revised global estimates, comparison with regional data and relationship to biogenic silica sedimentation. Global biogeochemical cycles, 9, 359-372.

Pitcher, G.C. (1986). Sedimentary flux and the formation of resting spores of selected *Chaetoceros* species at two sites in the southern Benguela system. South African Journal of marine Science, 4, 231-244.

Pitcher, G.C. (1990). Phytoplankton seed populations of the Cape Peninsula upwelling plume, with particular reference to resting spores of *Chaetoceros* (Bacillariophyceae) and their role in seeding upwelling waters. Estuarine Coastal Shelf Science, 31, 283-301.

Prell, W.L. (1984). Variation of monsoonal upwelling: A response to changing solar radiation. In: Hansen, J.E., Takahashi, T. (Eds.) Climate processes and climate sensitivity. American Geophysical Union, Geophysical Monograph Series, 29, 48-57.

Rixen, T., Haake, B., Ittekkot, V., Guptha, M.V.S., Nair, R.R., Schluessel, P. (1996). Coupling between SW monsoon related surface and deep ocean processes as discerned from continuous particle flux measurements and correlated satellite data.
Journal of Geophysical Research, 101, (12), 28569-28582.

Romero, O.E., Lange, C.B., Fischer, G., Treppke, U.F., Wefer, G. (1999). Variability in export production documented by downward fluxes and species composition of marine planktic diatoms: observations from the tropical and equatorial Atlantic. In: G. Fischer and G. Wefer (Eds.) Use of Proxies in Paleoceanography, Springer-Verlag, Berlin, Heidelberg, New York, Barcelona, Hong Kong, London, Milan, Paris, Singapore, Tokyo, pp. 365-392.

Sancetta, C. (1982). Distribution of diatom species in surface sediments of the Bering and Okhotsk Seas. Micropaleontology, 28, 221-257.

Sauter, L.R., Sancetta, C. (1992). Seasonal associations of phytoplankton and planktic foraminifera in an upwelling region and their contribution to the seafloor.
Marine Micropaleontology, 18, 263-278.

Schott, F. (1983). Monsoon response of the Somali Current and associated upwelling. Progress in Oceanography, 12, 357-381.

Schott, F., Swallow, J.C., Fieux, M. (1990). The Somali Current at the equator: annual cycle of currents and transports in the upper 1000m and connection to neighboring latitudes. Deep-Sea Research I, 37, 1825-1848.

Schrader, H.J. (1974). Proposal for a standardized method of cleaning diatom bearing deep-sea and land-exposed marine sediments. Nova Hedwigia, 45, 403-409.

Schuette, G., Schrader, H.J. (1981). Diatom taphocoenoses in the coastal upwelling area off southwest Africa. Marine Micropaleontology, 6, 131-155.

Smith, S.L., Codispoti, L.A. (1980). Southwest monsoon of 1979: chemical and biological response of Somali coastal waters. Science, 209, 597-600.

Smith, S.L. (1984). Biological indications of active upwelling in the northwestern Indian Ocean in 1964 and 1979, and a comparison with Peru and northwest Africa. Deep-Sea Research I, 31, 951-967.

Tabachnick, B.G., Fidell, L.S. (1996). Using multivariate statistics, Harper Collins College Publishers, 880 pp.

Tchernia, P. (1980). The Indian Ocean: Topography-Winds-Climatology-Currents. In: Descriptive Regional Oceanography, Pergamon Marine Series, Volume 3, Pergamon Press, Oxford, New York, Toronto, Sydney, Paris, Frankfurt, pp. 171-215.

Thunell, R.C., Pride, C.J., Tappa, E., Muller-Karger, F.E. (1994). Biogenic silica fluxes and accumulation rates in the Gulf of California. Geology, 22, 303-306.

Thunell, R.C. (1998). Particle fluxes in a coastal upwelling zone: sediment trap results from Santa Barbara Basin, California. Deep-Sea Research II, 45, 1863-1884.

Tomczak, M., Godfrey, J.S. (1994). Hydrology of the Indian Ocean. In: Tomczak, M. and Godfrey, J.S., Regional Oceanography, an Introduction, Pergamon Press, Oxford, New York, Toronto, Sydney, Paris, Frankfurt, pp. 221-236.

Tréguer, P., Nelson, D.M., van Bennekom, A.J., DeMaster, D.J., Leynaert, A., Quéguiner, B. (1995). The silica balance in the world ocean: a reestimate. Science, 268, 375-379.

Treppke, U.F., Lange, C.B., Wefer, G. (1996a). Vertical fluxes of diatoms and silicoflagellates in the eastern equatorial Atlantic and their contribution to the sedimentary record. Marine Micropaleontology **28**, 73-96.

Treppke, U.F., Lange, C.B., Donner, B., Fischer, G., Ruhland, G., Wefer, G.(1996b). Diatom and silicoflagellate fluxes at the Walvis Ridge: An environment influenced by coastal upwelling in the Benguela system. Journal of Marine Research, 54, 991-1016.

Van Weering, T.C.E., Helder, W. and Schalk, P. (1997). Netherlands Indian Ocean Programme 1992-1993, first results and an introduction. Deep-Sea Research II, 44, 6-7, 1177-1193.

Veldhuis, M.J.W., Kraay, G.W., Van Bleijswijk, J.D.L., Baars, M.A. (1997). Seasonal and spatial variability in phytoplankton biomass, productivity and growth in the northwestern Indian Ocean; the SW and NE monsoon, 1992-1993. Deep-Sea Research I, 44, 425-449.

Villareal, T.A. (1988). Positive buoyancy in the oceanic diatom *Rhizosolenia debyana*. H. Peragallo. Deep-Sea Research I, 35, 1037-1045.

Webster, P.J. (1987). The elementary monsoon. In: Fein, J.S., Stephens, P.L. (Eds.) Monsoons, Wiley, New York, pp. 3-32.

Wilkinson, L. (1988). SYSTAT, the system for statistics. SYSTAT, Chicago, USA.

CHAPTER 5

Biogenic silica accumulation and diatom species as tracers for paleo-upwelling in a Somalian Margin core.

Erica Koning, Tjeerd C.E. van Weering, Jolanda M. van Iperen,
Wim van Raaphorst and Willem Helder

ABSTRACT

A high-resolution biogenic silica accumulation record in a piston core from the Somalian Margin, directly below one of the present-day upwelling gyres, strongly reflects changes in upwelling intensity during the past 115 ky. In the Holocene, 2 long intervals of continuously increasing upwelling intensity occurred, terminated by abrupt cold events at 8.2 and 5.9 ky BP, respectively. The diatom species assemblage of selected samples was studied in detail to determine the preservation of upwelling-indicating diatoms and to assess the applicability of biogenic silica as a tracer for paleo-upwelling intensity. Biogenic silica accumulation rates in the sediment ranged from 0.01g cm^{-2} ky^{-1} in glacial periods to 1.02 g cm^{-2} ky^{-1} in the early Holocene. During intervals with elevated biogenic silica accumulation, 'upwelling' diatoms dominated, except for two samples in early isotope stage 3, when oceanic species dominated the assemblage. The biogenic silica accumulation record fluctuates in accordance with the SPECMAP marine $\delta^{18}O$ record indicating that the accumulation of biogenic silica on the Somalian Margin is related to global climate variations. Upwelling was more intense in the early Holocene and in the last interglacial than it is at present, but was of minor importance during glacial periods. The 50-year resolution biogenic silica record from the Holocene shows that accumulation of biogenic silica and thus upwelling intensity fluctuated at millennial and centennial time scales. The continuously increasing biogenic silica accumulation rates during the early Holocene suggest a gradual deglaciation of the Tibetan Plateau with abrupt returns to colder conditions at the Holocene cold event and at the late Holocene aridification. This study presents the first high-resolution biogenic silica record from the NW Indian Ocean Monsoon system and shows that in this area of the NW Indian Ocean biogenic silica is an excellent indicator for changes in paleo-upwelling intensity.

This chapter has been submitted to Paleoceanography

INTRODUCTION

The modern Somalian Margin of the northwestern Indian Ocean is characterized by intense summer upwelling, driven by the seasonal heating of the Tibetan Plateau. During boreal summer, differential heating of the plateau causes the formation of an area of low pressure over the warm Asian continent, in contrast to the relatively cold southern Indian ocean where pressure is high (Clemens et al., 1991; Brock et al., 1992; Clemens et al., 1996). The resulting strong, southwesterly winds over the Somalian Margin induce offshore transport of surface waters and upwelling of nutrient-rich deep waters at about 5 and 10°N (Schott, 1983; Schott et al, 1990; Fischer et al., 1996). In autumn, the air over the Tibetan Plateau cools, causing high pressure over Tibet and low pressure over the southern Indian Ocean and resulting in winds blowing from NE to SW, the NE monsoon. Surface circulation reverses and the Somali current flows southward until upwelling starts again in June. Although extent and intensity of monsoonal upwelling may vary widely on an annual basis (Smith and Codispoti, 1980; Smith, 1984; Hitchcock and Olsen, 1992; Rixen et al., 1996), the region is considered to be one of the most productive in the world oceans (Smith and Codispoti, 1980; Smith, 1984).

Climate changes that influence the strength of the monsoonal winds, and thus upwelling intensity, could be reflected in a direct response of diatom productivity that, in turn, is recorded in the sediments. To define changes in upwelling intensity in the geological record a 15m long piston core (TY93-905P, recovery 15m, water depth 1500m), covering 115 ky, was taken directly below the Somalian upwelling system (Fig. 1). From this core the oxygen isotope record from the foraminifera *Globigerina bulloides, Globigerinoides ruber* and *Neogloboquadrina dutertrei* and the foraminiferal records of *G. bulloides*, a species indicative for upwelling conditions, were studied in detail (Ivanova, 1999; Peeters, 2000). These studies attributed the increased productivity observed in interglacial periods to enhanced upwelling intensity.

Glacial-interglacial changes in productivity have been studied extensively in different areas of the world oceans. In contrast to the Atlantic and Pacific Oceans, where productivity was high during glacial periods (Abrantes, 1988; Schrader,1992), biogenic silica accumulation is low in glacial sediments from the Indian Ocean, indicating lower productivity during cold intervals (Sirocko, 1991). A number of studies have shown that the monsoonal system responds to changes in orbital forcing (Prell, 1984; Clemens et al, 1991; Clemens et al, 1996; Reichart et al, 1998). The associated variability of upwelling intensity was observed in sediment cores, ice cores, loess records, lake sediments and tree rings (e.g. Weedon and Shimmield, 1991; Shimmield and Mowbray, 1991; Feng et al, 1999; Altabet et al, 1995; Gasse and van Campo, 1994; Thompson et al; 1989; Thompson et al, 1997). The majority of these studies, however, focussed on the northern Arabian Sea and the upwelling area off Oman. Sediment cores from the northern Arabian Sea often show laminated, organic-rich bands, reflecting strong monsoonal productivity (Schulz et al., 1998; Reichart et al., 1998), but on the Somalian Margin, no laminated sediments are found. Tribovillard et al. (1996) attributed the lack of enhanced preservation of organic matter under upwelling conditions in sediment cores on the Somalian Margin to

increased mineralization at the sediment-water interface. The increased terrigenous content of the sediments and the high accumulation rates of eolian dust during the last glacial documents the high aridity during this period (Sirocko, 1991; Shimmield and Mowbray, 1991; Sirocko 1993). So far, no detailed studies have addressed the records of biogenic silica and diatoms of the Somalian Margin, that could reflect the direct response of diatom production to changes in monsoon-induced upwelling intensity.

Particulate settling fluxes, diatom assemblages and preservation of biogenic silica in the water column and at the sediment-water interface were discussed in earlier papers (Koning et al., 1997; Koning et al., 2001), but their main results are summarized below for the sake of establishing the comparison between the recent and past upwelling systems. Particulate settling fluxes of biogenic silica, as measured in a sediment trap at 268 mab, increased tenfold during the SW monsoon of 1992 and showed a distinct seasonal signal with a pré-upwelling, an upwelling and a post-upwelling period. This seasonal signal of biogenic silica was also reflected in the diatom species composition in the settling material. It was shown that 76% of the annual diatom species flux to the sediment was produced within the 112 days of the duration of the SW monsoon, and a distinct succession of dominant species over time could be recognized. Two well-silicified diatom species, *Thalassionema nitzschioides* and *Chaetoceros* resting spores characterized the SW monsoonal upwelling. Only a small fraction (8%) of the diatom flux was preserved in the surface sediment directly underneath the trap, due to the dissolution of weakly silicified species at the sediment-water interface. The two 'upwelling' species were shown to dominate the surface sediment, and thereby preserve the upwelling signal produced in the overlying waters.

The objective of this study is to relate the sedimentary biogenic silica record of the Somalian upwelling system to glacial-interglacial cycles and to fluctuations on millennial and centennial time-scales. We will show that periods of high biogenic silica accumulation occur associated with the presence of the two upwelling indicating diatom species that characterize the modern SW monsoon.

MATERIALS AND METHODS

All samples discussed in this paper were collected during the Netherlands Indian Ocean Programme (NIOP, 1992-1993; van Hinte et al., 1995), at site TY93-905, located at 10°47'N 51°56'E, 80km off the Somali coast on the mid-slope at a water depth of 1500m and directly below one of the main upwelling gyres (Fig. 1). At this site a 15m long piston core was recovered. In the laboratory, subsamples of the core were taken at 10cm intervals, which provides, given the sedimentation rate of approximately 20cm kyr^{-1} (Fig. 2a), a resolution of 500 years. The upper 400cm of the core, covering the last 14 ky, was sampled every cm, providing a resolution of about 50 years. All samples were dried, ground and analyzed for biogenic silica using a modified version of the automated wet chemical leaching method of Müller and Schneider (1993), following the methods described in Koning et al. (1997). To identify layers rich in magnetic minerals, i.e. Fe-bearing minerals, identifying eolian

dust input, magnetic susceptibility was measured at 2cm resolution using a Bartington MS2E1 handheld sensor and a high-resolution Fe-record was determined with the CORTEX XRF-scanner (Jansen et al., 1999).

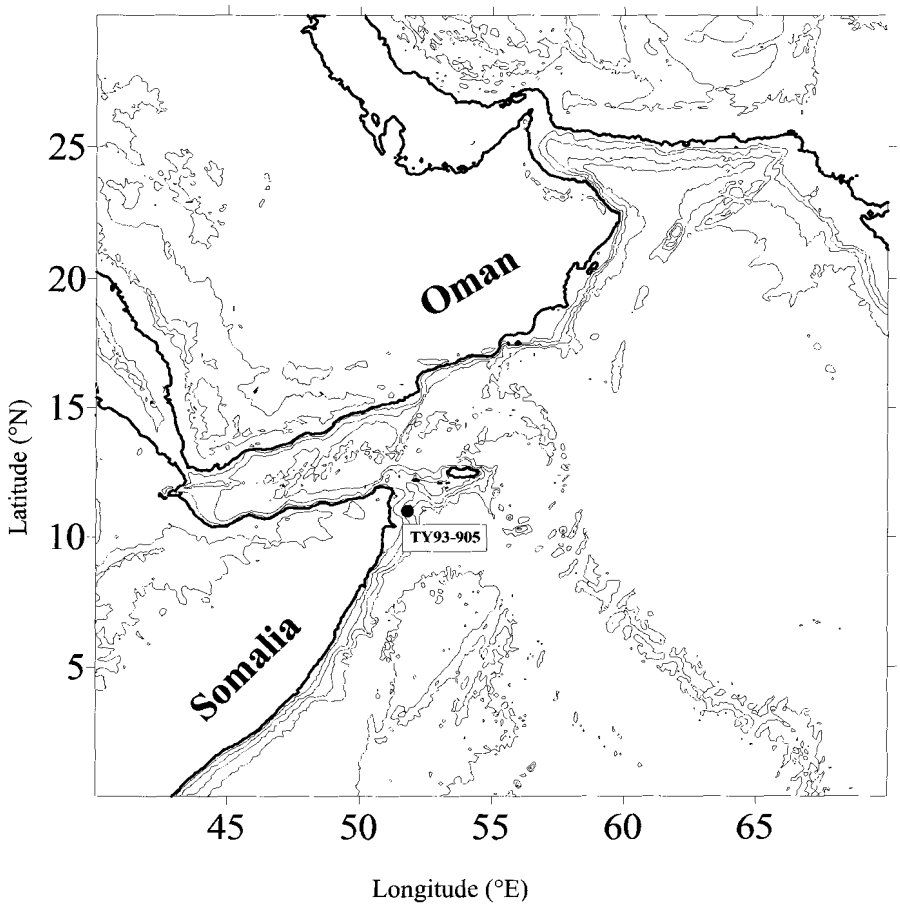

Fig. 1 A map of the study site on the Somalian Margin with the position of station TY93-905.

The age model for the core was derived from the correlation of the oxygen isotope records of *G. bulloides* and *N. dutertrei* to the SPECMAP timescale (Imbrie et al., 1984). Age control was based on 14 AMS ^{14}C datings (Fig. 2). Samples were dated at the R.J. van der Graaff Laboratory in Utrecht (Ivanova, 1999; Ganssen et al.,

1995). After subtracting 400 years for reservoir age (Bard, 1988) the radiocarbon ages were calibrated to calendar years BP (Bard et al., 1990; Bard et al., 1993). Age estimates for individual levels in the core are based on a linear interpolation between the age control points. From the age model, linear sedimentation rates (LSR) were calculated (Fig. 2). Dry bulk density (DBD) was determined by weighing a fixed volume of wet sediment after drying at 50°C. From DBD and LSR mass accumulation rates were calculated as: MAR (g cm^{-2} ky^{-1}) = DBD (g cm^{-3})* LSR (cm ka^{-1}).

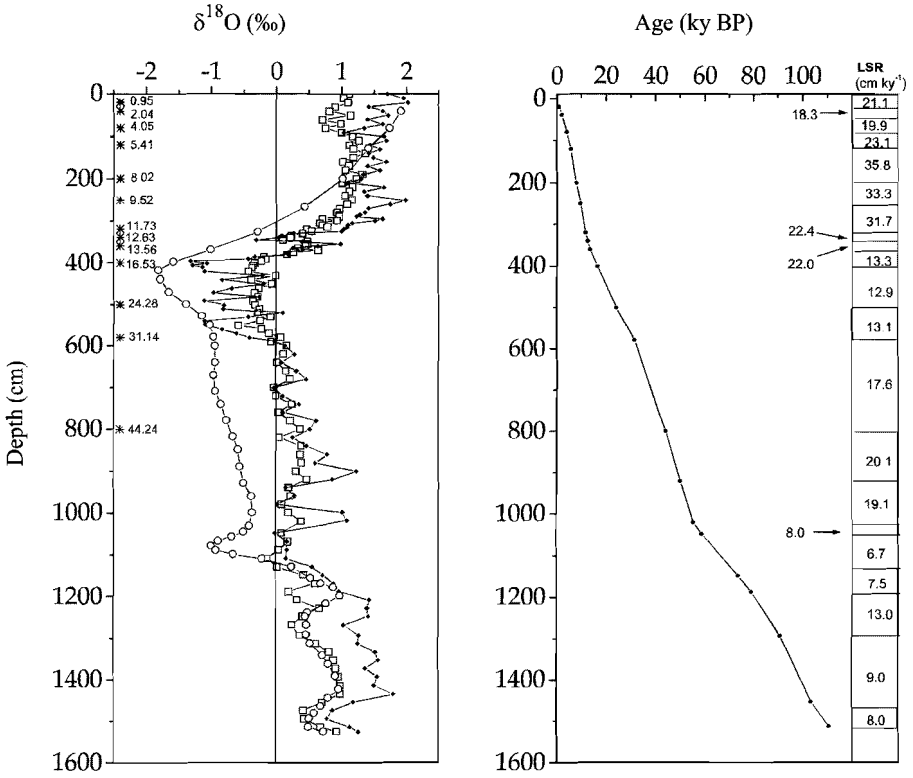

Fig. 2: Oxygen isotope records ($\delta^{18}O$) of *Globigerina bulloides* (open squares) and *Neogloboquadrina dutertrei* (solid diamonds) from core TY93-905P on the Somalian Margin and the SPECMAP $\delta^{18}O$ curve (open circles, Imbrie et al., 1994). Stars represent age control points (left panel). Age model and linear sedimentation rates calculated from the age model for core TY93-905P (right panel).

The selection of core samples for diatom species analysis was based on the biogenic silica content. Fourteen samples were selected from glacial and interglacial intervals, with high and low biogenic silica accumulation rates, respectively. A detailed

description of the methods for the determination of the diatoms as applied in sediment trap and surface samples is given in Koning et al. (2001). Total diatom burial flux was calculated as: DD (10^6 valves $gdry^{-1}$) * MAR, where DD is diatom density (Koning et al, 2001). Burial fluxes for single species in a sample were calculated by multiplying the total diatom burial flux with the fraction of the species in the sample.

RESULTS

The biogenic silica content ranged from ~0.2% during most of the last glacial to about 5% during the last interglacial and during the early Holocene (Fig. 3). The biogenic silica record of the core shows agrees with the SPECMAP global isotope record and indicates that biogenic silica content is usually high in warm interglacial and interstadial periods (Fig. 3).

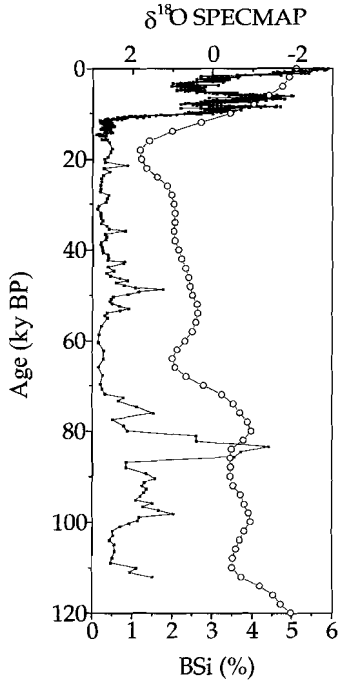

Fig. 3: Downcore record of biogenic silica content (solid squares) in %SiO2 of total dry mass and the SPECMAP $\delta^{18}O$ curve (open circles, Imbrie et al., 1994).

Fe- and Ti-records and magnetic susceptibility could give information on the presence of Fe-bearing minerals that would indicate enhanced dust transport in cold, arid intervals. The magnetic susceptibility record and the Fe record from the CORTEX XRF-scanner, however show low values (<1Fe%, based on calibration curves given by Jansen et al., 1998) throughout the core with little variation and no evidence for increased eolian input to the sediments on the Somalian Margin in glacial stages (Fig. 4).

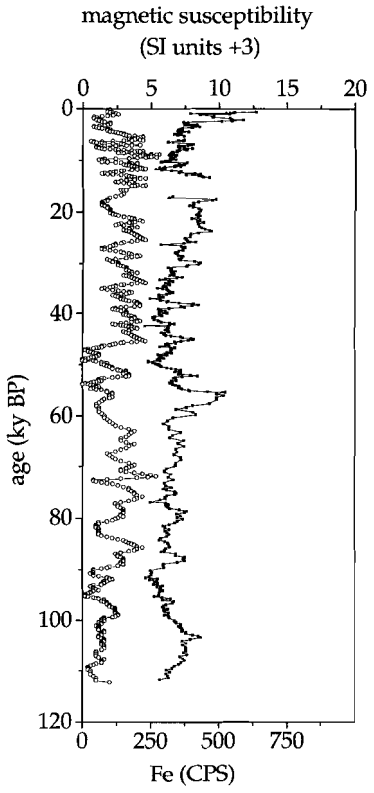

Fig. 4: Magnetic susceptibility record (open circles) and Fe-record (solid squares) as obtained with the CORTEX core scanner (units: counts per second).

Biogenic silica burial fluxes varied by two orders of magnitude (Fig. 5). Like the BSi content (Fig. 3), BSi accumulation is low in glacials and cold stages and high in interstadials and interglacials, indicating that the variations in BSi accumulation rates are not caused by changing mass accumulation rates. Biogenic silica accumulation rates varied from 0.01-0.06 g cm^{-2} ky^{-1} in the glacial periods, to 0.3-0.6 g cm^{-2} ky^{-1} in the last interglacial and in the Holocene, with maximum values

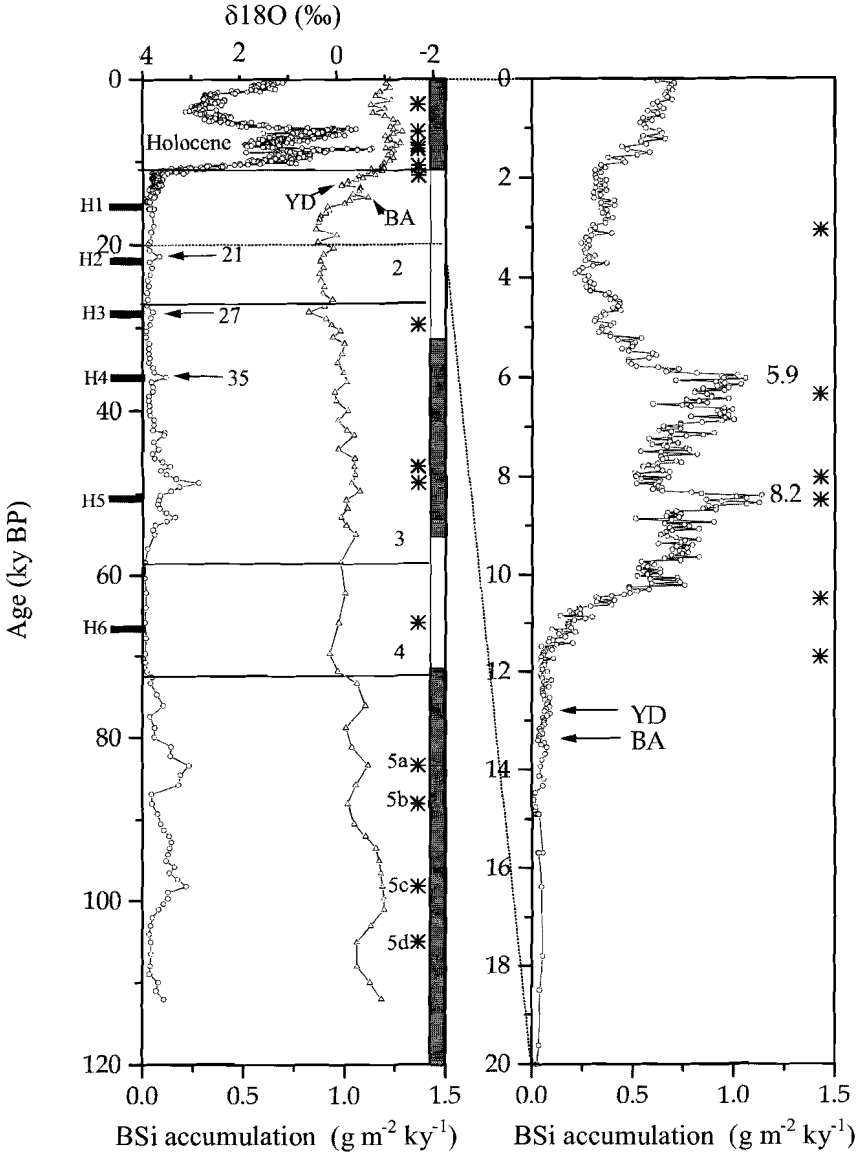

Fig. 5: Downcore biogenic silica accumulation record (open circles) for core TY93-905P and oxygen isotopes curve ($\delta^{18}O$) of *Globigerina bulloides* (open triangles) from the same core. Dates represent events discussed in the text. Black bars indicate Heinrich events. Stars represent samples analyzed for diatom species composition. The column on the right represents paleosols and loess deposits as recorded on the Chinese Loess Plateau. Dark intervals represent paleosols, light intervals represent Loess deposits (e.g. An et al., 1991; Porter and An, 1995).

of 1.13 g cm^{-2} ky^{-1} in the early part of the Holocene (Fig. 5a,b). In the early Holocene, two long intervals with continuously increasing BSi accumulation rates can be recognized, terminated by an abrupt cold event at 8.2 ky BP and 5.9 ky BP.
The biogenic silica accumulation record shows excellent correlation with the oxygen isotope record of the upwelling indicating foraminifera *G. bulloides* from the same core (Fig. 5a).

Burial fluxes of diatom species were in agreement with biogenic silica fluxes and varied by two orders of magnitude, with high diatom burial fluxes in warm intervals and very low diatom burial fluxes in the last glacial and the cold intervals of the last interglacial (Table 1). Highest diatom burial fluxes, up to 480 10^6 valves m^{-2} ky^{-1} were found in the early Holocene, at about 6 ky BP. In all interglacial samples, the "upwelling" diatom species *Thalassionema nitzschioides* and *Chaetoceros* resting spores dominated the assemblage, and oceanic diatoms were dominant only in the samples from isotope stage 3, at 46.7 and 48.7 ky BP (Table 1).

Table 1: Diatom burial fluxes for upwelling species, the oceanic species group and the total diatom flux for the modern sediment from the boxcore and for the samples selected from core TY93-905P. All fluxes are given in valves 10^6 cm^{-2} ky^{-1}.

Sample depth (cm)	Age (KY BP)	TNT	CHRS	oceanics	flux tot
Boxcore (9.5-25.5cm)		21.9	45.0	34.4	110.0
60.5	3.05	16.7	29.7	24.2	76.5
141	6.34	179.7	147.2	128.1	479.9
200	8.02	28.9	93.8	64.5	203.0
216	8.47	102.4	214.7	97.4	434.5
280	10.5	13.3	54.9	50.0	124.8
320	11.7	0.2	0.7	0.7	1.7
565	29.6	0.1	0.3	0.1	0.7
860	46.7	0.4	7.7	10.7	22.0
900	48.7	1.9	18.7	46.0	77.6
1089	65.9	0.3	0.7	0.2	1.1
1229	83.4	12.8	45.4	22.5	82.9
1268	88.1	0.3	2.6	1.3	4.4
1394	98.2	2.0	183.2	20.7	213.4
1474	105.0	0.2	1.0	0.4	1.7

The Paleo Burial Index (PBI) compares the diatom burial fluxes in a sample with modern burial fluxes. Modern burial is taken as the average diatom burial flux measured between 9.5 and 25.5 cm (averaging ~800 years) in a boxcore at this site,

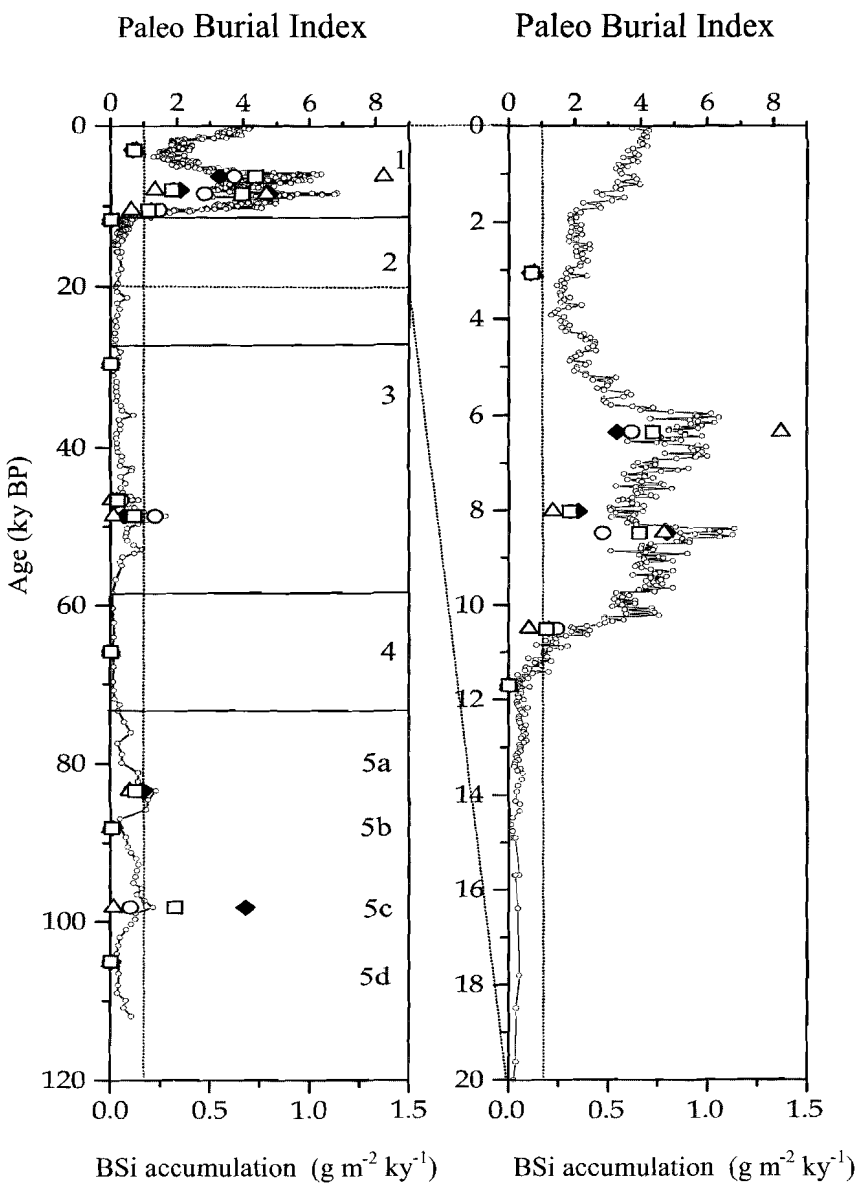

Fig. 6 Paleo Burial Index for the diatom species *Thalassionema nitzschioides* (open triangles), *Chaetoceros* resting spores (black diamonds), the oceanic species group (open circles) and the total diatom flux (open squares) in piston core TY93-905 on the Somalian Margin. The vertical line indicates PBI=1, paleo burial equal to modern burial. All diatom burial fluxes are given in Table 1. For comparison, the biogenic silica accumulation record is given.

well below the sediment mixing depth as determined from ^{210}Pb profiles [Koning et al., 2001]. PBI was calculated separately for the upwelling diatom species *Chaetoceros* resting spores and *Thalassionema nitzschioides*, for the oceanic species group and for the total diatom flux. Thus, PBI <1 indicates a burial flux lower than modern burial; PBI >1 indicates enhanced burial fluxes compared to the present. PBI values >1 were found in the warm stages of the last interglacial and in all samples from the early Holocene. Highest PBI values (8) were found at the Holocene climate optimum at about 6 ky BP for the upwelling diatom *Thalassionema nitzschioides*. For the oceanic species group PBI values >1 were found in early isotope stage 3 at 46.7 and 48.7 ky BP when BSi accumulation was relatively high (Fig. 6a, b).

DISCUSSION

Biogenic silica accumulation and monsoon variability

The sedimentary record from the Somalian upwelling area shows that during the last 150 ky biogenic silica accumulation rates have varied by two orders of magnitude, with little accumulation of biogenic silica during the last glacial and in stages 5b and 5d of the last interglacial. Relatively high biogenic silica accumulation occurred in the warm stages 5a and 5c of the last interglacial and in early isotope stage 3, at 46.7 and 48.7 ky BP. The highest biogenic silica accumulation took place in the early Holocene, from 10.3 - 6 ky BP (Fig. 5a, b). The biogenic silica accumulation record correlates well with the orbital based global chronostratigraphy (SPECMAP, Imbrie *et al.*, 1984), reflecting global ice volume (Fig. 3), and with oxygen isotope records from the NE Atlantic (Shackleton, 1977). This correlation suggests that the biogenic silica record is in phase with the millennial-scale variability in the North Atlantic Ocean and thus is a response to global climate change rather than a local feature, responding to conditions affecting the Indian Ocean only.

An excellent correlation exists between the biogenic silica record from the Somalian Margin and oxygen isotope records from the same core, indicating that biogenic silica accumulation is enhanced during warm intervals (Fig. 5a,b). Furthermore, biogenic silica fluctuations are in agreement with the foraminiferal record of *Globigerina bulloides*, a species that indicates coastal upwelling (Reichart, 1997; Ivanova, 1999). Apparently, the glacial-interglacial changes in biogenic silica accumulation as observed on the Somalian Margin are to be related to changes in upwelling intensity.

Diatom burial fluxes confirm the importance of upwelling. In all samples from interglacial periods that showed enhanced biogenic silica accumulation the "upwelling" diatom species *Thalassionema nitzschioides* and *Chaetoceros* resting spores dominated the diatom burial flux. Their PBI values confirm that diatom burial fluxes are directly related to upwelling intensity (Koning et al., 2001). All samples with high BSi have PBI values >1 for *Thalassionema nitzschioides* and/or *Chaetoceros* resting spores (Fig. 6). Apparently, the biogenic silica accumulation curve primarily reflects the increase and decrease of upwelling-induced diatom

productivity and thus the changes in monsoonal upwelling intensity. Only in early isotope stage 3, oceanic diatom species dominated the assemblage, suggesting that during this warm interval oceanic conditions prevailed, in contrast to the coastal upwelling conditions during the interglacial intervals.

Direct information on variations of both summer and winter monsoons is provided by loess records from central China and Lake Biwa, Japan (An et al, 1991; Xiao et al, 1997; Xiao et al, 1999). The succession of paleosols, deposited during wet periods, and wind-blown loess units, deposited during arid, cold periods, suggest increased summer monsoon intensity during isotope stages 1, 3, 5a and 5c, while winter monsoons were strengthened during isotope stages 2, 4, 5b and 5d (Fig. 5a). Our biogenic silica accumulation record complies with these records of monsoonal variability, thus we consider it evident that fluctuations in the biogenic silica burial fluxes on the Somalian Margin reflect changes in SW monsoon intensity.

As the annual biogenic silica fluxes to the sediment of the Somalian margin are largely determined by SW monsoon upwelling (Koning et al, 2001), the decreased biogenic silica flux during glacial periods would, by inference, indicate that upwelling weakened during these cold periods, as also shown by Duplessy (1982), Anderson and Prell (1993), Wang et al (1999) and Fang et al (1999). Sensitivity experiments in modeling studies have shown the importance of Northern Hemisphere glaciation and changes in snow cover and albedo in Asia on the intensity of the monsoons and Indian Ocean upwelling (Clemens et al., 1996; Prell and Kutzbach, 1992; Sirocko *et al.*, 1993; Sirocko, 1996). Changes in snow cover exert considerable control over the development of the continental heat low during summer, and affect the strength and duration of the SW monsoon (Anderson and Prell, 1993; Sirocko, 1993). In glacial periods, the ice and snow cover on the Himalaya was probably more extensive (Singh and Agrawal, 1976), thereby preventing spring heating on the Tibetan Plateau, resulting in a weakened low-pressure system during summer, and thus invoking less intense coastal upwelling. Indeed, Kuhle, (1998) proposed the existence of such a large ice sheet of 2.4 million km^2 covering the whole Tibetan Plateau during the last glacial. Thus, synchronous deglaciation and intensification of SW monsoon-induced upwelling appear to be related and in phase. Present day meteorological data reveal that in general a cold winter over the Northern Hemisphere is followed by a weakened heat low and weakened SW monsoon the following summer (Raman & Maliekal, 1985; Fang et al, 1999; Meehl, 1994). Accordingly, a prolonged period with intensive snow and ice cover on the Tibetan Plateau as could have occurred in glacial periods would have inhibited the formation of this heat low and would thus have reduced monsoonal upwelling. In early isotope stage 3, a period of maximum solar radiation within the last glacial, disappearing snowfields at high elevations and exposure of soil to this increasing solar radiation could have caused albedo changes that would have initiated a temporary intensification of monsoonal upwelling (Clemens et al, 1991).

Biogenic silica and diatom preservation and implications for the history of the SW monsoon

Last Interglacial - In the last interglacial, biogenic silica accumulation rates varied from about 0.05g cm^{-2} ky^{-1} in stages 5b and 5d to about 0.2g cm^{-2} ky^{-1} in stages 5a

and5c (Fig. 3a). Diatom burial fluxes fluctuated accordingly, with diatoms almost absent during cold stages and enhanced diatom burial fluxes during warm stages (Table 1). To relate diatom burial fluxes the Paleo Burial Index (PBI) was calculated (Fig. 6a-b). Fig. 6a shows that high PBI values are found in isotope stages 1,3 and 5, with burial of upwelling species being enhanced by a factor of up to 8. This high PBI suggests an increased flux of diatoms reaching the sediment, a better preservation of diatoms at these times or both. It is very unlikely that diatom preservation would have been enhanced by a factor of 4 to 8 without an enhanced diatom flux reaching the sediment. Our paleo burial index therefore suggests that during these warm stages, fluxes of diatoms in general and of upwelling species in particular were enhanced, in response to a more intense SW monsoon. In isotope stage 5c, around 98.000BP, burial fluxes of *Chaetoceros* resting spores were 4 times higher than at present, but for the oceanic species group, the PBI is <1, indicating that intense coastal upwelling occurred at that time. In contrast to the high PBI values in warm intervals, diatoms are virtually absent in the cold intervals (PBI values < 0.06 for all species and species groups).

Last glacial - During most of the last glacial, diatom burial fluxes were very low, more than two orders of magnitude lower than found in the early Holocene (Table 1). PBI values in isotope stages 2 and 4 were <0.01 for all species and species groups, confirming the decreased intensity of monsoonal upwelling compared to the present (Fig. 6a). Significant amounts of biogenic silica and higher diatom fluxes were buried in the early part of isotope stage 3. Here we find upwelling diatoms, but in lower numbers than the oceanic species. In the Atlantic Ocean, the early part of isotope stage 3 is considered to be an interval with more interglacial than glacial conditions (Boyle and Keigwin, 1982; Crowley, 1983). Apparently, less intense coastal upwelling and upwelling conditions like those of the present day NE monsoon characterized this slightly warmer interval and conditions were more favorable for the oceanic species assemblage. A second event with enhanced burial of biogenic silica can be recognized, the short interval of apparent warming at about 35.5 ky BP that was also revealed in the Dunde Ice core from the north-central Tibetan Plateau (Thompson et al, 1989, Fig. 5a).

On the Somalian Margin, brief episodes of enhanced biogenic silica accumulation appear to occur contemporary with the Heinrich events in the North Atlantic. These brief episodes could indicate increased productivity of diatoms due to a short-term warming event and/or to a strengthening of the NE monsoon (Fig. 5a). Semi-quantitative diatom analyses (smear slides) for these samples show that for the Heinrich-contemporary events at 27 and 35 ky BP, the increased biogenic silica accumulation resulted from an enhanced flux of species from the oceanic species group, suggesting a temporary warming analogous to the warm interval in early isotope stage 3. For the event at 21 ky BP neither the upwelling species nor the oceanic species were enhanced, and the diatom species composition resembled that from the last glacial. The increased biogenic silica preservation is in contrast to the total absence of diatoms during Heinrich-contemporary event H3 in records from Lake Baikal, Siberia, that have been attributed to short-term cooling events (Prokopenko et al, 2001). Leuschner and Sirocko (2000) reported evidence for Heinrich-contemporary events from magnetic susceptibility records in cores from the

northern Arabian Sea, located in an area where upwelling plays a minor role and where the main sediment supply is derived from eolian sources. Their records show increased sedimentation rates due to high eolian input during cold intervals. Our core on the Somalian Margin shows no evidence for increased eolian input during these Heinrich-contemporary events, since the contribution of wind transported material to the sediment is of minor importance in this area, as confirmed by the low magnetic susceptibility and Fe-content (Fig. 4). The minor fluctuations that can be observed in these records are not correlated and neither record is correlated with Heinrich-contemporary events. Furthermore, land-derived components (clay minerals and phytoliths) did not increase significantly during glacial periods. Apparently, eolian dust is of minor importance on the Somalian Margin, confirming that the major pathway of dust transport is well north of our sampling site.

Holocene - During the Holocene, the accumulation of biogenic silica fluctuated widely, and intervals of increased or decreased accumulation can be recognized (Fig. 5b). In general, the early Holocene is a warm period (Feng et al, 1999; Altabet et al, 1995; Gasse and van Campo, 1994; Thompson et al; 1989; Thompson et al, 1997; Fang et al, 1999; Marcantonio et al, 2001); however, in most of these records, the resolution is too low to detect even a millennial scale variability.

In our 50-year resolution record distinct millennial scale changes in biogenic silica accumulation in the Holocene can be attributed to global climate events. In the early Holocene, two prolonged intervals of continuously increasing biogenic silica accumulation rates and terminated by abrupt cold event can be recognized (Fig. 5b). Although the Younger Dryas is clearly visible in the oxygen isotope records from the Somalian Margin, it can not be detected in the biogenic silica accumulation record. In records from the northern Arabian Sea, Sirocko (1996) observed that the Younger Dryas was barely detectable in the productivity indicating Ba-record. Apparently, the Younger Dryas was not reflected in reduced diatom productivity on the Somalian Margin.

Other well-documented events, like the Holocene cold event, around 8.2 ky BP, are evident in our biogenic silica record (Fig. 5b). This global event has been recognized in ice-core records from Greenland (GISP2, Dansgaard et al, 1993), North American lakes (Barber et al, 1999) and in marine records (Alley et al, 1997). On the Somalian Margin, the Holocene cold event abruptly terminated an apparent interval of maximum monsoon intensity (Fig. 5b). Sirocko et al (1993) attribute the total absence of dolomite in their piston core on the Oman Margin in the interval from 8850-7850 BP to an Early Holocene SW monsoon maximum. Gasse and van Campo (1994) however, describe a major dry spell in pollen and lake records from West Asia and Africa from 8-7 ky BP. Our 50-year resolution record shows both the Early Holocene SW monsoon maximum at 8.53 – 8.38 ky BP, followed by an abrupt cooling towards the Holocene cold event at 8.2 ky BP. PBI values decreased by a factor of 2 during the 500 years of the transition from Early Holocene SW monsoon maximum to Holocene cold events, confirming the weakened monsoonal intensity during this cold event (Fig. 6b).

Another major event that can be observed was the Holocene climate optimum, around 6 ky BP, the final stage of a gradual increase in biogenic silica accumulation that started after the Holocene cold event (Sirocko, 1993; Thompson et al, 1989; Xiao

et al, 1997). This optimum was followed by the late Holocene aridification (Sirocko, 1993; Thompson et al, 1995), which started at approximately 5.9 ky BP and is clearly reflected in the abrupt decline in biogenic silica accumulation that occurred around that time (Fig. 5b). During the Holocene climate optimum, around 6000BP, PBI values show that the diatom burial flux was enhanced by a factor of 4 compared to the present-day burial flux, with burial fluxes of *Thalassionema nitzschioides* being enhanced by a factor of 8. These values are in line with continental records from north Africa, Rajasthan and Tibet (Bryson and Swain, 1981; Swain et al, 1983; Gasse and van Campo, 1994; DeMenocal et al, 2000) that suggest conditions wetter than today in the early-mid Holocene period, with major dry spells during the intervals 11.0-9.5 ky BP and 8-7 ky BP. In our biogenic silica record, major dry spells can be recognized around 10.2-9.5 ky BP, 8.9 ky BP and around 6.5 ky BP.

The long-scale continuous increase in biogenic silica accumulation observed during the early Holocene suggests a gradual deglaciation of the Tibetan Plateau that started around 11.7 ky BP, with returns to colder conditions at the Holocene cold event (8.2 ky BP) and the late Holocene aridification (5.9 ky BP). From ~1.7 ky BP monsoonal intensity increased continuously towards the present. Throughout the Holocene, fluctuations of monsoonal intensity on millennial and centennial scales can be recognized, indicating that the forcing mechanisms of the Indian Ocean summer monsoon are sensitive to short term local features.

CONCLUSIONS

Particulate biogenic silica and diatom fluxes on the Somalian Margin are largely determined by coastal upwelling during the SW monsoon. Two important upwelling indicators, *Thalassionema nitzschioides* and *Chaetoceros* resting spores preserve a residual upwelling record in the sediment. The Somalian Margin biogenic silica record fluctuates in accordance with isotope records from the NE Atlantic (Shackleton, 1987) and the orbital based global chronostratigraphy (SPECMAP, Imbrie et al., 1984), suggesting that the biogenic silica record and thus monsoonal intensity is a response to global climate change, but the high-frequency fluctuations observed in the Holocene appear to be related to local conditions affecting the Indian Ocean only. Biogenic silica and diatom burial fluxes in the last interglacial and the Holocene were 4 to 8 times higher than modern diatom burial fluxes, indicating a more intense SW monsoon. Maximum fluxes occurred during the Holocene climate optimum, around 6000BP. Biogenic silica and diatom burial fluxes were low during glacial periods, indicating that monsoonal upwelling appeared to be of minor importance in glacial periods. Our data show that on the Somalian Margin, biogenic silica is an excellent indicator for paleo-upwelling in the sediments.

ACKNOWLEDGMENTS

The cruises with R.V. TYRO to the NW Indian Ocean (1992/1993) were financially supported by the Netherlands Marine Research Foundation and by NIOZ. Without the skillful assistance of Captain J. de Jong, officers and crew of R.V. Tyro and the technicians of NIOZ, the core discussed in this study could not have been recovered. We are grateful to Katja Ivanova and Gerald Ganssen (Free University, Amterdam) who provided the age model for core TY93-905P and the DBD values. This is publication nr. 3594 of the Netherlands Institute for Sea Research

REFERENCES

Abrantes, F. (1988). Diatom assemblages as upwelling indicators in surface sediments off Portugal. Marine Geology, 85, 15-39.

Alley, R.B., Mayewski, P.A., Sowers, T., Stuiver, M., Taylor K.C., Clark, P.U. (1997). Holocene climate instability: a prominent, widespread event 8200 yr ago. Geology, 25, 483-486.

Altabet, M.A., Francois, R., Murray D.W., Prell, W.L. (1995). Climate-related variations in denitrification in the Arabian Sea from sediment $^{15}N/^{14}N$ ratios. Nature, 373, 506-509.

An, Z., Kukla, G.J., Porter S.C., Xiao, J. (1991). Magnetic susceptibility evidence of monsoon variation on the Loess Plateau of central China during the last 130,000 years. Quaternary Research, 36, 29-36.

Anderson, D.M., Prell, W.L. (1993). A 300 kyr record of upwelling off Oman during the late Quaternary: evidence of the Asian southwest monsoon. Paleoceanography, 8, 193-208.

Barber, D.C., Dyke, A., Hillaire-Marcel, C., Jennings, A.E., Andrews, J.T., Kerwin, M.W., Bilodeau, G., McNeely, R., Southon, J., Morehead M.D., Gagnon, J.-M. (1999). Forcing the cold event of 8,200 years ago by catastrophic drainage of Laurentide lakes. Nature, 400, 344-348.

Bard, E. (1988). Correction of accelerator mass spectrometry ^{14}C AMS ages measured in planktic foraminifera: Paleoceanographic implications, Paleoceanography, 3, 635-645.

Bard, E., Hamelin, B., Fairbanks R., Zindler, A. (1990). Calibration of the ^{14}C timescale over the past 30,000 years using mass spectrometric U-Th ages from Barbados corals, Nature, 345, 405-409.

Bard, E., Arnold, M., Fairbanks, R. Hamelin, B. (1993). ^{230}Th-^{234}U and ^{14}C ages obtained by mass spectrometry on corals, Radiocarbon, 35, 191-199.

Boyle, A.E., Keigwin, L.D. (1982). Deep circulation of the North Atlantic over the last 200,000 years: Geochemical evidence. Science, 218, 784-787.

Brock, J.C., McClain, C.R., Hay, W.W. (1992). A southwest monsoon hydrographic climatology for the northwestern Arabian Sea. Journal of Geophysical Research, 97, 9455-9465.

Bryson, R.A., Swain, A.M. (1981). Holocene variations of monsoonal rainfall in Rajasthan. Quaternary Research, 16, 135-145.

Clemens, S.C., Prell, W.L., Murray, D.W., Shimmield, G., Weedon, G.(1991). Forcing mechanisms of the Indian Ocean monsoon. Nature, 353, 720-725.

Clemens, S.C., Murray, D.W., Prell, W.L. (1996). Nonstationary phase of the Plio-Pleistocene Asian monsoon. Science, 274, 943-948.

Crowley, T..J. (1983). Calcium-carbonate preservation patterns in the central North Atlantic during the last 150,000 years. Marine Geology, 51, 1-14.

Dansgaard, W., Johnsen, S.J., Clausen, H.B., Dahl-Jensen, D., Gundestrup, N.S., Hammer, C.U., Hvidberg, C.S., Steffensen, J.P., Sveinbjörnsdottir, A.E., Jouzel, J., Bond, G. (1993). Evidence for general instability of past climate from a 250-kyr ice-core record. Nature, 364, 218-220, 1993.

DeMenocal, P., Ortiz, J., Guilderson, T., Adkins, J., Sarnthein, M., Baker, L., Yarusinsky, M. (2000). Abrupt onset and termination of the African humid period: rapid climate responses to gradual insolation forcing. Quaternary Science Reviews, 19, 347-361.

Duplessy, J.C. (1982). Glacial to interglacial contrasts in the northern Indian Ocean. Nature, 295, 494-498.

Fang, X.-M., Ono, Y., Fukusawa, H., Bao-Tian, P., Li, J.-J., Dong-Hong, G., Oi, K., Tsukamoto, S., Torii, M., Mishima, T. (1999). Asian summer monsoon instability during the past 60,000 years: magnetic susceptibility and pedogenic evidence from the western Chinese Loess Plateau. Earth and Planetary Science Letters, 168, 219-232.

Feng, X., Cui, H., Tang, K., Conkey, L.E. (1999). Tree-ring δD as an indicator of Asian monsoon intensity. Quaternary Research, 51, 262-266.

Fischer, J., Schott, F., Stramma, L. (1996). Current and transports of the Great Whirl-Socotra Gyre system during the summer monsoon, August 1993. Journal of Geophysical Research, 101, 3573-3587.

Ganssen, G., Troelstra, S.R., van Weering, T.C.E.(1995). Younger Dryas style-event and the possible correlation with Heinrich events in deep-sea cores offshore Somalia (Indian Ocean), In: S.R. Troelstra, J.E. van Hinte and G.M. Ganssen (Eds.), The Younger Dryas. Koninklijke Academie van Wetenschappen Verhandelingen, afdeling Natuurkunde, 44, 149-154.

Gasse, F., van Campo, E.(1994). Abrupt post-glacial climate events in West Asia and North Africa monsoon domains. Earth and Planetary Science Letters, 126, 435-456.

Hitchcock, G.L., Olsen, D.B. (1992). NE and SW monsoon conditions along the Somali coast during 1987. In: B.N. Desai (Ed.) Oceanography of the Indian Ocean. Oxford & IBH, New Delhi, 583-593.

Imbrie, J., Hays, D., Martinson, D.G., McIntyre, A., Mix, A.C., Morley, J.J., Pisias, N.G., Prell, W.L., Shackleton, N.J. (1984). The orbital theory of Pleistocene climate: Support from a revised chronology of the marine $\delta^{18}O$ record. In: Milankovitch and Climate. A. Berger et al (Eds.) D. Reidel, Dordrecht, 269-305.

Ivanova, E.M. (1999). Late Quaternary monsoon history and paleoproductivity of the western Arabian Sea. PhD thesis, Vrije Universiteit Amsterdam, pp 1- 172, 1999.

Jansen, J.H.F., van der Gaast, S.J., Koster, B., Vaars, A.J. (1998). CORTEX, an XRF-scanner for non-destructive chemical analyses of split sediment cores, Marine Geology, 151, 143-154.

Koning, E., Brummer, G.-J.A., van Raaphorst, W., van Bennekom, A.J., Helder, W., van Iperen, J.M. (1997). Settling, dissolution and burial of biogenic silica in the sediments off Somalia (northwestern Indian Ocean). Deep-Sea Research II, 44,6-7, 1341-1360.

Koning, E., van Iperen, J.M., van Raaphorst, W., Helder, W., Brummer, G.-J.A., van Weering, T.C.E. (2001). Selective preservation of upwelling-indicating diatoms in sediments off Somalia, NW Indian Ocean. (Deep-Sea Research I, 48, 2473-2495.

Kuhle, M. (1998). Reconstruction of the 2.4 million km^2 late Pleistocene ice sheet on the Tibetan Plateau and its impact on the global climate. Quaternary International, 45/46 , 71-108.

Leuschner, D.C., Sirocko, F. (2000). The low-latitude monsoon climate during Dansgaard-Oeschger cycles and Heinrich events. Quaternary Science Reviews, 19, 243-254.

Marcantonio, F., Anderson, R.F., Higgins, S. , Fleisher, M., Stute, M., Schlosser, P. (2001). Abrupt intensification of the SW Indian Ocean monsoon during the last glaciation: constraints from Th, Pa and He isotopes. Earth and Planetary Science Letters, 184, 505-514.

Meehl, G.A. (1994). Coupled land-ocean-atmosphere processes and South Asian monsoon variability. Science, 266, 263-267.

Müller, P.J., Schneider, R. (1993). An automated method for the determination of opal in sediments and particulate matter. Deep Sea Research I, 40, 425-444

Peeters, F.J.C. (2000). The distribution and stable isotope composition of living planktic foraminifera in relation to seasonal changes in the Arabian Sea, PhD thesis, Free University, Amsterdam, 184pp.

Porter, S.C., An, Z. (1995). Correlation between climate events in the North Atlantic and China during the last glaciation. Nature, 375, 305-308.

Prell, W.L. (1984). Variation of monsoonal upwelling: a response to changing solar radiation, In: J. Hasen and T. Takahashi (Eds.) Climate processes and climate sensitivity. 29. AGU, Washington DC, 48-57.

Prell, W.L., Kutzbach, J.E. (1987). Sensitivity of the Indian monsoon to forcing parameters and implications for its evolution, Nature, 360, 647-652.

Prokopenko, A.A., Williams, D.F., Karabanov, E.B., Khursevich, G.K. (2001). Continental response to Heinrich events and Bond cycles in sedimentary record of Lake Baikal, Siberia, Global and Planetary Change, 28, 217-226.

Raman, C.R.V., Maliekal, J.A. (1985). A 'northern oscillation' relating northern hemisphere pressure anomalies and the Indian summer monsoon, Nature, 314, 430-432.

Reichart, G.J. (1997). Late quaternary variability of the Arabian Sea monsoon and oxygen minimum zone, PhD thesis. Utrecht University. 171 pp, 1997.

Reichart, G.J., Lourens, L.J., Zachariasse, W.J. (1998). Temporal variability in the northern Arabian Sea oxygen minimum zone (OMZ) during the last 225,000 years, Paleoceanography, 13, 607-621.

Rixen, T., Haake, B., Ittekkot, V., Guptha, M.V.S., Nair, R.R., Schluessel, P. (1996). Coupling between SW monsoon related surface and deep ocean processes as discerned from continuous particle flux measurements and correlated satellite data,
Journal of Geophysical Research, 101, (12), 28569-28582.

Schott, F. (1983). Monsoon response of the Somali Current and associated upwelling. Progress in Oceanography, 12, 357-381.

Schott, F., Swallow, J.C., Fieux, M. (1990). The Somali Current at the equator: annual cycle of currents and transports in the upper 1000m and connection to neighboring latitudes. Deep-Sea Research, 37, 1825-1848.

Schrader, H. (1992). Coastal upwelling and atmospheric CO2 changes over the last 400,000 years: Peru, Marine Geology, 107, 239-248.

Schulz, H., von Rad, U., Erlenkeuser, H. (1998). Correlation between Arabian Sea and Greenland climate oscillations of the past 110,000 years, Nature, 393, 54-57.

Shackleton, N.J. (1977). Carbon-13 in Uvigerina: Tropical rainforest history and the Equatorial Pacific carbonate dissolution cycles. In: The fate of fossil fuel CO2 in the oceans. N.R. Anderson and A. Malahoff (Eds.). Plenum Press, New York, 401-428.

Shimmield, G.B., Mowbray, S.R. (1991). The inorganic geochemical record of the northwest Arabian Sea: a history of productivity variation over the last 400 K.Y. from sites 722 and 724, In: Prell, W.L., Niitsuma, N., et al., (Eds.) Proceedings of the Ocean Drilling Program, Scientific Results, Vol. 117, 409-429.

Singh, G., Agrawal., D.P. (1976). Radiocarbon evidence for deglaciation in north-western Himalaya, India, Nature, 260, 232.

Sirocko, F. (1991). Deep-sea sediments of the Arabian Sea: a paleoclimatic record of the Southwest-Asian summer monsoon, Geologische Rundschau, 80/3, 557-566.

Sirocko, F., Sarnthein, M., Erlenkeuser, H., Lange, H., Arnold, M., Duplessy, J.C. (1993). Century-scale events in monsoonal climate over the past 24,000 years, Nature, 364, 322-324.

Sirocko, F. (1996). Past and present subtropical summer monsoons, Science 274, 937-938.

Smith, S.L. (1984). Biological indications of active upwelling in the northwestern Indian Ocean in 1964 and 1979, and a comparison with Peru and northwest Africa, Deep-Sea Research I, 31, 951-967.

Smith, S.L., Codispoti, L.A. (1980). Southwest monsoon of 1979: chemical and biological response of Somali coastal waters, Science, 209, 597-600.

Swain, A.M., Kutzbach, J.E., Hastenradt, S. (1983). Estimates of Holocene Precipitation for Rajasthan, India, based on pollen and lake-level data, Quaternary Research, 19, 1-17.

Thompson, L.G., Thompson-Mosley, E., Davis, M.E., Bolzan, J.F., Dai, J., Yao, T., Gundestrup, N., Wu, X., Kleinand, L., Xie, Z. (1989). Holocene-late Pleistocene climate ice core records from Qinghai-Tibetan Plateau, Science, 246, 474-477.

Thompson, L.G., Yao, T., Davis, M.E., Henderson, K.A., Thompson-Mosley, E., Lin, J. Beer, P.-N., Synal, H.-A., Cole-Dai, J., Bolzan, J.F.(1997). Tropical climate instability: the last glacial cycle from a Qinghai-Tibetan ice core, Science, 276, 1821-1825.

Tribovillard, N.-P., Caulet, J.-P., Vergnaud-Grazzini, C., Moureau, N., Tremblay, P. (1996). Lack of organic matter accumulation on the upwelling-influenced Somalia margin in a glacial-interglacial transition, Marine Geology, 133, 157-182.

Van Hinte, J.E., van Weering, T.C.E, Troelstra, S.R.(1995). Tracing a seasonal upwelling, Cruise Report, National Museum of Natural history, Leiden, The Netherlands, 146pp.

Wang, L., Sarnthein, M., Erlenkeuser, H., Grimalt, J., Grootes, P., Heilig, S., Ivanova, E., Kienast, M., Pelejero, C., Pflaumann, U.(1999). East Asian monsoon climate during the late Pleistocene: high-resolution sediment records from the South China Sea, Marine Geology, 156, 245-284.

Weedon, G., Shimmield, G. (1991). Late Pleistocene upwelling and productivity variations in the northwest Indian Ocean deduced from spectral analyses of geochemical data from sites 722 and 724, In: Prell, W.L., Niitsuma, N., et al., (Eds.) Proceedings of the Ocean Drilling Program, Scientific Results, Vol. 117, 431-443.

Xiao, J., Inouchi, Y., Kumai, H., Yoshikawa, S,. Kondo, Y., Liu, T., An, Z. (1997). Biogenic silica record in Lake Biwa of central Japan over the past 145,000 years, Quaternary Research, 47, 277-283.

Xiao, J.L., An, Z.S., Liu, T.S., Inouchi, Y., Kumai, H., Yoshikawa, S., Kondo, Y.(1999). East Asian monsoon variation during the last 130,000 years: evidence from the Loess Plateau of central China and Lake Biwa of Japan, Quaternary Science Reviews, 18, 147-157.

CHAPTER 6

Concluding remarks and perspectives

CURRENT STATUS OF BIOGENIC SILICA RESEARCH

Given the importance of diatoms as primary producers that dominate the early stages of phytoplankton blooms, it is not surprising that the cycle of production of diatoms, regeneration of silicic acid and burial of biogenic silica has been the object of intensive study in the last decades. A major problem, however, is to relate the sedimentary BSi content to the original production of diatoms that took place in the surface waters. The extent of dissolution of diatoms in the water column varies widely, depending on the local hydrographic conditions of the area sampled. For example, high dissolved iron concentrations in the water column may lead to more silicified and faster sinking diatoms, thereby promoting preservation in the sediments (Hutchins and Bruland, 1998; Tanaka, 1998). Furthermore, large uncertainties exist in the measured biogenic silica content of the sediments (as illustrated in chapter 2, fig. 12) and, as a consequence, in the burial efficiencies calculated from these sediment biogenic silica data.

So far, research carried out all over the world ocean encompassed studies of the production and dissolution processes that take place in the water column (e.g. Brzezinski et al., 1998; Nelson et al., 1995; Treguer et al., 1991), sediment trap studies of vertical rain rates of BSi (e.g. Treppke et al, 1996; Romero et al., 2001), studies that related the production of BSi in the surface waters to the efflux of silicic acid from the pore waters (e.g. DeMaster et al., 1991; Archer et al., 1993; Schluter and Sauter, 2000), taxonomic studies of species assemblages in the top layer of the sediments (e.g. Abrantes, 1999) and paleoceanographic studies that looked at fluctuations in biogenic silica accumulation fluxes on glacial-interglacial timescales (e.g. Mortlock et al., 1991; Sirocko et al., 1993). In a study carried out in the Amazon delta, Michalopoulos and Aller (1995) showed that neoformation of clay minerals could be a alternative pathway in the early diagenesis of biogenic silica. In recent years, scientists have tried to construct global silica budgets, based either on conventional mass balance calculations (e.g. Treguer et al., 1995; Nelson et al., 1995; Ragueneau et al., 2000) or on global models, thereby linking the silica cycle to the global carbon cycle (e.g. Heinze et al., 1999; Harrison, 2000; Archer et al., 2000). A requisite for constructing global budgets is the availability of reliable data to validate the model calculations. For large areas of the oceans, however, little data are available, and different methods have been applied to obtain these data. Few studies have been devoted to the cycle of biogenic silica in the northwestern Indian Ocean, even though the upwelling in this area generates rates of primary production that are among the highest in the world oceans.

In this thesis the biogenic silica cycle below the upwelling area on the Somalian Margin in the northwestern Indian Ocean was studied, focussing both on biogenic silica and on diatom species fluxes. Furthermore, we have developed a method to analyze biogenic silica in complex sediments as found in large areas of the oceans, with low biogenic silica and high lithogenic contents.

THIS STUDY

On the Somali Margin, annual production of diatoms can be related directly to upwelling during the northwest monsoon. Diatom settling fluxes increase by an order of magnitude when the upwelling season starts, followed by a distinct species succession. Approximately 50% of the biogenic silica produced in the surface layer dissolves in the upper water column during surface mixing and settling. Of the BSi that escapes dissolution in the upper water column, 90% dissolves at the sediment-water interface or in the upper mm's of the sediment. At the sediment-water interface, a major shift in species composition takes place, due to selective dissolution or preservation. The small, weakly silicified diatom species that dominate the pre-upwelling and mid-upwelling periods dissolve as soon as they reach the sediment-water interface, and disappear from the diatom assemblage. Part of the well-silicified species that dominate the beginning and end of the upwelling period, however, survive dissolution at the sediment-water interface and are buried in the sediments. Once buried in the sediments, diatom species remain remarkably intact over timescales of a few thousand years, indicating that the processes that control preservation of BSi in the sediments take place at the sediment-water interface during early diagenesis.

In older sediments of the Somalian Margin, the fluctuations in BSi accumulation coincide with warm and cold periods in the geological past as recorded in the SPECMAP global temperature curve (Imbrie et al., 1984). In all periods when enhanced burial of biogenic silica was observed, diatom species that are diagnostic for the upwelling season dominate the assemblage in the sediment, with accumulation fluxes of up to eight times the present-day flux preserved in the early Holocene and in isotope stage 5, 100,000 BP. In cold, glacial periods, however, biogenic silica fluxes were very low and upwelling indicating diatoms were absent from the sediment assemblage. These results suggest that an upwelling system analogous to the present-day system was present in the warm interglacials and interstadials, but of minor importance during cold, glacial periods. The massive diatom fluxes that were preserved in the early Holocene and in isotope stage 5 confirm that the presence of biogenic silica in deeper sediments is primarily controlled by early diagenetic processes at the sediment-water interface, and not by dissolution in the sediments.

FUTURE RESEARCH

The study presented in this thesis confirms that, although a major part of the dissolution of biogenic silica occurs in the water column thereby determining which fraction of the biogenic silica produced in the surface waters reaches the sediment surface, the actual preservation of biogenic silica is controlled by processes at the sediment-water interface. So far, the dissolution of biogenic silica has been studied mainly under hydrodynamic and chemical conditions representative for the water column (Kamatani and Riley, 1979, Greenwood et al., 2001; Dixit et al., 2001), hence underrepresenting the specific conditions prevailing at the sediment-water interface. It can be hypothesized that the transition from turbulent conditions with relatively low concentrations of relevant solutes in the ambient water, to a diffusive regime with high concentrations in the interstitial water is crucial for the preservation of biogenic silica. Previous research has provided evidence that diagenetic alterations, such as the incorporation of aluminium into the SiO_2 matrix, lower the solubility and dissolution rate of biogenic silica and, hence, promote its preservation (van Bennekom et al., 1989; Van Cappellen, 1996; Van Cappellen and Qiu, 1997; Dixit et al., 2001). Little, however, is known about the physical and chemical conditions and even less about their synergistic effects that favor Al incorporation upon deposition at the sea floor. In order to identify and quantify the key-processes for preservation we will, in a recently started project, conduct a step-wise simulation of the relevant changes in the physico-chemical environment encountered by biogenic silica as it is transferred from the water column to the sediment. The following aspects will be taken into account:

Processes in the water column- Before biogenic silica can be subjected to diagenetic processes at the sediment-water interface, dissolution in the water column determines the fraction of the primary production that reaches the sediment surface. Living diatoms are protected by organic coatings, but after death of the organisms, bacteria will degrade these coatings and thereby promote dissolution of the silica cell walls (Bidle and Azam, 1999). Between the different diatom species, large differences in size, pore volume, specific surface and extent of silification are observed, depending on the hydrographic conditions during growth. The size of the diatoms is of importance because it influences their sinking speed. Larger diatoms will sink more rapidly and will thus have a shorter residence time in the water column and be less susceptible to dissolution. Since dissolution of BSi is a surface process, the rate of dissolution is proportional to the specific surface of the diatom cells (Kamatani and Riley, 1979; Dixit et al., 2001). To study the influence of these species characteristics, experiments will be carried out on different cultured species of diatoms to study their specific dissolution behavior.

Aging- Aging takes place as diatoms sink through the water column and during their residence time on the sediment-water interface. As result of aging, the specific surface area and thus the reactivity of the diatoms decreases, because the more reactive sites on the diatom surface and irregularities such as spines are removed preferentially when dissolution takes place. In the laboratory, aging can be simulated by pre-treating diatoms in seawater for different periods of time at controlled temperatures and pH.

Diagenetic alterations- The incorporation of small amounts of aluminium in the matrix of biogenic silica has been shown to effectively lower the solubility of biogenic silica (Lewin, 1961; van Bennekom et al., 1989). Aluminium can be incorporated in the diatom frustule during biosysthesis, but levels will not exceed 0.8%, even at high dissolved aluminium concentrations in the culture medium. Since up to 6% of aluminium has been found in diatom frustules in Angola Basin sediments, additional post-mortem processes must be responsible, most likely at the sediment-water interface where elevated concentrations of dissolved aluminium diffusing from the pore waters are available. In laboratory experiments, we will try to mimick the early diagenetic incorporation of aluminium. Cultured diatoms will be suspended in flow-through reactors and dissolution kinetics, solubilities and diagenetic alterations will be monitored, first at turbulent conditions at low concentrations of solutes such as those observed in the water column, and secondly in a diffusive regime at slowly increasing concentrations of dissolved aluminium. As a final step, the combined effect of complex chemical gradients (e.g. Al^{3+}, H_4SiO_4, pH, redox) on aluminium incorporation will be studied by incubating the diatoms in sediments of different biochemical characteristics.

Hopefully, the experiments described above will contribute to our knowledge of the processes that control the diagenetic alteration of biogenic silica in the sediment. Only if the mechanisms that control preservation are better understood, the biogenic silica remains that are observed in deep-sea sediments can eventually be related to the original primary production in the surface waters.

REFERENCES

Abrantes, F., Moita, M.T. (1999). Water column and recent sediment data on diatoms and coccolithophorids, off Portugal confirm sediment record of upwelling events. Oceanologica Acta, 22, 67-84.

Archer, D., Lyle, M., Rodgers, K., Froelich, P. (1993). What controls opal preservation in tropical deep-sea sediments. Paleoceanography, 8, 7-21.

Archer, D., Winguth, A., Lea, D., Mahowald, N. (2000). What caused the atmospheric pCO_2 cycles? Reviews of Geophysics, 38, 159-189.

Bidle, K.D., Azam, F. (1999). Accelerated dissolution of diatom silica by marine bacterial assemblages. Nature, 397, 508-511.

Brzezinski, M.A., Villareal, T.A., Lipschultz, F. (1998). Silica production and the contribution of diatoms to new and primary production in the central North Pacific. Marine Ecology Progress Series, 167, 89-104.

DeMaster, D.J., Nelson, T.M., Harden, S.L., Nittrouer, C.A.(1991). The cycling and accumulation of biogenic silica and organic carbon in Antarctic deep-sea and continental margin environments. Marine Chemistry, 35, 489-502.

Dixit, S., Van Cappellen, P., van Bennekom, A.J. (2001). Processes controlling the solubility of biogenic silica and pore water build-up of silicic acid in marine sediments. Marine Chemistry, 73, 333-352.

Greenwood, J.E., Truesdale, V.W., Rendell, A.R. (2001). Biogenic silica dissolution in seawater- in vitro chemical kinetics. Progress in Oceanography, 48, 1-23.

Harrison, K.G. (2000). Role of increased marine silica input on paleo-pCO_2 levels. Paleoceanography, 15, 292-298.

Heinze, C., Maier-Reimer, E., Winguth, A.M.E., Archer, D. (1999). A global oceanic sediment model for long-term climate studies. Global biogeochemical cycles, 13, 221-250.

Hutchins, D.A., Bruland, K.W. (1998). Iron-limited diatom growth and Si:N uptake ratios in a coastal upwelling regime. Nature, 393, 561-564.

Imbrie, J., Hays, D., Martinson, D.G., McIntyre, A., Mix, A.C., Morley, J.J., Pisias, N.G., Prell, W.L., Shackleton, N.J. (1984). The orbital theory of Pleistocene climate: Support from a revised chronology of the marine $\delta^{18}O$ record. In: Milankovitch and Climate. A. Berger et al (Eds.) D. Reidel, Dordrecht, 269-305.

Kamatani, A., Riley, J. P. (1979). Rate of dissolution of diatom silica walls in seawater. Marine Biology, 55, 29-35.

Lewin, J.C. (1961). The dissolution of silica from diatom walls. Geochimica et Cosmochimica Acta, 21, 182-198.

Michalopoulos, P., Aller, R.C. (1995). Rapid clay mineral formation in Amazon delta sediments: Reverse weathering and oceanic elemental cycles. Science, 270, 614-617.

Mortlock, R.A., Charles, C.D., Froelich, P.N., Zibello, M.A., Saltzman, J., Hays, J.D., Burckle, L.H. (1991). Evidence for lower productivity in the Antarctic Ocean during the last glaciation. Nature, 351, 220-223.

Nelson, D.M., Tréguer, P., Brzezinski, M.A., Leynaert A., Quéguiner, B. (1995). Production and dissolution of biogenic silica in the ocean: Revised global estimates, comparison with regional data and relationship to biogenic silica sedimentation. Global Biogeochemical Cycles, 9, 359-372.

Ragueneau, O., Tréguer, P., Leynaert, A., Anderson, R.F., Brzezinski, M.A., DeMaster, D.J., Dugdale, R.C., Dymond, J., Fischer, G., François, R., Heinze, C., Maier-Reimer, E., Martin-Jézéquel, Nelson, D.M., Quéguiner, B. (2000). A review of the Si cycle in the modern ocean: recent progress and missing gaps in the application of biogenic opal as a paleoproductivity proxy. Global and planetary change, 26, 317-365.

Romero, O.E., Hebbeln, D., Wefer, G. (2001). Temporal and spatial variability in export production in the SE Pacific Ocean: evidence from siliceous plankton fluxes and surface sediment assemblages. Deep-Sea Research I, 48, 2673-2697.

Schlüter, M., Sauter, E. (2000). Biogenic silica cycle in surface sediments of the Greenland Sea. Journal of Marine systems, 23, 333-342.

Sirocko, F., Sarnthein, M., Erlenkeuser, H., Lange, H., Arnold, M., Duplessy, J.C. (1993). Century-scale events in monsoonal climate over the past 24,000 years, Nature, 364, 322-324.

Tanaka, S. (1998). Influence of iron availability on nutrient consumption ratio of diatoms in oceanic waters. Nature, 393, 774-777.

Tréguer, P., Nelson, D.M., van Bennekom, A.J., DeMaster, D.J., Leynaert, A., Quéguiner, B. (1995). The silica cycle in the world ocean: A reestimate. Science, 268, 375-379.

Treguer, P., Lindner, L., van Bennekom, A.J., Leynaert, A., Panouse, M., Jacques, G. **(1991). Production if biogenic silica in the Wedell-Scotia Seas measured with 32Si. Limnology and Oceanography, 36, 1217-1227.**

Treppke, U.F., Lange, C.B., Donner, B., Fischer, G., Ruhland, G., Wefer, G.(1996b). Diatom and silicoflagellate fluxes at the Walvis Ridge: An environment influenced by coastal upwelling in the Benguela system. Journal of Marine Research, 54, 991-1016.

Van Bennekom, A.J., Jansen, J.H.F., van der Gaast, S.J., van Iperen, J.M., Pieters, J. (1989). Aluminium-rich opal: an intermediate in the preservation of biogenic silica in the Zaire (Congo) deep-sea fan. Deep-Sea Research I, 36, 173-190.

Van Cappellen, P. (1996). Reactive surface area control of the dissolution kinetics of biogenic silica in deep-sea sediments. Chemical Geology, 132, 125-130.

Van Cappellen, P., Qiu, L. (1997). Biogenic silica dissolution in sediments of the Southern Ocean. II. Kinetics. Deep-Sea Research II, 44, 1129-1149.

Samenvatting

DE KRINGLOOP VAN SILICAAT IN DE OCEANEN

Silicium is een van de meest voorkomende elementen op aarde. In gesteenten en mineralen is het hoofdzakelijk als silicaat (SiO_2) aanwezig. Silicaat komt door verwering in rivieren en uiteindelijk in het oppervlaktewater van de oceanen terecht. De aanvoer van silicaat naar de oceanen, via rivieren, uit hydrothermale bronnen en ingeblazen door de wind is in evenwicht met de hoeveelheid silicaat die uit de oceanen verdwijnt doordat het in de zeebodem begraven wordt. Kiezelzuur, de vorm waarin silicaat in zeewater voorkomt, is een belanrijke voedingsstof in het marine milieu, omdat het door diatomeeën en andere organismen wordt gebruikt om hun skeletjes uit op te bouwen. Wanneer deze organismen sterven, kunnen de skeletjes enige tijd door menging in de bovenste waterkolom circuleren, maar uiteindelijk zinken ze door de waterkolom en komen op de zeebodem terecht. Omdat de waterkolom onderverzadigd is wat betreft kiezelzuur lost gemiddeld 60% van het biogeen gevormde silicaat (BSi) dat in het oppervlaktewater geproduceerd wordt op voordat het de zeebodem bereikt. Dit heeft tot gevolg dat de concentratie kiezelzuur laag is in het oppervlaktewater en toeneemt met de diepte. De oplossing van BSi gaat verder op de bodem en in het bovenste laagje van het sediment, resulterend in hoge concentraties kiezelzuur in het poriewater. Uiteindelijk zal slechts een klein gedeelte van de BSi productie, ~2.5%, begraven worden in het sediment, waaruit het na miljoenen jaren, via tectonische processes zoals zeebodemspreiding, gebergtevorming en erosie weer terug komt in de oceanische kringloop.

BIOGEEN SILICAAT IN OPWELLINGSGEBIEDEN

Wanneer er in het oppervlaktewater voldoende voedingsstoffen aanwezig zijn, zijn de diatomeeën de eerste organismen die daarvan gebruik kunnen maken. In het voorjaar leidt dit vaak tot uitgestrekte algenbloeien in grote delen van de oceaan en in kustzeeën. Diatomeeën hebben echter, naast de stikstof en fosfaat die voor alle autotrofe organismen essentieel zijn, een absolute behoefte aan kiezelzuur. Wanneer kiezelzuur op raakt in het oppervlaktewater stagneert de groei van de diatomeeën en verschuift de samenstelling van het fytoplankton in de richting van flagellaten, die geen kiezelzuur nodig hebben. In opwellingsgebieden wordt voortdurend water dat rijk is aan voedingsstoffen aangevoerd vanuit de diepere waterkolom. Hierdoor blijven de omstandigheden gedurende langere perioden gunstig voor de productie van diatomeeën. Tijdens zo'n periode van upwelling zal, afhankelijk van de hydrografische condities van het moment, een opeenvolging van diatomeeënsoorten de fytoplanktonpopulatie domineren. Na hun dood zinken de resten van de

diatomeeën naar de bodem, waarbij soorten met een zwaar skeletje de grootste kans hebben om de bodem te bereiken.

PRESERVATIE VAN BIOGEEN SILICAAT IN HET SEDIMENT

Hoewel slechts een klein gedeelte van de diatomeeën die in het oppervlaktewater worden gevormd begraven wordt in het sediment, weerspiegelt het biogeen silicaatgehalte van de sedimenten de productiviteitspatronen zoals die zichtbaar zijn in het oppervlaktewater. De soortensamenstelling in het sediment verschilt echter vaak van het levende fytoplankton, omdat de dunne en kleine skeletjes, met een groot specifiek oppervlak, oplossen terwijl de dikke, zwaar verkiezelde soorten bewaard blijven. Hoewel BSi oplost in het oppervlaktesediment, lijkt het erop dat oplossing dieper in het sediment van ondergeschikt belang is (hoofdstuk 4). Kennelijk is de overgang van de waterkolom naar het sediment-water grensvlak en vervolgens naar het sediment de cruciale stap voor de preservatie van biogeen silicaat. In het bovenste laagje van de bodem vinden processen plaats die de oplossingsgevoeligheid van biogeen silicaat verminderen. De reactieve plaatsen op het silicaatoppervlak worden geëlimineerd, bijvoorbeeld doordat aluminiumionen worden ingebouwd in het silicaatrooster. De aanwezigheid van biogeen silicaat is aangetoond in sedimenten die enkele honderdduizenden jaren oud zijn, en er zijn aanwijzingen dat de aan- en afwezigheid van BSi in oude sedimentlagen een weerspiegeling is van de variatie in opwellingsintensiteit in het geologisch verleden. Voordat biogeen silicaat echter gebruikt kan worden als een indicator voor deze paleo-productiviteitsprocessen is een goed begrip van de mechanismen die de kringloop van productie, oplossing en preservatie van biogeen silicaat reguleren, van groot belang. Een eerste vereiste daarvoor is een betrouwbare methode om BSi te analyseren, zowel in de waterkolom als in sedimenten.

OPWELLINGSGEBIEDEN

Opwelling is het belangrijkste transportmiddel dat diep water, rijk aan kiezelzuur en andere voedingsstoffen, naar het oppervlak brengt, waar het benut kan worden door fytoplankton. De belangrijkste opwellingsgebieden vinden we rond de evenaar in de Atlantische en Stille Oceaan en rond Antarctica. Verder is opwelling een belangrijk proces langs de westelijke randen van de continenten, bijvoorbeeld bij Peru en Namibië, waar het oppervlaktewater van de kust wordt weggeblazen door de daar heersende passaatwinden. Een ander belangrijk opwellingsgebied is de noordwestelijke Indische Oceaan, waar 's zomers opwelling plaatsvindt die gekoppeld is aan de moesson.

De moesson in de Indische Oceaan beïnvloedt grote delen van Afrika en Azië en is een van 's werelds belangrijkste klimaatsystemen. Het afwisselend optreden van

zuidwestelijke en noordoostelijke winden, en de daaraan gekoppelde stroomrichting van het oppervlaktewater, is het gevolg van het grote warmte-regulerende vermogen van de oceanen. In de wintermaanden is het Tibetaans Hoogland koud vergeleken met het oppervlaktewater van de Indische Oceaan, wat resulteert in de vorming van een hogedrukgebied boven de Himalaya, een noordoostelijke moessonwind en een noord-zuid stroming van het oppervlaktewater voor Oost Afrika, de Somali Current. In het voorjaar warmt het Tibetaans Plateau snel op, terwijl de temperatuur van het water van de zuidelijke Indische Oceaan nauwlijks verandert. Boven de Himalaya vormt zich een lagedrukgebied, dat sterke, zuidwestelijke winden tot gevolg heeft boven Somalië en de Arabische Zee. De Somali Current verandert van richting en stroomt vervolgens van zuid naar noord, terwijl aflandige winden het oppervlaktewater wegblazen van de kust. Dit oppervlaktewater wordt vervangen door voedselrijk water afkomstig van grotere diepten. De aanvoer van voedingsstoffen, en de daaraan gekoppelde fytoplanktonproductie, is hoog tijdens de zuidwest moesson, en laag tijdens de wintermaanden, wanneer de noordoost moesson waait. Van jaar tot jaar kunnen echter grote verschillen optreden. Na een winter met weinig sneeuw kan het Tibetaans Hoogland vroeg opwarmen en zal de moesson sterk zijn. Na een koude winter op het noordelijk halfrond wordt slechts een zwak lagedrukgebied gevormd boven de Himalaya en zal de moesson zwak zijn. Een langdurige periode met zware sneeuwval en ijsbedekking op het Tibetaans Plateau, zoals waarschijnlijk heeft plaats gevonden tijdens de ijstijden, zou daarom een langdurige verzwakking van het moesson systeem tot gevolg hebben gehad.

DE MOESSON, VROEGER EN NU

Het woord moesson, afkomstig van het Arabische *mausim,* betekent een seizoen, een periode. Hiermee werd de seizoenale verschijning van zon en regen aangeduid. Al ongeveer 5000 jaar maken kooplieden gebruik van de handelsroutes van de Middellandse Zee naar de Perzische Golf en de Arabische Zee. In de oudste scheepsverslagen, daterend van 2600 v. Chr., wordt echter nauwelijks gewag gemaakt van periodieke veranderingen in windrichting. Dat de windrichting veranderde met de seizoenen moet deze vroege zeelui zeker opgevallen zijn, en mogelijk hielden zij met hun reisschema's zelfs rekening met de heersende moessonwinden. Na de val van het Romeinse Rijk verdwenen de kooplui van het Middellandse-Zeegebied uit de Indische Oceaan en het duurde tot de 7de eeuw, toen de Arabieren het gebied veroverden, voordat het handelsverkeer op de Indische Oceaan weer volop op gang kwam. Uit deze periode dateert ook de volgende beschrijving:

> *De zee stroomt tijdens de zomermaanden naar het noord-oosten, en tijdens de wintermaanden naar het zuid-westen – Ibn Khordazbeh, 9de eeuw.*

De middeleeuwse geografen hadden geen besef van oceaancirculatie, en zij beschouwden de moesson als een soort van jaarlijks getij. In de zomermaanden was

het hoog water in het oosten, in de wintermaanden aan de Somalische kust, een beschrijving die redelijk nauwkeurig is voor de noordelijke Indische Oceaan wat betreft stroomrichting van het oppervlaktewater.

Vanaf de 17de eeuw onwikkelde de moderne wetenschap zich in Europa. Experimentele studie, vooral een nauwkeurige beschrijving van waarnemingen, gevolgd door een theoretische interpretatie met behulp van wis- en natuurkunde, moest leiden tot een beter begrip van de waargenomen natuurverschijnselen. Deze aanpak kon bij uitstek worden toegepast op atmosferische verschijnselen, en vanwege het grote belang voor het leven en de handel rond de Indische Oceaan was de moesson een van de eerste grootschalige atmosferische systemen die werd bestudeerd. Veel van de vroege observaties werden gedaan door koopvaardijschepen van de Oost Indische Compagnie, die lange tijd de handel naar het Verre Oosten domineerde. De waarnemingen werden verzameld in atlassen die bestemd waren voor navigatiedoeleinden. Vanaf het einde van de 19de eeuw bezochten gespecialiseerde onderzoeksschepen de Indische Oceaan met een louter wetenschappelijk doel, waaronder de Challenger Expeditie, Snellius I, 19929-1930, de John Murray Expeditie, 1933-1934 en de International Indian Ocean Expedition, 1959-1960.

Recent zijn diepzeesedimenten, ijskernen, boomringen, loesskernen en meersedimenten bestudeerd om een verklaring te vinden voor de drijvende krachten achter het moessonsysteem. Deze studies laten zien dat de intensiteit van de moesson in de Indische Oceaan en de daaraan verbonden opwelling varieert op tijdschalen die overeenkomen met de ijstijden en dat de processen die het klimaat van de Indische Oceaan sturen gekoppeld zijn aan klimaatprocessen in de rest van de wereld. De weerspiegeling van glaciaal-interglaciale variaties in opwellingsintensiteit en de daarmee verbonden productie van diatomeeën kan worden teruggevonden in het biogeen silicaat dat in de sedimenten begraven is.

DIT PROEFSCHRIFT

Dit proefschrift beschrijft een studie naar de kringloop en de preservatie van biogeen silicaat en diatomeeën op de Somalische continentale helling in de noordwestelijke Indische Oceaan.

In hoofdstuk 2 wordt een methode beschreven om gelijktijdig biogeen silicaat en aluminium te analyseren, speciaal geschikt voor monsters met een laag BSi en een hoog kleigehalte. Het meten van aluminium vergemakkelijkt het onderscheid tussen silicaat afkomstig van de biogene en de niet-biogene fractie van het sediment, omdat aluminium vrijwel geheel afkomstig is van de lithogene fractie. De methode werd getest met fijn-korrelig silicagel, standaard kleimineralen, kunstmatige sedimenten en natuurlijke monsters varierend van verse diatomeeën tot oude sedimenten afkomstig uit verschillende oceanen. Om het BSi gehalte van de monsters te bepalen werd gebruik gemaakt van 4 modellen van een toenemende complexiteit, waarna voor elk monster het optimale model werd geselecteerd met behulp van een statistische F-test. Voor mengsels van silicagel en kleimineralen bleek de bijdrage van silicaat afkomstig

van de klei verwaarloosbaar ten opzichte van de silicagel. De natuurlijke monsters vertoonden complexer oplosgedrag, maar voor de meeste kon het onderscheid tussen silicaat van biogene oorsprong en silicaat afkomstig uit klei gemaakt worden op basis van de Si:Al verhouding en de reactiviteitsconstanten berekend met de modellen.

De hoofdstukken 3, 4 en 5 beschrijven de kringloop van biogeen silicaat op twee stations 80 en 270 km uit de kust op de Somalische continentale helling (NW Indische Oceaan). Dit gebied werd bezocht tijdens het Nederlands Indische Oceaan Programma (NIOP) in 1992 en 1993. Gedurende 9 maanden waren op beide stations sedimentvallen geplaatst, om de naar de bodem zakkende deeltjes te onderscheppen. Het station bij de kust bevond zich direct onder een van de belangrijkste opwellingswervels terwijl het tweede station verwijderd was van de directe opwelling nabij de kust. Op de zeebodem onder de vallen werden sedimentmonsters genomen en werd de afgifte van kiezelzuur vanuit de bodem naar het bovenliggende water gemeten. Op basis van de resultaten werd een massabalans voor biogeen silicaat opgesteld voor deze beide stations (hoofdstuk 3). In de sedimentval bij de kust, op de Somalische helling, werd veel BSi onderschept tijdens de ZW moesson, en weinig tijdens de wintermaanden. De sedimentval verder van de kust, in het Somalische Bekken, vertoonde een soortgelijk patroon, maar de hoeveelheid BSi die werd onderschept was lager. Op beide stations bleek minder dan 10% van het biogeen silicaat dat op het sediment aankomt begraven te worden, doordat efficiente recycling plaats vindt op het sediment-water grensvlak.

In hoofdstuk 4 werd de soortensamenstelling van de diatomeeënpopulatie die door de sedimentvallen onderschept werd tot in detail bestudeerd en vergeleken met het oppervlaktesediment. Op beide stations was de aanvoer van diatomeeën naar de sedimentval tijdens de ZW moesson een orde groter dan gedurende de wintermaanden. In de sedimentval bij de kust kon een duidelijke opeenvolging van pre-opwellers, opwellers en oceanische soorten worden aangetoond. In het Somalisch Bekken werd een soortgelijk patroon aangetroffen, maar het totale aantal diatomeeën was lager. Op het sediment-water grensvlak lossen de kleine, zwak verkiezelde diatomeeën op, maar dieper in de bodem blijkt oplossing van ondergeschikt belang te zijn. Twee diatomeeënsoorten die karakteristiek zijn voor het opwellingsseizoen, *Thalassionema nitzschioides* en de sporen van *Chaetoceros* domineren de assemblages in het sediment en weerspiegelen daarmee de opwelling in het oppervlaktewater.

In hoofdstuk 5 worden de conclusies die in het vorige hoofdstuk werden getrokken toegepast op een piston core, een 15 m lange sedimentkern genomen onder de sedimentval op de Somalische helling. De fluctuaties in BSi accumulatie in deze kern weerspiegelen de veranderingen in de intensiteit van opwelling gedurende de laatste 115.000 jaar. Tijdens het Holoceen traden twee lange perioden op waarin de opwellingsintensiteit geleidelijk toenam, abrupt onderbroken door een terugkeer naar koudere omstandigheden rond 8200 BP en 5900 BP. Van een aantal monsters werd de diatomeeënsamenstelling in detail vastgesteld om de preservatie te bepalen van soorten die karakteristiek zijn voor opwelling. Tijdens perioden met een verhoogde biogeen silicaataccumulatie bleken diatomeeën die karakteristiek zijn voor opwelling

de populatie te domineren. Tijdens IJstijden en koude perioden was de accumulatie van BSi laag en waren er nauwlijks diatomeeën aanwezig in het sediment. In het vroege Holoceen en tijdens isotopenstadium 5c, ongeveer 110.000 jaar geleden, was de accumulatie van de opwellingsdiatomeeën *Thalassionema nitzschioides* en de sporen van *Chaetoceros* tot 8 maal hoger dan tegenwoordig, wat er op wijst dat de aan opwelling gerelateerde productie van diatomeeën verhoogd was tijdens die perioden. Kennelijk was opwelling intenser tijdens het vroege Holoceen en het laatste Interglaciaal, maar van ondergeschikt belang tijdens de IJstijden.

Samenvattend laat deze studie zien dat biogeen silicaat dat in de sedimenten van de Somalische continentale helling gepreserveerd is een afspiegeling is van de aan opwelling gerelateerde productie van diatomeeën in het oppervlaktewater. Hoewel een belangrijk deel van het biogeen silicaat oplost in de waterkolom en op het sediment-water grensvlak en de skeletjes van de kleine, zwak verkiezelde soorten uit de populatie verdwijnen blijven twee belangrijke soorten die karakteristiek zijn voor de opwelling bewaard in het sediment. In het sediment kan de opwellings geschiedenis van de Indische Oceaan worden afgeleid uit de fluctuaties in BSi accumulatie en uit de aan- en afwezigheid van opwellingsdiatomeeën in het sediment.

Dankwoord

Voorjaar 1989 besloot ik om na 10 jaar werken in het lab mijn vaste baan op te zeggen en mij in te schrijven voor de propedeuse scheikunde als voorbereiding op een bovenbouwstudie geochemie. De reacties in mijn omgeving waren zeer uiteenlopend van aard. Van "ik wou dat ik zoiets kon doen" tot "waar begin je aan, je hebt toch een vaste baan, dat geef je toch niet op" en alles wat daar tussen zit. Natuurlijk, die hele onderneming ook had misschien ook minder goed af kunnen lopen.....
In de 11 jaar die sindsdien zijn verstreken hebben een aantal toevalligheden en gelukkige keuzes er toe geleid dat dit proefschrift de kringloop van silicaat behandeld en niet, bijvoorbeeld, de varkensmestproblematiek in de provincie Noord Brabant. Gert de Lange vroeg mij als tweedejaars student mee op de TYRO voor een expeditie naar de anoxische bekkens van de Middellandse Zee, en maakte mij daarmee enthousiast voor de mariene geochemie. Op het NIOZ selecteerde Johan van Bennekom enkele jaren later een OIO, die na een jaar voor de studie theologie koos. De twee jaar tijd die na haar vertrek op dat contract overgebleven waren betekenden mijn overstap van de CO_2 groep naar de groep elementencycli en het silicaatonderzoek.

Een groot aantal mensen op het NIOZ en daarbuiten heeft in mindere of meerde mate bijgedragen aan het welslagen van het onderzoek dat in dit boekje beschreven is. Allen wil ik bij deze daarvoor hartelijk bedanken. Enkele mensen wil ik speciaal vermelden. In de eerste plaats Wim Helder en Wim van Raaphorst. Zij bliezen het silicaatonderzoek op het NIOZ nieuw leven in op het moment dat het in de reorganisatie ten onder dreigde te gaan, boden mij de gelegenheid om het uit te voeren en stonden klaar wanneer dat nodig was. Belanrijke steun kreeg ik verder van Eric, Henk, Claar, Tjeerd, Geert-Jan, en tenslotte van Jan, die altijd klaar zat met de koffie. Philippe van Cappellen wil ik ervoor bedanken dat hij als promotor heeft willen optreden.

Zonder Nita en Rijk en de aanwezigheid van José, Wim, Roos, Erik, Margriet, Bram, Annemarie en Huib waren de afgelopen jaren niet half zo plezierig geweest. Bedankt voor alles!

Curiculum Vitae

F. A. (Erica) Koning werd geboren op 23 september 1957 te Utrecht. Na het doorlopen van de middelbare school en het volgen van een HBO-opleiding tot medisch analist was zij gedurende bijna 10 jaar werkzaam als analist in een ziekenhuislaboratorium. In september 1989 begon zij met de studie scheikunde aan de Universiteit Utrecht. Na het behalen van de propedeuse in 1990 vervolgde zij de studie bij de vakgroep geochemie, waar in oktober 1995 het doctoraal examen werd behaald. Sinds oktober 1993 is Erica werkzaam bij het Nederlands Instituut voor Onderzoek der Zee, achtereenvolgens als analist, als toegevoegd projectonderzoeker, als projectonderzoeker en sinds 1 september 2001 als postdoc.